AN EXPERIMENTAL STUDY OF THE MOTION RESPONSE IN REGULAR WAVES OF A SEMI-SUBMERSIBLE UNDER DAMAGE CONDITIONS

BARRY MICHAEL STONE

AN EXPERIMENTAL STUDY OF THE MOTION RESPONSE IN REGULAR WAVES OF A SEMISUBMERSIBLE UNDER DAMAGE CONDITIONS

by

Barry Michael Stone, B.Eng., P.Eng.

A thesis submitted in partial fulfillment of
the requirements for the degree of

Master of Engineering

Faculty of Engineering and Applied Science
Memorial University of Newfoundland

May 1986

St. John's Newfoundland

ISBN 0-315-33635-8

ABSTRACT

The determination of motion response characteristics, and therefore operating limits, of semisubmersibles in normal even keel conditions has been extensively reported in the literature. However, the extension of this work to vessels which have undergone some form of damage leading to loss of buoyancy and abnormal heel and trim angles is limited.

To establish the motion response of a typical semisubmersible in both even keel and damage conditions, and resulting changes relative to severity and direction of damage, a model study using a 1/100 scale model of a moored, four column, twin pontoon semisubmersible has been conducted. For each wave direction of head, beam and quartering seas, tests were undertaken at five angles of trim and heel: even keel, two towards (windward damage), and two away (leeward damage) from the waves in 7 m regular seas with periods of 7 to 25 sec. In all cases six degrees of freedom motion response was obtained.

The RAO curves for small angles of trim and heel show little change from even keel, operating draft. However,

at large angles, with pontoons and deck structure piercing the water surface, substantial increases in roll and, particularly pitch motion, occurred over a band of wave periods of 9 to 13 sec. Over this band all motions contained not only the wave frequency but also a significant subharmonic component at half the wave frequency. Under these conditions leeward damage consistently produced the largest motion. The most extreme motion measured resulted in a pitch RAO of 2.9 or 19.8° for a wave height of 6.9 m at a wave period of 12 sec. in quartering seas.

Further work using realistic irregular seas to obtain additional insight into nonlinear effects over the subharmonic or parametric resonance frequency band has been recommended.

ACKNOWLEDGEMENTS

I wish to thank my supervisor Dr. D.B. Muggeridge for his encouragement, guidance and financial support throughout the research.

A special thank you to Mr. M. Sullivan, Mr. B. Wilkie, Mr. H. Mesh and Mr. L. Little of the Ocean Engineering Research Group for their patience and invaluable assistance during the experiment, and to Dr. H. El-Tahan for our many long hours of discussion which proved most helpful.

The assistance of the technical staff of the Faculty of Engineering and Applied Science and Department of Technical Services, Engineering Division, is gratefully acknowledged.

Financial support was provided by the Natural Sciences and Engineering Research Council of Canada through Grant A4885. I am also grateful for the financial support provided by the School of Graduate Studies of Memorial University of Newfoundland.

Furthermore, I express my appreciation to Mrs. M. Brown for typing of the manuscript on short notice and with considerable care.

TABLE OF CONTENTS

LIST OF TABLES

LIST OF FIGURES

NOMENCLATURE

BM	Height of metacenter above KB
d	Distance
GM	Metacentric height
GZ	Righting arm
I	Mass moment of inertia
K	Spring stiffness
KB	Center of buoyancy
KG, CG	Center of gravity
k	Radius of gyration
L	Total mooring line length
M_h	Heeling Moment
m	Mass
S	Mooring line catenary arc length
T	Mooring line tension
T_x, T_y	x and y components of T
U	Horizontal distance from anchor to free end of catenary mooring
U'	Length of mooring line in contact with sea floor
W	Displacement or weight
ν	Water depth
T	Period of oscillation
ϕ	Angle of heel
ψ	Angle of mooring with horizontal at the fairleader
ψ_o	Angle of mooring line at the sea floor

1.0 INTRODUCTION

In its quest to meet the ever increasing demand for energy during this century, the petroleum industry has extended its operations progressively further offshore. The resulting evolution of mobile offshore drilling units (MODU) and their capabilities have been well documented by such authors as Danforth (1977), McTaggart (1976) and others. Of the available configurations, semisubmersibles have, as a result of superior motion response characteristics, become the "work horse" of the industry particularly in harsh environment regions such as the North Sea and off Eastern Canada.

Semisubmersibles can be described as floating, column stabilized platforms, comprised of a deck structure supported above water by an array of vertical columns attached to large underwater displacement hulls in the form of individual footings or, more commonly today, twin pontoons. This geometry provides a low waterplane area to displacement ratio resulting in high natural periods relative to dominant wave periods thus achieving mihimal dynamic response. In addition, given the exponential decay of wave motion with increasing depth, the wave excitation forces experienced by

the pontoons are also reduced at operational and survival drafts. The development of the modern day twin-pontoon semisubmersible has been specifically dealt with in some detail by Rodnight (1983).

The operating limits of a semisubmersible is largely a function of its motion response characteristics. Its prediction using both mathematical and physical modelling has been extensively reported in the literature. A review of the various mathematical techniques is provided by Hsiung (1984); and Mathisen and Carlsen (1980), while Takagi et al. (1985) have provided a comprehensive comparison of calculation methods with physical modelling based on a large, twin pontoon, eight column semisubmersible.

However, this work has been limited to platforms in normal even keel condition at transit, operating and survival drafts. The motion response that can be expected after a semisubmersible has undergone some form of damage producing significant heel and trim angles and its potential impact on vessel stability has received relatively little attention.

Since the loss of the semisubmersibles ALEXANDER KIELLAND in 1980 and the OCEAN RANGER in 1982 the stability regulations, although incorporating many changes, remain based on free floating, still water conditions and do not consider the dynamic motion response of the structure. The regulations relating to damage stability and loss of buoyancy would be most affected by vessel motion. In the more strict cases these rules generally state:

- maximum inclination angle of 15° after defined damage.

- maximum inclination angle of 35° with minimum freeboard to downflooding of 0.6 m and minimum righting arm (GZ) of 1.0 m after complete loss of buoyancy of any one column.

Additional detail concerning the development of the present regulations, comparison of the rules of various certifying and government authorities, discussion of the adequacy of existing regulations and validity of recent changes can be found in Springett and Praught (1986), Praught et al. (1985), Morland et al. (1985), Hammett (1983), Hoff (1982) and others.

The motion characteristics of a vessel in damage condition meeting these requirements may still permit progressive downflooding through intermittently submerged openings leading to capsizing.

The following investigation, using rigid body modeling, addresses this problem by providing a quantitative measure of the motion response characteristics of a semisubmersible in both even keel, operating draft and damage conditions. The resulting comparison will provide a definitive indication of the changes in response that can be expected relative to severity and direction of damage.

2.0 REVIEW OF LITERATURE

Numata et al. (1976) provided the first insights to the motion response of a semisubmersible in extreme conditions. Models of a typical footing and pontoon type semisubmersible were tested in varying conditions of: extreme wind and sea state, deck load (metacentric height), draft (air gap), vessel heading, and moorings. Wind heeling moments resulted in static heel angles up to 12.5 deg. It was, however, demonstrated that for an intact vessel and without downflooding, capsizing was unlikely to occur. The above model tests also provided the early observations of wave induced steady heel of a semisubmersible in regular waves.

The extension of this work to the dynamic motion response of damaged semisubmersibles in waves has, with few exceptions, not been considered in the published literature.

The Mobile Platform Stability (MOPS) Project of the Norwegian Maritime Directorate used both a physical model and theoretical approach in studying this problem. Initially, experimental data was obtained through a series of regular wave, head sea model tests based on an idealized

eight column , twin pontoon semisubmersible similar to the Aker H-3 design at various drafts and trim angles. The model tests were followed by and compared with numerical calculations of the motions using a number of techniques.

Huang et al. (1982) provides the heave and pitch response from these tests. The influence of trim angle is small, as long as the pontoons remain fully submerged, and the results agree satisfactorily with linear strip theory calculations. However, when the pontoons or deck pierce the surface nonlinear effects become significant and, as can be expected, agreement with linear strip theory cannot be maintained. These effects are clearly illustrated by marked asymmetry of the motion response curve relative to trim angle. With the pontoons piercing the surface the motion becomes more severe at trim angles in the direction of wave travel (i.e. leeward). This situation is reduced and reversed in the case of the largest draft and trim angle tested where the pontoons remain fully immersed but the deck enters the water.

For large draft and trim angles with both pontoons and deck piercing the water surface, the motion response was not sinusoidal but contained, in addition to the wave frequency,

a significant subharmonic component at half the wave frequency. This parametric resonance effect existed over a specific wave frequency band about twice the natural frequency, outside of which the motion was sinusoidal. To simulate this nonlinear phenomenon a simplified time simulation method was used and had limited success in reproducing the general trends and, at some wave frequencies, double frequency behaviour of the data. Additional details of this work can be found in Huang et al. (1983).

The simplified time domain simulation method used above was improved and extended to the general six degrees of freedom problem by Naess and Hoff (1984) using a strip theory approach and a time stepping procedure. It should be noted that the method does not consider wave forces on the deck structure (Huse and Nedrelid, 1985). Added mass and damping coefficients, which are calculated as a function of submergence, go through an abrupt change as the pontoons move through the water surface. Another important factor is the nonlinear restoring force term in the equations of motion discussed by Huang et al. (1983). The extended method showed improved correlation with the experimental results discussed earlier and also provided the following observations:

- the nonlinear nature of the equations of motion of a vessel with pontoons piercing the surface was clearly illustrated by different response curves produced for different wave amplitudes.

- motion response was shown to be relatively insensitive to positive trim angles (i.e. inclined towards waves).

- increasing draft produces a significant decrease in the asymmetry of the motion response.

When applied to a vessel in beam seas with a heel angle the heave response was asymmetric as previously discussed for head seas. However, the roll response curves for positive and negative heel angles cross at a frequency of 5.3 rad/sec; positive (towards waves) heel angle roll motion was greater below this frequency.

Further model test results and numerical predictions are provided by Naess et al. (1985). In this instance a much larger model (1:40) of an ODECO eight column, twin pontoon semisubmersible was used. During irregular,

quartering sea tests at operating draft dynamic roll and pitch amplitude was insensitive to increasing windward damage (inclined into the waves). In addition, it was demonstrated that surge and sway motions were larger for windward damage while the reverse occurs for pitch and roll motions. The latter indicates that leeward damage (inclined in the direction of wave travel) is more critical to progressive flooding which may lead to capsizing. These conclusions were further supported by tests in survival condition.

Naess et al. (1985) also conducted regular sea tests of the same model "soft" moored in head and beam seas for comparison with time domain simulation calculations. In this comparison, with more realistic model tests than those of Huang et al. (1982), the theory, although showing the general trends, does not provide satisfactory agreement with model tests. The asymmetric motion with respect to inclination angle is clearly reproduced in both cases. The subharmonic (parametric) resonance effects were not apparent in the time simulation method results given by the authors.

In addition to the MOPS project, detailed and parallel model studies of a 1/40 scale model of the OCEAN RANGER, an

eight column, twin pontoon semisubmersible, were carried out by both the National Research Council of Canada and the Norwegian Hydrodynamics Laboratory on behalf of the Royal Commission on the OCEAN RANGER Marine Disaster. Indeed, some of the tests were undertaken in collaboration with the MOPS project and have previously been discussed by Naess et al. (1985).

Full details are provided by Mogridge (1984), Huse et al. (1983) and summarized by The Royal Commission on the OCEAN RANGER Marine Disaster (1984). The tests were intended to assist in examining possible causes of the disaster and modelled specific wind and wave conditions, and directions existing at the location during the time in question. The tests demonstrated that capsizing of the model, although possible, was predominantly due to hydrostatic effects resulting from both progressive downflooding and inappropriate ballasting of the foreward tanks, and not dynamic wave forces.

Due to the specific nature of both model and environmental test conditions the extension of the results to the more general problem of motion response of a semisubmersible under damage conditions is difficult.

The minor influence of small angles of inclination on motion response is also illustrated and confirmed by experimental results presented by DeSouza and Miller (1978) for a three column, caisson type semisubmersible and El-Tahan (1985) for an eight column, twin pontoon type semisubmersible. In the latter case the motion response in damage condition was reduced and the existence of a sub-harmonic component was noted.

3.0 THE HYDRODYNAMIC MODEL

The 1/100 scale model designed and constructed for the study is considered similar in geometry and mass properties to the four column, twin pontoon semisubmersible drilling unit GVA 4000 (Fig. 3.1) of Gotaverken Arendal AB, Gothenberg, Sweden. A general arrangement drawing of the model is presented in Fig. 3.2 while Table 3.1 gives principal characteristics of both the prototype (Gotaverken Arendal, 1984; Jacobsson and Dyne, 1983; Kallstrom, 1983; Mathison et al., 1982 and Lundgren and Berg, 1982) and the model as measured during tests (Section 3.2 to 3.4).

All model parameters and test results have, for the convenience of comparison, been scaled up and are presented, unless otherwise noted, as full scale or prototype values. The Froude scaling factors between model and prototype are given in Table 3.2.

3.1 Model Design and Fabrication

The model was constructed entirely of rigid polyvinyl chloride (PVC): 1/8 in. sheet for the box deck structure and pontoons; machined thick wall tubing for the columns; and

machined round rod for the cross bracing and pontoon corners. The deck structure, columns, bracing and pontoons were initially constructed separately as components and then assembled. Underwater joints were hot air welded with glue joints being used throughout the box deck structure.

Both pontoons were equipped with two "ballast tubes" running parallel through the length of the pontoon. A threaded rod attached to the O'ring sealed end caps of these tubes permitted the placement of ballast weights anywhere along the length of each ballast tube. Access was gained to these tubes through a removable and resealable bow on each pontoon. A watertight drain plug was located on the bottom of each pontoon to facilitate the removal of water should any leaks occur.

Each column was also equipped with an end cap and threaded rod allowing the placement and adjustment of ballast vertically in the columns. An air valve was installed in the end caps of the stern columns. By filling the model with low pressure air via these valves any leaks could be quickly located. It is worthy of noting that no leaks whatsoever occurred during testing.

Ballast weights could also be placed at the center of the deck structure within the moon pool and on deck.

Fig. 3.3 shows the model near the end of construction with the ballast, threaded rod, end cap and bow removed from the starboard pontoon and ballast, threaded rod and end cap from the starboard bow column. Fig. 3.4 shows the model moored in the test basin just prior to testing.

3.2 Mass Properties

To obtain the model displacement at the required operating draft the model was allowed to float freely in still water. Ballast was then added and adjusted such that the model assumed a level position at the unmoored draft. The model and ballast were then weighed and the resulting weight adjusted to the moored draft of 20.5 m.

The difference in displacement between prototype and model is attributed to sharper curves in the model at both the pontoon corners and ends. This reduced buoyancy in the model resulted in a higher center of buoyancy (KB). To obtain the correct model metacentric height (GM) of 2.4 m it was therefore necessary to increase the center of gravity

(KG) from 20.05 m to 20.97 m according to the formula: GM = (KB + BM) - KG.

To establish this KG position and the required radii of gyration the model and ballast were placed on a tilting platform shown in Figs. 3.5 and 3.6. Prior to placing the model on the platform the adjustable KG, i.e. the distance between table and knife edge, was set to the desired distance of 20.97 m. The empty table was then levelled, i.e. once placed in a level position it remains so thus showing that the center of gravity (CG) is somewhere on the vertical plane through the two knife edges, by moving small weights on the platform. This levelling procedure was repeated about both the pitch and roll axis, thereby positioning the CG of the empty platform somewhere on the vertical axis passing through the intersection of the pitch and roll axis at the platform center.

The counterweights were then adjusted vertically to raise or lower the platform center of gravity bringing it in line with the axis of rotation. The empty platform was thus balanced, i.e. the CG is now on the axis of rotation and once tilted to any angle about this axis the platform will remain at that position.

The model was then placed and centered on the platform. The position of ballast weights within the model was adjusted to both level and balance the platform and model together as previously described, thus setting the desired model KG.

The model radii of gyration in both pitch and roll was measured using the period of oscillation of the empty platform, and of the model and platform together. The measured period was used in the following formula developed from the natural frequency of a simple undamped torsional spring system (MacDuff and Curreri, 1958):

$$k^2 = I/m = \frac{I_{P+M} - I_P}{m} = \frac{\Sigma K_i d_i^2}{4\pi^2 m} (T^2_{P+M} - T^2_P) \qquad (3.1)$$

where:

I = mass moment of inertia

k_i = radii of gyration about axis of interest

$K_i d_i^2$ = torsional spring stiffness where K = spring constant and d = distance

m = mass of the model

T_{P+M} = period of oscillation of platform and model

T_P = period of oscillation of platform

The measured initial k for pitch and roll was then adjusted to the desired value by moving ballast weights towards or away from the axis of rotation.

The spring system provided the restoring force necessary to oscillate the platform. Period was measured using a Bruel and Kjaer 8306 accelerometer and Hewlett Packard 5420B Digital Signal Analyzer which provided an accuracy of 0.01 sec.

3.3 Metacentric Height

To measure metacentric height (GM) about both the transverse (pitch) and longitudinal (roll) axis a simple inclining experiment was carried out. Fig. 3.7. shows the experimental arrangement. An external heeling moment was applied to the model using equal calibrated weights attached to eye bolts installed equal distance from the axis of rotation. The angle of inclination was measured using a Spectron L210 Two Axis Electrolytic Level Sensor and a Bruel and Kjaer 1526 Digital Display.

The resulting static stability curve is shown in Fig. 3.8. A longitudinal and transverse GM of 2.4 m was then calculated using the formula:

$$GM = M_h / W \sin \phi \qquad (3.2)$$

where:

M_h = heeling moment (wt x distance)
W = model displacement or weight
ϕ = angle of inclination

The experimental GM obtained was confirmed by calculation using a computer program (Deb, 1986). The calculated values confirm those of the inclining experiment. The discrepancies occur as a result of approximations used in defining the vessel geometry program input.

3.4 Natural Periods

The model natural periods of heave, pitch and roll were measured in both the freefloating (unmoored) and mopred condition. Pitch and roll periods were measured using the

Spectron Level Sensor via the analog output of the B and K Digital Display. Freefloating heave was obtained using a B and K 4343 accelerometer while the moored period was measured using a linear rotary potentiometer. In all instances the HP Digital Signal Analyzer was used to process the transducer signal.

The prototype (Lundgren and Berg, 1982) and model natural periods are in close agreement, with the pitch and roll periods lower in the moored case, as would be expected, and heave period unaffected by the mooring.

4.0 MOORING SYSTEM

A flexible chain of uniform weight per unit length forms a catenary when supported by the two ends. From Alexandrov (1971) the main features of the catenary form are:

1. the horizontal component of tension is constant along the length of line

2. minimum line tension is equal to the horizontal component of tension

3. tension at a given point along the line is linearly related to the y-coordinate of the point.

As the tension at the upper end of the mooring line increases, line geometry progresses from the slack mode; mooring line makes tangential contact with the seabed applying no vertical force component to the anchor, to the taut mode; the mooring line contacts the seabed at some finite angle thus applying a vertical force component on the anchor.

The elasticity of the line (effective Young's Modulus) can be neglected at low tensions but becomes increasingly significant as the tension approaches the breaking strength of the chain. Compensation for elastic stretch in the chain is accomplished by increasing the length using effective Young's Modulus (Korkut and Herbert, 1970). At the point of transition from slack to taut this procedure becomes more difficult due to the vertical force at the seabed contact point no longer being zero.

Conventional anchors are designed to resist horizontal rather than vertical force with even small amounts of uplifting severely degrading holding capacity (Adams, 1967 and Bryant, 1983). It is therefore considered good practice, and indeed required by regulation (Norwegian Maritime Directorate, 1983), to lay sufficient mooring line length to ensure suspended line length is always less than total line length.

To obtain the geometric configuration and stiffness (line tension and horizontal line attachment angle versus horizontal and vertical excursion) characteristics of this system a static analysis using the traditional catenary equations (Korkut and Herbert, 1970 and Rothwell, 1979)

neglecting chain elasticity, can be used. For the slack mode, the following equations apply:

$$T_x = T - W\nu \tag{4.1}$$

$$\alpha = 1 + [1/(T_x/W\nu)] = 1/\text{Cos } \psi \tag{4.2}$$

$$T_y = T_x\sqrt{\alpha^2-1} \tag{4.3}$$

$$S = T_y/W \tag{4.4}$$

$$U = T_x/W\ [\text{Log}(\alpha+\sqrt{\alpha^2-1}) - \sqrt{\alpha^2-1}] + L \tag{4.5}$$

$$U' = L - S \tag{4.6}$$

For the taut mode, the following apply:

$$\sin \psi = 1/2\ W\nu/T\ (L/\nu - \nu/L) + \nu/L \tag{4.7}$$

$$\cos \psi_o = \text{Cos } \psi/[1-(W\nu/T)] \tag{4.8}$$

$$T_x = T \text{ Cos } \psi \tag{4.9}$$

$$T_y = T \text{ Sin } \psi \tag{4.10}$$

$$S = L \tag{4.11}$$

$$U' = 0.0 \tag{4.12}$$

$$U = T_x/W \log (\sec \psi + \tan \psi/\sec \psi_o + \tan \psi_o) \tag{4.13}$$

where (Fig. 4.1):

T = line tension

T_x, T_y = component of line tension in horizontal and vertical directions

W = weight per unit length of the mooring line

ν = water depth

ψ = angle of mooring line with horizontal at the fairleader

ψ_o = angle of mooring line at the sea floor

S = catenary arc length

L = total mooring line length

U = horizontal distance from anchor to free end of the catenary mooring

U' = length of line in contact with sea floor

4.1 Prototype Mooring

The prototype spread mooring system used as a basis in earlier model tests (Lundgren and Berg, 1982, Mathisen et al., 1982) consisted of an 8-point all chain system deployed in a 45° symmetrical pattern as shown in Fig. 4.2. The 76 mm chain had a total length of 900 m pretensioned to 1275 kN (130 tonnes) in a water depth of 195 m.

The above, with additional information from Price and Wu, (1983); The Naval Architect, (1981); Gotaverken Arendal, (1984); and Ljusne Katting, (1984) enabled the formulation of the following prototype mooring specification as a basis for the proposed tests.

Anchor Chain	76 mm Grade K4
Linear Weight	135 kg/m (1.3239 kN/m)
Proof Load	4730 kN
Breaking Load	6010 kN
Total Chain Length	900 m
Pretension	1275 kN (130 tonnes)
Water Depth	195 m
Fairleader Depth	5.33 m[1]

The prototype mooring line tension as a function of horizontal and vertical excursion, shown in Figs. 4.3 and 4.4, were calculated using equations 4.1 to 4.13 in a computer program given in Appendix A.

---

[1] From Price and Wu, (1983). Approximately equal to depth shown on GA drawing, The Naval Architect (1981). More recent information (Gotaverken Arendal AB, 1984) shows this depth as approximately 3 m.

For the mooring characteristics versus horizontal excursion during the slack mode an initial tension, T, is set and T_x, T_y, ψ, S, U and U' are calculated. T is then incrementally increased and new values calculated. When arc length, S, exceeds 900 m, total mooring length, the mooring becomes taut and ψ_o, ψ, T_x, T_y, U and U' are calculated using the appropriate formula. To solve the equations as a function of vertical excursion an intial tension is set and a lower than expected vertical displacement assumed. U is then calculated based on these values and compared to the known value of U at pretension from the previous program. If the two values do not match within a reasonable tolerance, the assumed vertical displacement is increased by a small increment until U calculated equals U at pretension thereby providing the correct vertical displacement for the given tension and horizontal pretension distance. T_x, T_y, ψ, ψ_o, S and U' are now calculated as before.

4.2 Model Mooring System

The 4.57 m width of the wave tank did not permit full length modelling of the prototype mooring on the basis of weight per unit length. The mooring system was simulated by

compound springs. The stiffness of the springs, permissible stretch and initial attachment angle were selected to correctly model horizontal and vertical mooring stiffness or restoring force as a function of horizontal displacement over a defined range.

The spring or mooring stiffness is defined as:

$$\partial T/\partial U = K \cos \psi \quad (4.14)$$

$$\partial T_x/\partial U = K \cos^2 \psi \quad (4.15)$$

$$\partial T_y/\partial U = K \cos \psi \sin \psi \quad (4.16)$$

$$\tan \psi = (\partial T_y/\partial U)/(\partial T_x/\partial U) \quad (4.17)$$

where:

∂T, ∂T_x, ∂T_y = change in line tension, horizontal component, vertical component respectively

∂U = horizontal displacement

K = stiffness

ψ = mooring angle with horizontal

In modelling a specific prototype mooring as in this case, $\partial T_x/\partial U$ and $\partial T_y/\partial U$ for a specific range is obtained from the prototype characteristics as determined from the catenary formulas (Figs. 4.3 and 4.4) and equivalent model values

obtained using the appropriate scale factor (Table 3.2). A spring stiffness, contact angle, and permissible stretch for the excursion range selected (-5.3 m to + 5.3 m) is then obtained using equations 4.15 and 4.16 thus modelling the prototype mooring stiffness, vertical and horizontal, as a function of horizontal excursion.

To extend the model mooring range additional excursion ranges above (+5.3 m to +15.0 m) and below (-5.3 m to -14.7 m) the initial range (-5.3 m to +5.3 m) were selected and new spring stiffness and permissible stretch defined using Eq. 4.15 for horizontal stiffness, and the previously calculated contact angle..

The required stiffness of individual springs was then adjusted to account for the three springs (one for each excursion range) being connected in series in a mooring line. Figs. 4.5 and 4.6 show the tension versus horizontal and vertical excursion characteristics of the model mooring and compares these to the prototype mooring.

The resulting compound spring system provides the correct horizontal and vertical stiffness as a function of horizontal excursion over the initial range of -5.3 m to

+5.3 m. The T_x and T_y curves of the prototype mooring are approximated by a straight line. At the excursion ranges above and below the initial range, the mooring contact angle has already been determined from the previous calculation. Given the predominant influence of the mooring system in providing horizontal restoring force relative to vertical restoring force which is largely determined by hydrostatic characteristics, the model mooring system spring stiffness in these ranges was based on horizontal mooring stiffness as a function of horizontal excursion (Eq. 4.15). The resulting spring system, in these ranges, thus provided correct horizontal stiffness while closely approximating the less important vertical stiffness (Fig. 4.5).

In fact, examination of the characteristics of the resulting compound spring mooring system as a function of vertical excursion shows very close approximation, compared to the prototype, of both the horizontal and vertical stiffness although the overall magnitude of vertical tension, T_y, is only about half that of the prototype (Fig. 4.6).

5.0 EXPERIMENTAL STUDY

5.1 Experimental Arrangement

The tests were conducted in 1.95 m water depth in a 58 m wave flume described in detail by Muggeridge and Murray (1981). The flume measures 58.27 m (length) x 4.57 m (width) x 3.04 m (depth) and is equipped at one end with an MTS servohydraulic piston type wave generator. A 0 to 5 m/s towing carriage runs on parallel rails 4.88 m apart on top of the tank walls. To accommodate testing at various water depths the carriage operating platform can be adjusted to different height positions. By using this feature and the carriage model brake, a model can be rigidly held in a center position anywhere along the length of the tank.

Having previously surveyed in the relative positions of the tow carriage, model, mooring touchdown (at the tank wall) and mooring termination points for each orientation, the model was rigidly held in position at the correct draft during mooring set-up and pretensioning. Fig. 5.1 illustrates a typical arrangement. With the model rigidly held in the correct position the compound spring mooring assembly was connected into the mooring line just below the fair-

leader. 0.6 mm nylon coated, stainless steel miniature cable constituted the remaining portion of the mooring line, running from the top end of the spring assembly via the fairleader to a rigid attachment under the main deck. From the lower end, the cable ran through a pulley, located at the touchdown point on the tank wall, up the tank wall to a cantilever beam load cell mounted underneath the tow carriage rails.

5.2 Instrumentation and Calibration

A block diagram of the instrumentation and data recording system is provided in Fig. 5.2.

Instrumentation on the model was limited to four SELSPOT light emitting diodes (LEDs) at the four corners and a Spectron electrolytic two axis level sensor mounted on the longitudinal centerline at the stern. The level sensor is basically a resistance potentiometer and can be used in an A.C. bridge circuit as a half-bridge. This feature enabled the use of a Bruel and Kjaer 1526 Digital Strain Indicator for both signal conditioning and display. The sensor and indicator were calibrated together against a high precision machinist level and tilting vise with indicator adjustments

being set to provide a direct digital display in degrees of the tilt about both the pitch and roll axis.

The SELSPOT (selective spot recognition) System, manufactured by Selective Electronic Co. (SELCOM) of Sweden, is an optical electronic device capable of three dimensional position measurement of up to 30 points defined by infrared Light Emitting Diodes (LEDs). The LEDs are pulsed on sequentially every 3.2 ms allowing a maximum sampling rate of 312.5 frames per second. Two electronic cameras with photosensitive detectors provide a digitized output of the angular displacement of each LED from the origin of its focal plane. The x, y and z co-ordinates of each LED is calculated using vector calculus from the actual position of the cameras and the line vectors to the LEDs. In theory, the line vectors from both cameras should intersect at the LEDs but due to imperfections in the optical lens, nonlinearities in the digitization of the signals, and errors in measuring the initial positions this does not occur. To accommodate this an orthogonal line between the two line vectors is calculated and the actual position of the LED is defined as the point midway between the two points of intersection of the orthogonal line and line vectors. The distance between these two points is then used

as a measure of the error of the LEDs position. To minimize this error the cameras should be placed 90 degrees from one another with respect to the object being measured.

Using at least 3 noncolinear LEDs the translations and rotations (six degrees of freedom) motion response of a rigid body can be calculated as a function of displacement versus time using the system software.

The primary system hardware components consisted of the 4 LEDs mounted on the model, a LED control unit secured above the model, to an external power supply at the tank wall, two cameras mounted 90° apart on custom mounts underneath the two carriage rails, and an administration unit.

The initial x, y and z co-ordinates, in the tank axis system, of the LEDs and cameras are calculated using azimuth and inclination measured with a transit. The same initial positions are then measured with the SELSPOT System.

Using this data as input the system software calculates two transformation matrices (one for each camera) enabling measurements made by the cameras to be transferred to the

tank co-ordinate system. To minimize error, the rotations and translations which transform the camera co-ordinates to the tank co-ordinates are calculated by a least squares method. The difference between the transit measured final co-ordinates and the rotated and translated camera co-ordinates is used as a measure of error. By obtaining the first and second derivates of the displacement data, the velocity and acceleration of the six degrees of freedom can also be calculated.

The SELSPOT System will give translation accuracies to within 0.2 cm and rotational accuracies to within 0.2 degrees.

Laurich (1984) provides an indepth description of the SELSPOT System and associated software.

All eight model mooring lines were terminated via a turnbuckle to a strain-gauged cantilever beam load cell mounted underneath the carriage rails directly above the mooring touchdown points. A Vishay Instruments 2100 Strain Gauge Conditioner and Amplifier System connected to a digital multimeter was used to both establish and monitor mooring line pretension. All mooring line load cells were

calibrated insitu prior to each series of tests. Calibrated weights in 50 gm intervals from 50 to 400 gm were hung from a D-ring and turnbuckle which remained attached to the cantilever after calibration. Gain adjustments were made on the signal conditioning unit such that .5 mv output equalled 1 gm..

This system permitted the setting of initial level keel mooring pretension to within 7% of the desired value in all instances and to within 3% in the vast majority of tests.

The wave profiles being produced during the tests were measured at two locations using standard twin wire linear resistance wave probes. One positioned on the tank center-line/x-axis, approximately 1.5 m upstream of the model, served as the primary probe; a backup was positioned along the tank transverse/y-axis approximately 1 m from the model center.

Prior to the start of tests each day and after the wave generator had been run for 10 minutes to eliminate any water temperature differential both probes were calibrated by raising and lowering the probe ± 5 cm about its zero position and measuring the voltage accross the wires at each

centimeter interval of immersion. For control, calibration of both probes was also done at the completion of each day of testing. No significant differences between daily calibrations occurred. The linearity correlation coefficient was always 0.999 or better.

5.3 Test Program and Procedure

The model tests were carried out in regular waves, in three orientations (head, beam and quartering seas), and in both normal operational and simulated damage condition. Wave periods ranged from 7 to 25 sec. full scale at a wave height (double amplitude) of approximately 7 m. Damage conditions, defined as a major loss of buoyancy in one column, were simulated by adding weight to a column at the center of gravity height thus inclining the model with equal amounts of heel and trim towards that column. To produce two angles, one where pontoons remain fully immersed and the deck remains above the water surface, and a larger angle where the pontoons are piercing the water surface and/or the deck enters the water, two weights, 500 and 1000 tonne respectively, were added. For each orientation, and after completion of the normal operational, even keel tests, the weights were first added to the column nearest the wave

generator (inclined towards the waves, windward damage) and secondly in the column furthest from the generator (inclined away from the waves, leeward damage). Thus for each orientation, tests were conducted at five angles: even keel, two towards, and two away from the waves.

5.4 Data Recording and Analysis

Time histories of the wave profile measured by both probes were recorded on an HP 3968A Instrumentation Tape Recorder. This 8-channel, 6 speed recorder is capable of FM recording over a bandwidth of dc to 5 kHz and/or direct recording of signals up to 64 kHz.

To obtain both wave frequency and height the record[redacted] analog signal from Probe 1 was used as input to an HP 5420A Digital Signal Analyzer which provided wave frequency directly using the Fourier transform. To obtain wave height an HP-86 computer was programmed to read the data from the analyzer and calculate average wave height over a specified time window (Little, 1985).

Corresponding SELSPOT data over the same time interval was recorded on the hard disk of an HP 2100 Fourier Analyzer

and later transferred to computer compatible magnetic tape. Due to data storage constraints the maximum SELSPOT scan rate of 312.5 samples/sec. was reduced by a factor of 4 to 78.1 samples/sec. At this rate 32.8 sec. of data per test required 10 blocks of disk space permitting the completion of 11 tests before transferring data to computer tape was necessary.

As discussed by Laurich (1984) filtering is normally required to reduce the effect of noise. This was done by averaging several consecutive frames further reducing the scan rate to 13.0 samples/sec. This increased the accuracy of the signal while still providing a band width well in excess of the 3 Hz required. The system software was then used to calculate the rotations and translations and transform these motions from the fixed reference axis system (i.e. tank co-ordinate system) to the body co-ordinate system. The resulting output provided both a data table and plot of displacement versus time for all six degrees of freedom. To obtain the double amplitude of motion the data table is used as input to a program similar to that previously discussed for the HP-86 which calculates wave height.

The same time interval of 0 to 20 seconds was used in the analysis of both the wave and motion records. Data recording was initiated (0 sec.) after several waves had passed the model and steady state conditions established.

6.0 RESULTS AND DISCUSSION

6.1 Even Keel, Operating Draft

The response amplitude operators (RAO) obtained from the double amplitude of motion divided by the wave height for even keel, operating draft are given in Figures 6.1 to 6.7 for all three wave directions: head, beam and quartering seas. For comparison, the experimental results for head and beam seas provided by Lundgren and Berg (1982) have also been reproduced.

The typical shape of the response curves for a twin pontoon semisubmersible is evident throughout. Surge and sway showing a small peak at extremely low periods with a gradual increase as wave period increases. The peak is not particularly evident in quartering seas. The magnitude of surge, head seas, and sway, beam seas is similar. Although the magnitude is reduced, this similarity is maintained between these motions in quartering seas.

Heave shows a gradual increase from the low periods peaking at a 14 sec. wave then decreasing to a period of 19 sec. whereupon a sharp climb peaking at the heave resonance

period of 21 sec. occurs. Head seas produced the largest heave motion, particularly in wave periods up to 19 sec., with beam seas producing the lowest.

The pitch and roll motion in head and beam seas shows a gradual increase to a wave period of 11 sec. then a small steady decline to 25 sec,, the highest period tested. In quartering seas the same trends can be seen but magnitude is greatly reduced.

No significant yaw was measured in any of the even keel tests. RAO's were typically less than 0.05.

Comparison of the present test results with those of Lundgren and Berg (1982) indicates good agreement up to 19 sec. for heave, pitch and roll. The discrepancies which occur in heave near the resonant period are not to be unexpected given the sensitivity to damping near resonance. A small shift in test wave period or model natural period will produce a large shift in motion response. The resonant peak in both head and beam seas occurs at a wave period of 21 sec., the heave resonant period, slightly lower than the 23 sec. head sea and 22 sec. beam sea peaks reported by Lundgren and Berg (1982). The measured heave resonance

period both moored and freefloating was 21 sec. for both series of tests (Table 3.1).

At 19 sec. differences begin to occur in pitch and roll. Lundgren and Berg (1982) show a rapid increase occurring in pitch and a much smaller increase peaking at 22 sec. in roll, compared to a continued gradual decline in both motions for the present study. This peaking of pitch and roll, and in addition surge, with heave in the earlier tests tends to indicate the existence of coupling effects (Mathisen et al., 1982) which are not apparent in the present model.

To ensure that the present tests did provide the correct motions head sea tests for wave periods above 19 sec. were repeated and extended with the same results. The extended tests for wave periods to 40 sec. showed the pitch motion beginning to increase at a wave period of 28 sec. peaking sharply, as expected, at the moored natural period for pitch of 37 sec.

The present model study resulted in higher surge and sway motions, particularly sway, than those measured by Lundgren and Berg (1982). This difference in horizontal

linear motion is sensitive to, and indicative of, differences in mooring horizontal restoring forces. This sensitivity was illustrated by Lundgren and Berg (1982) when resonance periods for surge and sway decreased substantially with increasing mooring pretension. Pitch and roll periods were affected to a much lesser degree and heave remained unaffected. The sensitivity of surge and sway to mooring characteristics was also reflected in the results of Price and Wu (1983). In the present study the compound spring-mooring system used provides the correct stiffness, i.e. restoring force, over the necessary excursion range as shown by Fig. 4.5 and 4.6 relative to the prototype defined by Sect. 4.1.

6.2 Damage Condition

In addition to even keel, operating draft, tests were also carried out in simulated damage condition (Sect. 5.3). The 500 and 1000 tonne weights added to the columns at the vertical center of gravity can be equated to volumes of 487.8 and 975.6 m^3 or column lengths of 3.73 and 7.46 m respectively. This is equivalent to 9.3% and 18.2% of total flooding of one column from keel to main deck or 14.6% and 29.3% of one column from top of pontoon to lower deck.

Fig. 6.8 illustrates with respect to the wave direction the three orientations tested while Table 6.1 provides a summary of the measured damage conditions. Figs. 6.9 and 6.10 show the model in head seas at an angle of 11.6° and 19.5° towards the corner column.

6.2.1 Head Seas

Figs. 6.11 to 6.17 provide the RAO for both damage conditions and, for comparison, even keel operating draft. To facilitate comparison a cubic spline smooth curve has been drawn through the even keel operating draft experimental points.

In many instances the general observations of Huang (1982), (1983), and Naess and Hoff (1984) (Sect. 2.0) from tests using an idealized eight column model under different trim angles and zero heel angle also apply to the present tests. In all six degrees of freedom the smaller angle of inclination had little influence on motion response relative to even keel. Comparison with even keel heave, surge and pitch show, in most cases, a slight reduction, if any difference, in motion at both +11.6° and -12.3°. Signif-

icant sway, yaw and roll does not occur. Neither the deck structure nor the pontoons pierce the water surface during testing at these angles.

However, this situation changes dramatically at the sharper angles of inclination where both deck structure and pontoon now pierce the surface. The asymmetry of the response curves with wave direction, i.e. windward damage (inclined into the waves) versus leeward damage (inclined in direction of wave travel), although present to some degree in heave, pitch and roll, is not as distinctive as that reported earlier by Huang et al. (1982), (1983) and Naess and Hoff (1984). The larger positive angle (windward damage) produces a heave resonant peak at the slightly lower period of 20 sec. compared to 21 sec. in other cases. For both damage directions the general trends are maintained with leeward damage (negative angle) consistently producing larger motions.

Huang et al. (1982), (1983), and Naess and Hoff (1985) also demonstrated the existence, at certain wave periods about half the natural period of heave, of significant subharmonic motions in heave and pitch. This phenomenon occurred during tests where both pontoons and deck pierced

the water surface at a negative angle of trim (i.e. leeward damage). During the present tests subharmonics occurred to some degree in all motions at both +19.5 deg. and -19.5 deg. angle of inclination.

Fig. 6.18 provides a typical time history of the 11 sec. wave test at an angle of -19.5 deg. clearly showing the subharmonic component. The translations show a modulation in amplitude with a clear component at the wave period (1.1 sec. model scale) plus a subharmonic component. In many circumstances this modulation produces two distinct amplitudes, one larger than the other. In such cases the larger amplitude is used to calculate the RAO for that test. The rotations show the primary component with a period of 22 sec. (2.2 sec model scale) or twice the wave period with only a minor component, if any, at the wave period.
The tests wherein subharmonic motion occurred are summarized in Table 6.2.

The presentation of results in "nondimensional" form as RAO's is normally considered valid given the assumption of a totally linear problem where motion response is a function of wave period only. Such assumptions are clearly no longer valid for a vessel under damage conditions. As a result the

response curves presented cannot be considered a linear transfer function between response and wave period. It must be emphasized that, as in the earlier MOPS tests (Sect. 2.0), the curves are specifically applicable to the particular wave amplitude tested only and the larger amplitude used to calculate the RAO for tests in which the subharmonic effect produced two modulating amplitudes must be noted.

Except for surge the larger angles of inclination produce significant changes in the motion response in not only the frequency band over which the subharmonic effect occurs (9 to 13 sec. for an angle of inclination of -19.5 deg.) but also in a region about the natural period of heave, 21 sec. The peaking of RAO curves over both these bands is more pronounced for negative angles (leeward damage) in all cases with a particularly strong influence in pitch where the RAO for a wave of 12 sec. reaches 2.5. Significant motion in sway, roll and yaw does not occur except at the larger angles over the frequency bands about the heave period and half the heave period. Negative angles produce the greatest motion over the subharmonic band but not necessarily over the frequency band about the heave natural period (i.e. half the subharmonic frequency band).

6.2.2 Beam Seas

Figs. 6.19 to 6.25 provide the RAO for both damage condition and, for comparison, even keel operating draft.

It is significant that the previous discussion for head sea tests (Sect. 6.2.1) can also be applied directly to the beam sea results. The same trends are maintained throughout the six degrees of motion for the damage condition angles of inclination and even keel heave, sway and roll.

The substantial pitch motion present in head sea tests at large negative angles within the subharmonic effect frequency band (waves at 9 to 13 sec.), is also present in beam sea tests. Tests at even keel and small angles contained no significant pitch motion while within the frequency band (at 11 sec.) the pitch motion peaks at an RAO of 2.4

6.2.3 Quartering Seas

Figs. 6.26 to 6.32 provide the RAO for both damage conditions, and for comparison, even keel operating draft. The number of wave periods at which tests were conducted were reduced in the last two series of tests (-13.1 deg. and -20.2 deg damage condition) due to time constraints.

The previous discussions for head and beam sea tests (Sect. 6.2.1 and 6.2.2) are also directly applicable to quartering seas.

Pitch motion has, again, become extremely large within the 9 to 13 sec. wave periods which result in the existence of significant subharmonics. Producing the largest motion measured, 19.8° of double amplitude pitch for a wave height of 6.9 m at a period of 12 sec. and an angle of inclination of -20.2 deg. towards column 5-6 (leeward damage in quartering seas).

7.0 CONCLUSIONS

Test results available to date (Huang et al. 1982, 1983; and Naess et al. 1985), showing heave and pitch only, have largely been limited to an idealized model at trim angles, in head seas with wave periods up to about 12.5 sec.

The present study, using a model similar in geometry and mass properties to an existing prototype, has provided complete six degrees of freedom motion response measurements over a full range of regular wave periods (7 to 25 sec.) for both even keel and damage conditions in each of head, beam and quartering seas. Damage conditions, simulating partial flooding/loss of buoyancy in one column, represented a somewhat realistic scenario considered in recent stability regulations.

Extreme care was taken to ensure correct calibration and accurate measurements in all aspects of the experiment. The model was designed and constructed to provide reliable watertight integrity at all seams and connections. Mass properties were established using accurate scales, machinist tools, accelerometers and a signal analyzer, and are reflected in the measured GM and natural periods. Each

spring and combination of springs in each mooring line were individually and collectively calibrated for correct stiffness and permissible stretch. The cantilever load cells were calibrated in-situ after each series of tests and monitored throughout the tests. All relative positions of model, mooring touchdown, and mooring termination points for each orientation were surveyed and marked prior to installation. These, and other efforts, resulted in accurate and reliable results using a 1/100 scale model that could be considered, by some, to be small.

The resulting comprehensive comparison of the time histories and RAO curves has provided a measure of the changes in motion response of a twin pontoon semisubmersible that can be expected relative to both severity and direction of damage. Small angles (Fig. 6.9) of inclination both windward and leeward produce only a small change in motion response relative to even keel operating draft. However, at larger angles (Fig. 6.10) with pontoons and deck piercing the water surface, significant changes do occur producing substantial increases in both roll and, particularly pitch, over two frequency bands: about the heave natural frequency (period of 18 to 25 sec.) and about twice the heave natural

frequency (periods of 9 to 13 sec. containing the subharmonic motions).

Pitch amplitude, although large over both frequency bands and in both windward and leeward damage, is consistently and substantially higher for leeward damage in waves of 9 to 13 sec. (e.g. RAO of 2.9 for a wave period of 12 sec. in quartering seas, Fig. 6.31). The occurrence and extent of the subharmonic resonance phenomenon in unidirectional and multidirectional irregular waves remains open to question. However, when considering an irregular sea state this frequency band would contain significant wave energy indicating the potentially critical nature of such a situation should it occur.

Progressive downflooding through intermittently submerged openings leading to capsizing becomes a real possibility. This would be of particular concern in semisubmersibles with an open deck structure and little, if any, reserve buoyancy. In order to meet recent changes to stability regulations (Sect. 1.0) many new designs, including the model tested, have incorporated a watertight box deck structure which provides significant reserve

buoyancy enabling the vessel to withstand high inclination angles before downflooding is reached.

Given the present inadequacies of existing mathematical techniques (Sect. 2.0) further work using rigid body modelling in realistic irregular seas is recommended. Such tests would provide additional insight into nonlinear effects particularly over the subharmonic or parametric resonance frequency band, thus further facilitating consideration of the problem in the design and operation of twin pontoon semisubmersibles.

REFERENCES

Adams, R., 1969, "Analysis of Spread Moorings by Dimensionless Functions", Proceedings of the Offshore Technology Conference, May 18-21, Houston, Texas, Paper No. OTC 1077.

Alexandrov, M., 1971, "On the Dynamics of Cables with Application to Marine Use", Marine Technology, January, pp. 84-92.

Bryant, F.A., 1983, "Floating Structures and Mooring Cable Systems - Industry Practice", Continuing Engineering Education Centre, Memorial University, Symposium on Offshore Mechanics and Cold Ocean Engineering, St. John's, Nfld.

Danforth, L.J., 1977, "Environmental Constraints on Drill Rig Configurations", Marine Technology, Vol. 14, No. 3, pp. 244-264.

Deb, M.K., "Statics and Dynamics of Tension Leg Platforms in Intact and Damaged Conditions", M.Eng. Thesis, In Preparation, Memorial University of Newfoundland.

DeSouza, P.M.E.M. and Miller, N.S., 1978, "The Intact and Damaged Stability Behaviour of Two Semisubmersible Models Under Wind and Wave Loading", Proceedings of the Offshore Technology Conference, May 8-11, Houston, Texas, Paper No. 3298.

El-Tahan, H.W., 1985, "Dynamic Response of a Hydroelastic Model of a Typical Semisubmersible to Waves and Bergy Bit Impact", Ph.D. Thesis, Memorial University of Newfoundland, May, 373 pp.

Gotaverken Arendal AB, 1984, "Outline Specification for a Semisubmersible Drilling Unit; GVA 4000", Jan. 2, Goteborg, Sweden.

Hammett, D.S., 1983, "Future Semisubmersible Drilling Units", Proceedings of the RINA International Symposium Semisubmersible: The New Generation, March 17-18, London.

Hoff, J., 1982, "Survey of Stability Rules for Mobile Platforms", Norwegian Hydrodynamics Laboratories, Trondheim, Norway, Report No. 182047.

Hsiung, C.C., 1984, "Computing Responses (Motions and Wave Loads) for Floating Marine Structures in Waves - A State-of-the-Art Review", Symposium on Computer Methods in Offshore Engineering, May 23-25, Halifax, N.S., pp. 99-139.

Huang, X., Hoff, J.R. and Naess, A., 1982, "On the Behaviour of Semisubmersible Platforms at Large Angles", Proceedings of the Offshore Technology Conference, May 3-6, Houston, Texas, Paper No. 4246.

Huang, X., Naess, A. and Hoff, J.R., 1983, "MOPS Subproject 03 - Theoretical Calculation of Platform Responses (MOPS Report No. 8)", Norwegian Hydrodynamics Laboratories, Trondheim, Norway, Report No. 183171.

Huse, E., Brevig, P., Furunes, I., Nedrelid, T., Thronsen, H.J., 1983, "OCEAN RANGER ModelTests", Sept., Norwegian Hydrodynamics Laboratories, Trondheim, Norway, Report No. 183275.

Huse, E. and Nedrelid, T., 1985, "Hydrodynamic Stability of Semisubmersibles Under Extreme Weather Conditions", Proceedings of the Offshore Conference, May 6-9, Houston, Texas, Paper No. 4987.

Jacobsson, P. and Dyne, G., 1983, "Reynolds Number Effects in Model Tests with a Four-Column Semisubmersible", Second International Symposium on Ocean Engineering and Ship Handling, Sept. 17-18, Gothenburg, Sweden, pp. 343-362.

Kallstrom, C.G., 1983, "Mooring and Dynamic Positioning of a Semisubmersible - A Comparative Simulation Study", Second International Symposium on Ocean Engineering and Ship Handling, Sept. 17-18, Gothenburg, Sweden, pp. 417-442.

Korkut, M.D. and Hebert, E.J., 1970, "Some Notes on Static Anchor Chain Curve", Proceedings of the Offshore Technology Conference, April 22-24, Houston, Texas, Paper No. 1160.

Laurich, P.H., 1984, "The Selspot System", National Research Council of Canada, Ottawa, Technical Report No. 23187.

Little, L., 1985, "Hardware and Software Modifications to Equipment at MUN Wave Tank", Memorial University of Newfoundland, Ocean Engineering Research Group, St. John's, Newfoundland.

Ljusne Katting AB, 1984, "Ljusne (Swedish) Anchor Chain", Ljusne, Sweden.

Lundgren, J. and Berg, A., 1982, "Wave Induced Motions on a Four-Column Semisubmersible Obtained from Model Tests", Proceedings of the Offshore Technology Conference, May 3-6, Houston, Texas, Paper No. 4230.

MacDuff, J.N. and Curreri, J.R., 1958, "Vibration Control", McGraw-Hill Book Co., Toronto.

Mathisen, J., Borresen, R. and Lindberg, K., 1982, "Improved Strip Theory for Wave-Induced Loads on Twin Hull Semisubmersibles", First Offshore Mechanics/Arctic Engineering/Deepsea Systems Symposium, May 7-10, New Orleans, Louisiana, Vol. 1, pp. 1-9.

Mathisen, J., and Carlsen, C.A., 1980, "A Comparison of Calculations Methods for Wave Loads on Twin Pontoon Semisubmersibles", International Symposium on Ocean Engineering and Ship Handling, Sept. 17-18, Gothenburg, Sweden, pp. 7.1-7.23.

McTaggart, R.G., 1976, "Offshore Mobile Drilling Units", The Technology of Offshore Drilling, Completion and Production, Petroleum Publishing Co., Tulsa, pp. 3-32.

Mogridge, G.R., 1984, "A Hydrodynamic Model Study of the Mobile Offshore Drilling Unit "Ocean Ranger", Vol. 1", National Research Council of Canada, Ottawa, Canada, Report No. CTR-HY-001, 318 pp.

Morland, M., Uliborg, J., Lotveit, S.A. and Sigurdsen, M., 1985, "Floating Stability and Seaworthiness - Trends and Development", Proceedings of the International Conference on Behaviour of Offshore Structures, Amsterdam, pp. 187-194.

Muggeridge, D.B. and Murray, J.J., 1981, "Calibration of a 58 m Wave Flume", Canadian Journal of Civil Engineering, Vol. 8, pp. 4[illegible]-455.

Naess, A. and Hoff, J.R., 1984, "Time Simulation of the Dynamic Response of Heavily Listed Semisubmersible Platforms in Waves", Norwegian Maritime Research, Vol. 12, No. 1, pp. 2-14.

Naess, A., Hoff, J.R. and Herfjord, K., 1985, "Modelling of the Dynamic Behaviour of Damaged Platforms by Time Simulation Methods and Model Tests", Proceedings of the International Conference on Behaviour of Offshore Structures, Amsterdam, pp. 195-203.

Naval Architect, 1981, "GVA 4000 - and the New 2000", Sept., pp. E211-E213.

Norwegian Maritime Directorate, 1983, "Mobile Drilling Platforms, Regulations Laid Down by Norwegian Official Control Institutions", Oslo, Norway.

Numata, E., Michel, W.H., McClure, A.C., 1976, "Assessment of Stability Requirements for Semisubmersible Units", SNAME Transactions, Vol. 84, pp. 56-74.

Price, W.G. and Wu, Y., 1983, "Hydrodynamic Coefficients and Responses of Semisubmersibles in Waves", Second International Symposium on Ocean Engineering and Ship Handling, Sept. 17-18, Gothenburg, Sweden, pp. 393-414.

Praught, M.W., Hammett, D.S., Hampton, J.B. and Springett, C.N., 1985, "Industry Action on Stability of Mobile Offshore Drilling Units: A Status Report", Proceedings of the Offshore Technology Conference, May 6-9, Houston, Paper No. 4986.

Rodnight, T.V., 1983, "Development of the Modern Semisubmersible Drilling Unit", Proceedings of the RINA International Symposium Semisubmersibles: The New Generations, March 17-18, London.

Rothwell, A., 1979, "A Graphical Procedure for the Stiffness of a Catenary Mooring", Journal of Applied Ocean Research, Vol. 1, Nov. 4, pp. 217-219.

Royal Commission on the OCEAN RANGER Marine Disaster, 1984, "Report One: The Loss of the Semisubmersible Drill Rig OCEAN RANGER and its Crew", Aug., St. John's, Newfoundland, 400 pp.

Springett, C.N. and Praught, M.W., 1986, "Semisubmersible Design Considerations - Some New Developments", Marine Technology, Vol. 23, No. 1, pp. 12-22.

Takagi, M., Arai, S., Takezawa, S., Tanaka, K., and Takarada, N., 1985, "A Comparison of Methods for Calculating the Motion of a Semisubmersible", Journal of Ocean Engineering, Vol. 12, No. 1, pp. 45-97.

TABLES

TABLE 3.1 PRINCIPAL CHARACTERISTICS OF PROTOTYPE AND MODEL

Dimensions			
Pontoon			
	Length		80.56 m
	Width		16.00 m
	Height		7.50 m
	Bilge radius		1.35 m
Column			
	Diameter		12.90 m
	Transverse/Longitudinal spacing, C-C		54.72 m
Brace			
	Diameter		2.06 m
	Height C above keel		11.20 m
Deck			
	Lower Deck	Length	54.72 m
		Beam	54.72 m
	Tween Deck	Length	62.32 m
		Beam	54.72 m
	Main Deck	Length	67.00 m
		Beam	57.50 m
Height			
	Keel to Lower Deck		33.00 m
	Keel to Main Deck		41.00 m

	Prototype	Model (1:100)
Draught (operational)	20.50 m	20.50 m
Displacement (operational)	24,860 m^3 [1]	24,368 m^3
CG from Keel	20.05 m	20.97 m
GM	2.4 m	2.4 m

Natural Periods	Freefloating	Moored	Freefloating	Moored
Heave	21 sec.	21 sec.	21 sec.	21 sec.
Pitch	41	36	41	37
Roll	50	43	52	46
Surge		73		
Sway		89		

Radius of Gyration		
pitch (about y-axis)	~~27.3 m~~	27.8 m
roll	29.6 m	29.2 m

[1] Calculated from geometry. Cotaverken Arendal (1984) gives a displacement of 25,835 tonnes (25,205 m^3)

TABLE 3.2 FROUDE SCALE FACTOR FOR 1:100 SCALE MODEL

Parameter	Scale Law	For 1:100 Model
Length	$\lambda_l = 100.0$	100.0
Velocity	$\lambda_v = \sqrt{\lambda_l}$	10.0
Acceleration	$\lambda_a = 1.0$	1.0
Time	$\lambda_t = \sqrt{\lambda_l}$	10.0
Density	$\lambda_\rho = 1.025$	1.025
Force	$\lambda_f = 1.025\lambda_l^3$	1,025,000

TABLE 6.1 SUMMARY OF MEASURED MODEL TEST CONDITIONS

Orientation	wt./column (tonnes)	Heel/Trim (deg.)[2]	Angle Inclination towards/Column (deg.)[3]
Head	-	+0.4/+0.5	-0.6/3-4
	500/7-8	-8.2/-8.2	+11.6/7-8
	1000/7-8	-13.5/-13.8	+19.5/7-8
	500/5-6	-8.3/+9.0	-12.3/5-6
	1000/5-6	-13.0/+14.3	-19.5/5-6
Beam	-	+0.1/+0.5	+0.4/3-4
	500/1-2	+8.9/-8.6	+12.4/1-2
	1000/1-2	+14.5/-13.9	+20.5/1.2
	500/7-8	-8.6/-8.3	-12.0/7-8
	1000/7-8	-14.2/-13.6	-19.9/7-8
Quartering	-	+0.2/+0.3	±0.4/3-4
	500/1-2	+9.0/-8.2	+12.2/1-2
	1000/1-2	+14.6/-13.6	+20.2/1-2
	500/5-6	-8.5/+9.9	-13.1/5-6
	1000/5-6	-13.5/+14.7	-20.2/5-6

[2]Sign convention follows right hand rule

[3]Positive angle corresponds to inclination towards the waves (windward damage). Negative angle corresponds to inclination away from the waves (leeward damage).

TABLE 6.2 SUMMARY OF TEST CONDITIONS PRODUCING SUBHARMONIC EFFECT

Orientation	Wave Period (sec.)	Angle of Inclination Towards/Column (deg.)
Head	10	+19.5/7-8
	11	
	12	
	9	-19.5/5-6
	10	
	11	
	12	
	13	
Beam	10	+20.5/1-2
	11	
	12	
	9	-19.9/7-8
	10	
	11	
	12	
Quartering	10	+20.2/1-2
	11	
	12	
	11	-20.2/5-6
	12	
	13	
	14	

FIGURES

Fig. 3.1 Four Column, Twin Pontoon Semisubmersible Drilling Unit; GVA 4000

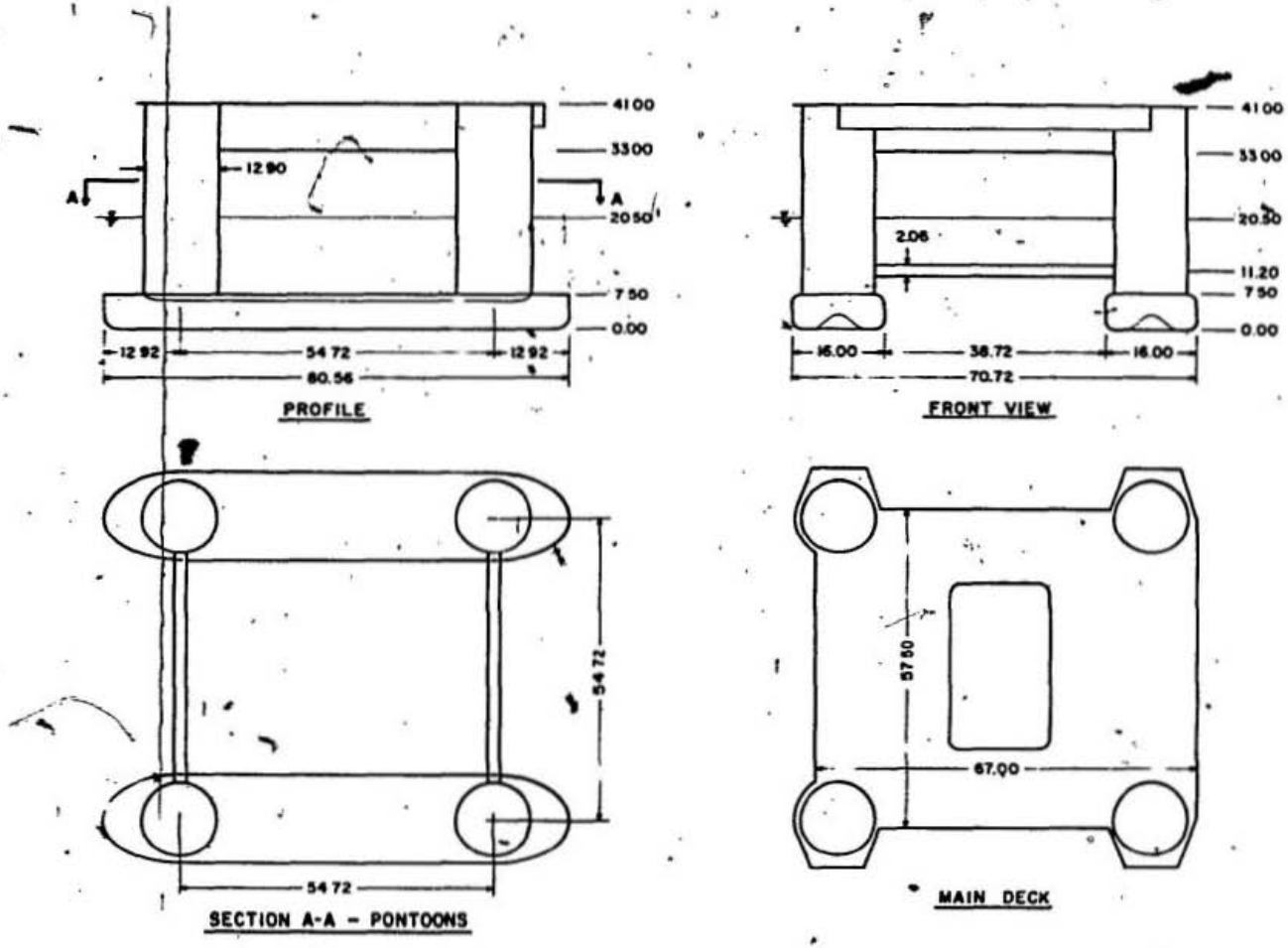

Fig. 3.2 1/100 Scale Model, General Arrangement

Fig. 3.3 1/100 Scale Model, During Construction

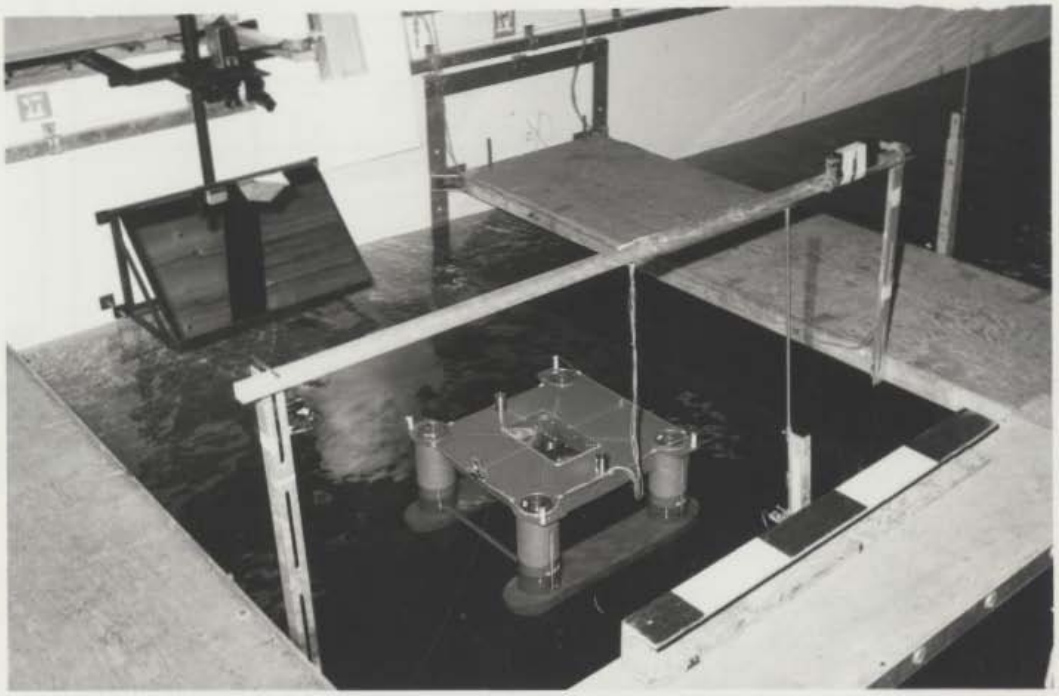

Fig. 3.4 1/100 Scale Model, Head Sea, Even Keel

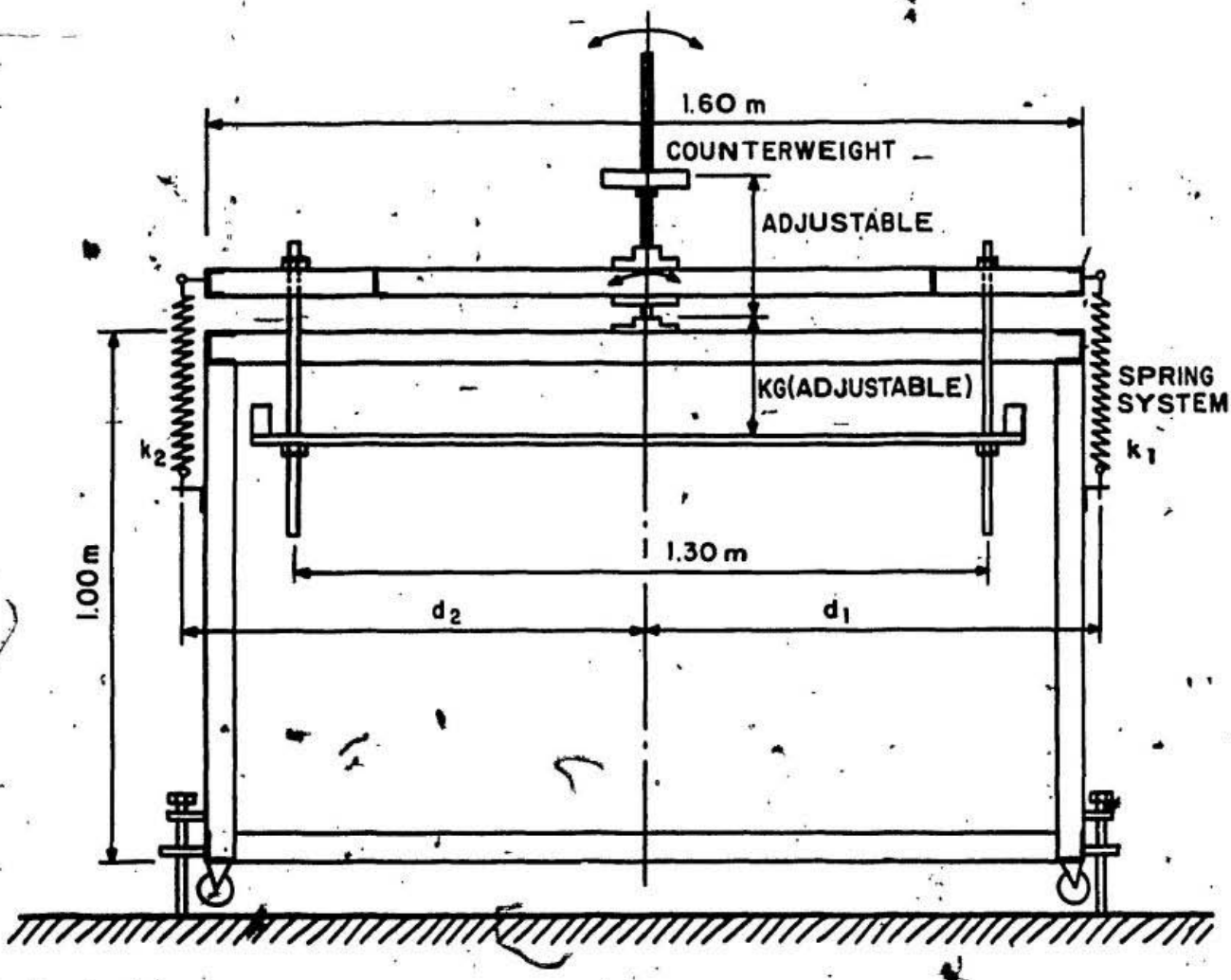

Fig. 3.5 Tilting Platform

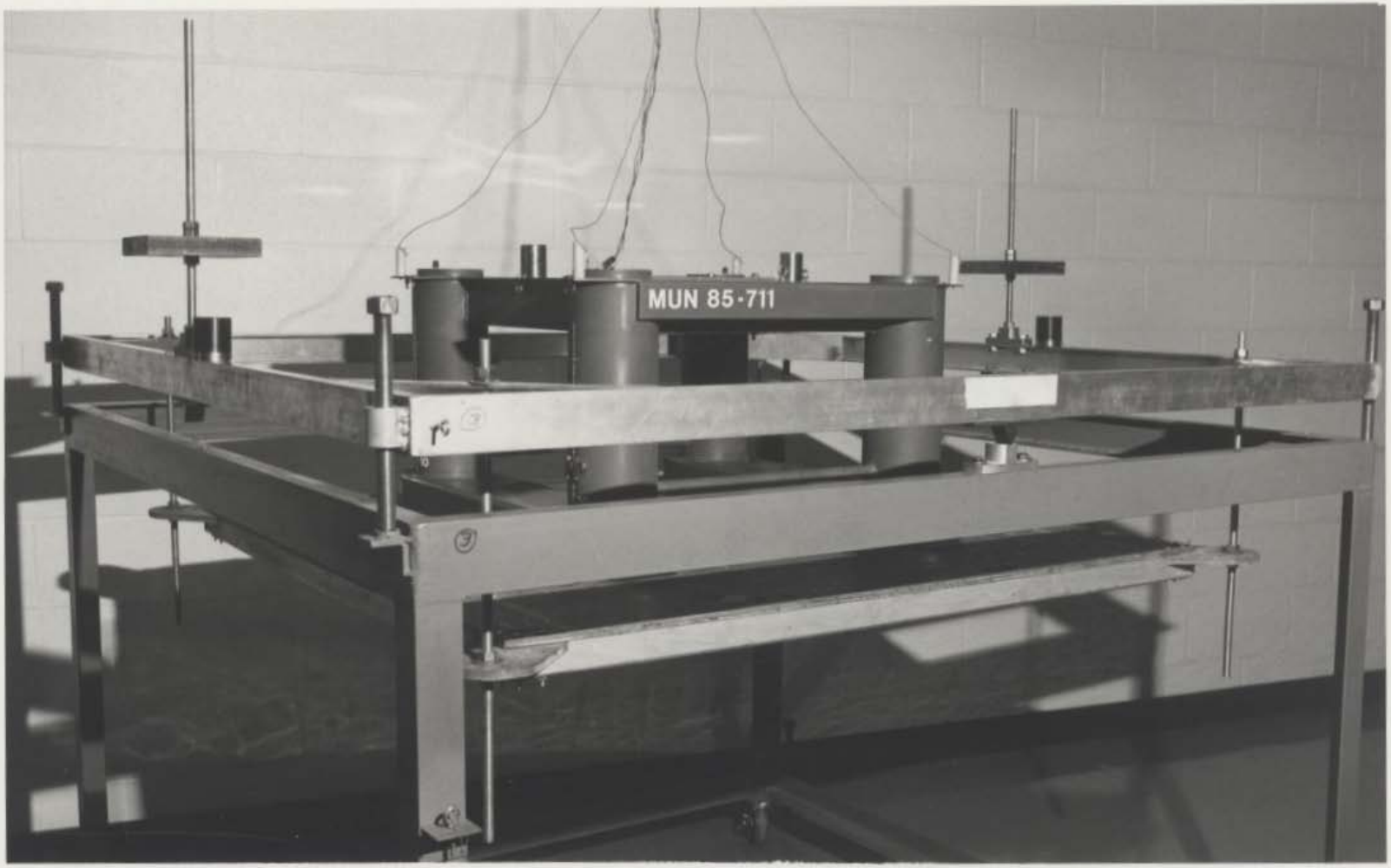

Fig. 3.6 Tilting Platform With Model

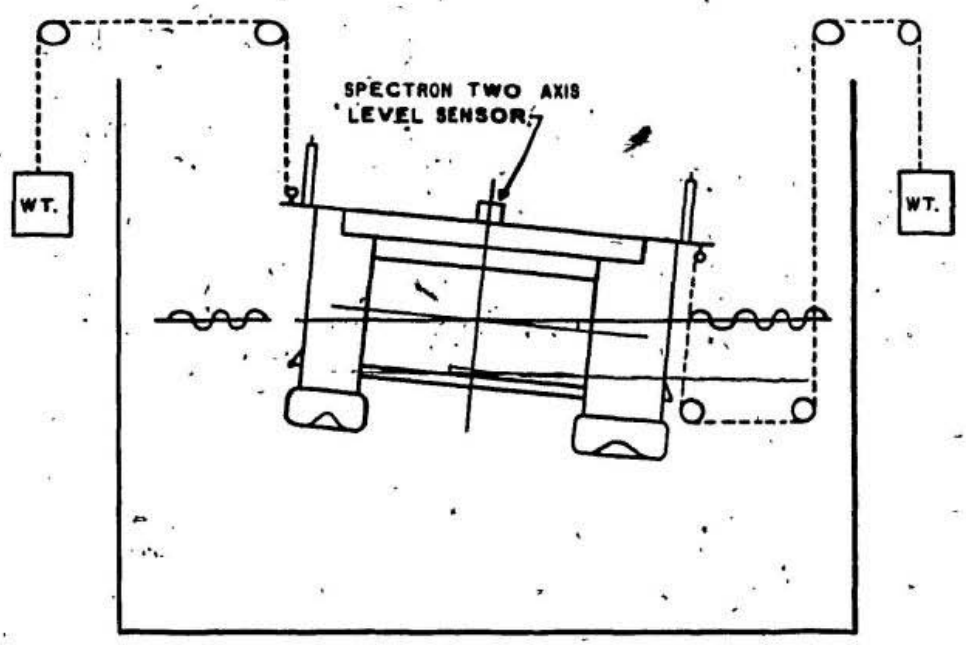

Fig. 3.7 Inclining Experimental Arrangement

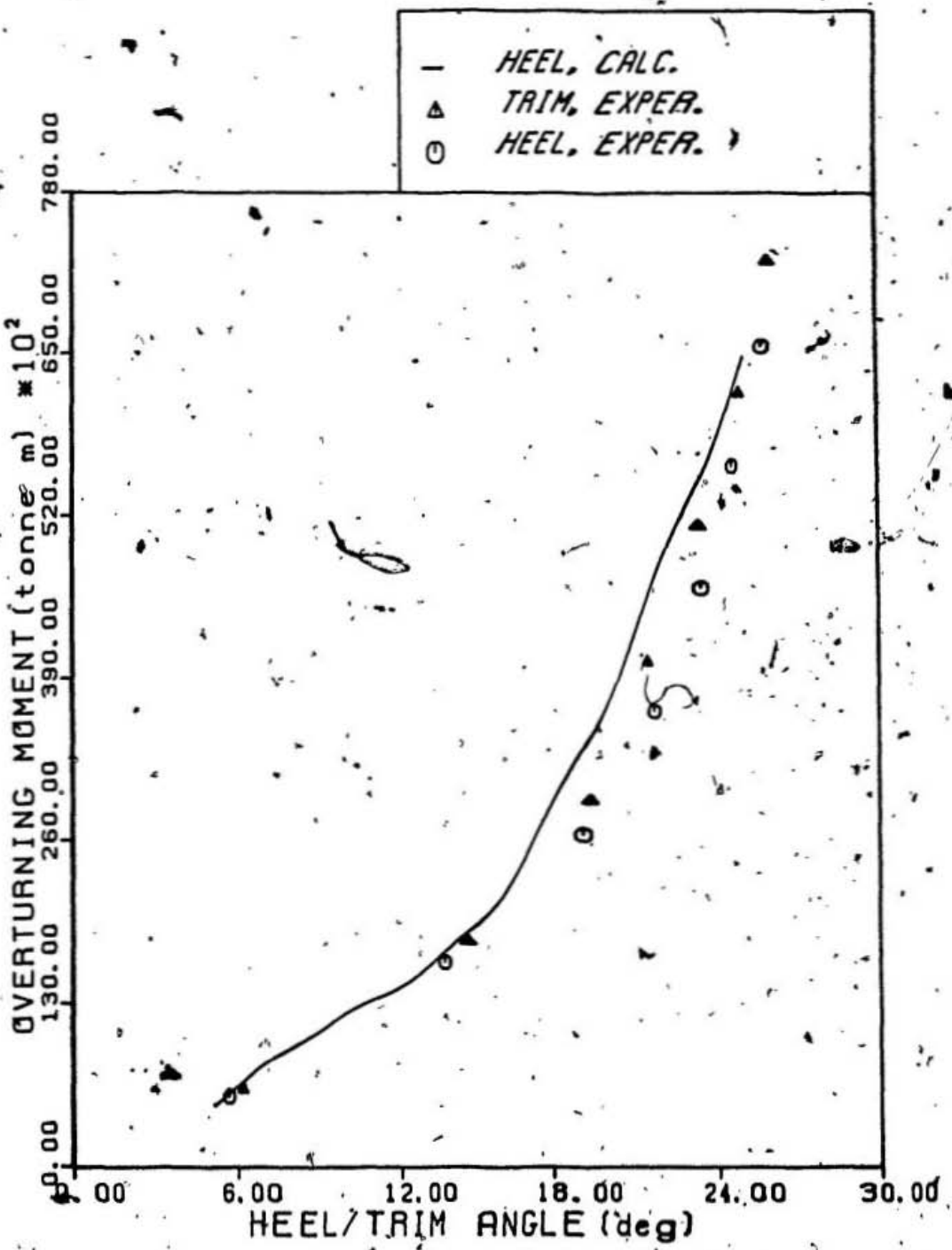

FIG. 3.8 STATIC STABILITY CURVE

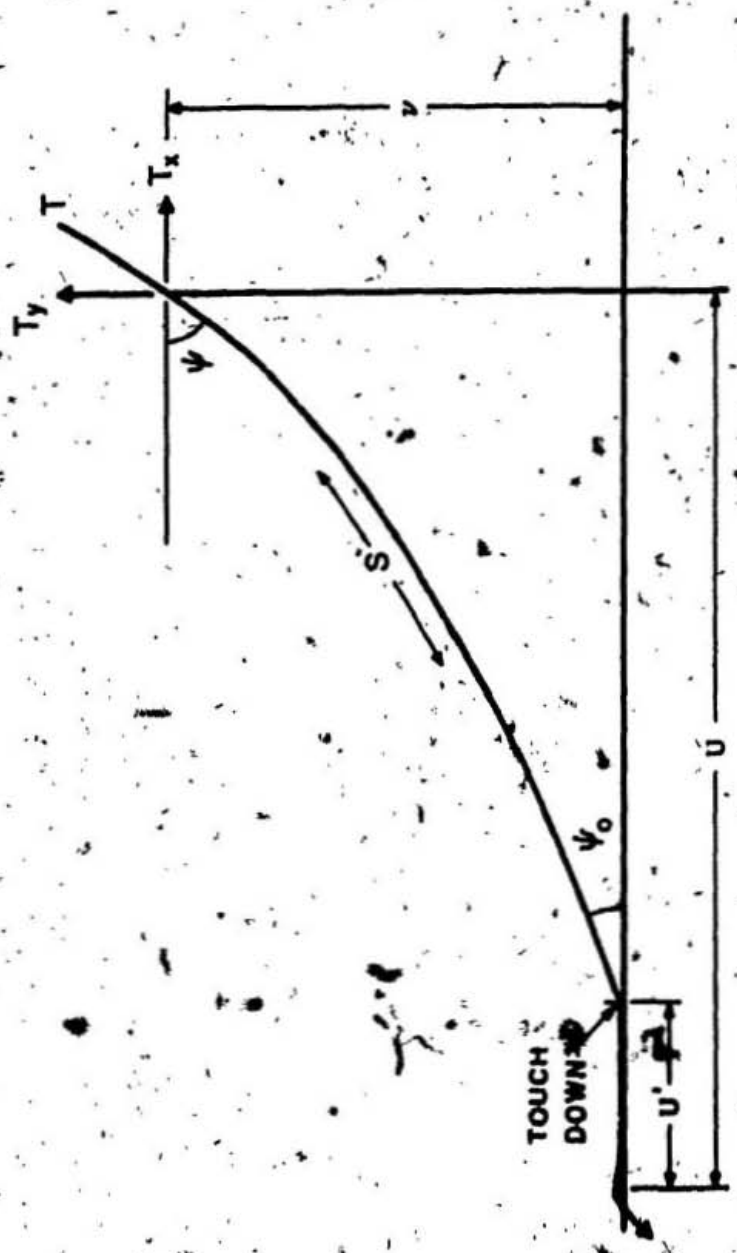

FIG. 4.1 PROTOTYPE MOORING ANALYSIS

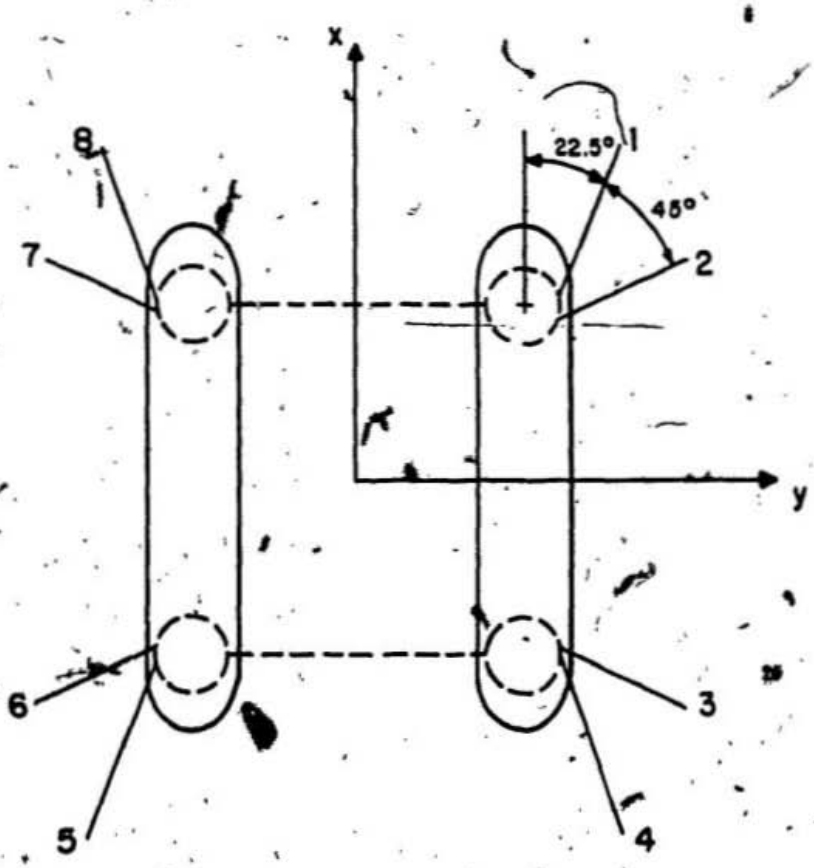

FIG. 4.2 MOORING CONFIGURATION

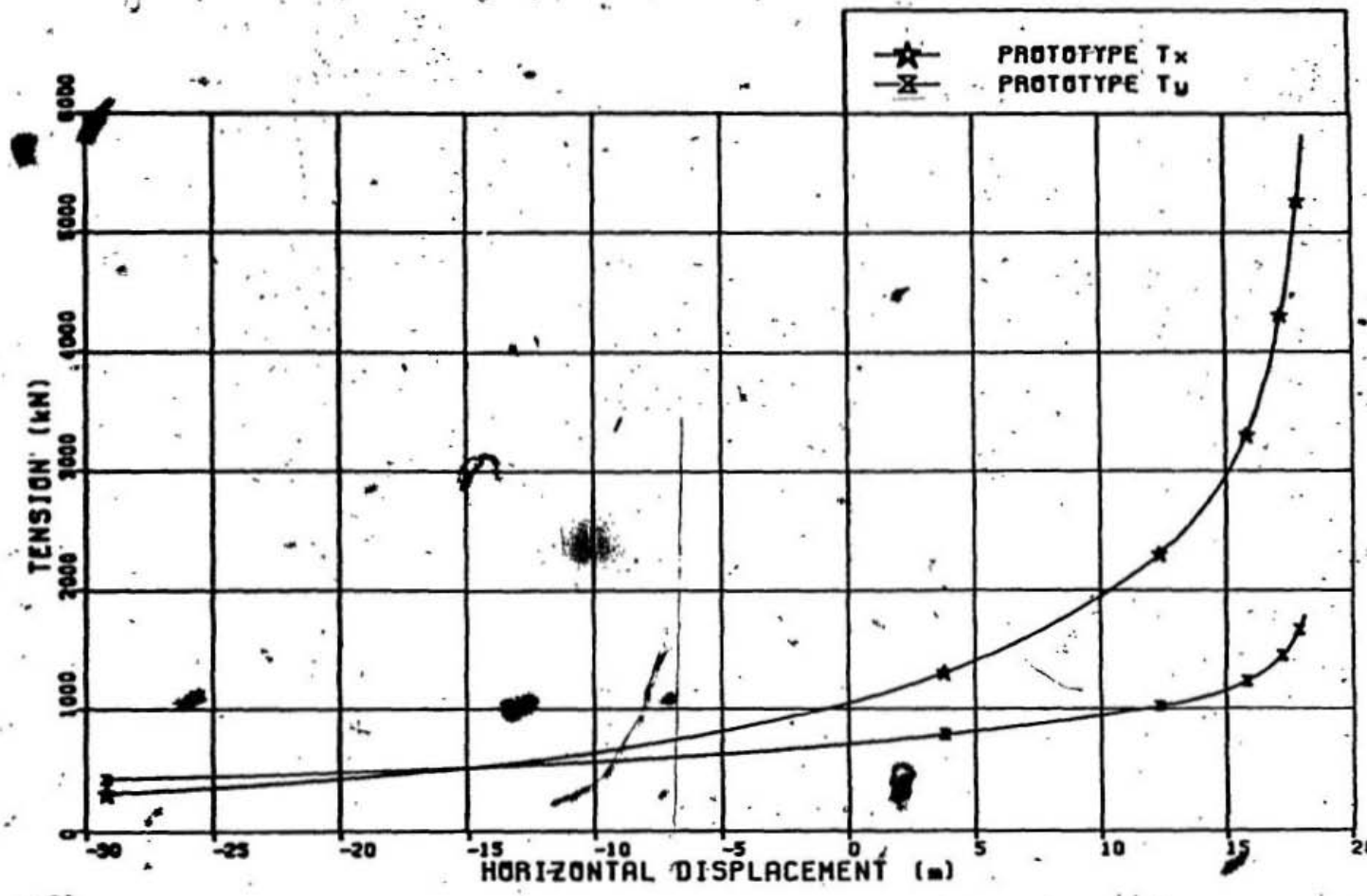

FIG. 4.3 PROTOTYPE MOORING; LINE TENSION AS A FUNCTION OF HORIZONTAL EXCURSION

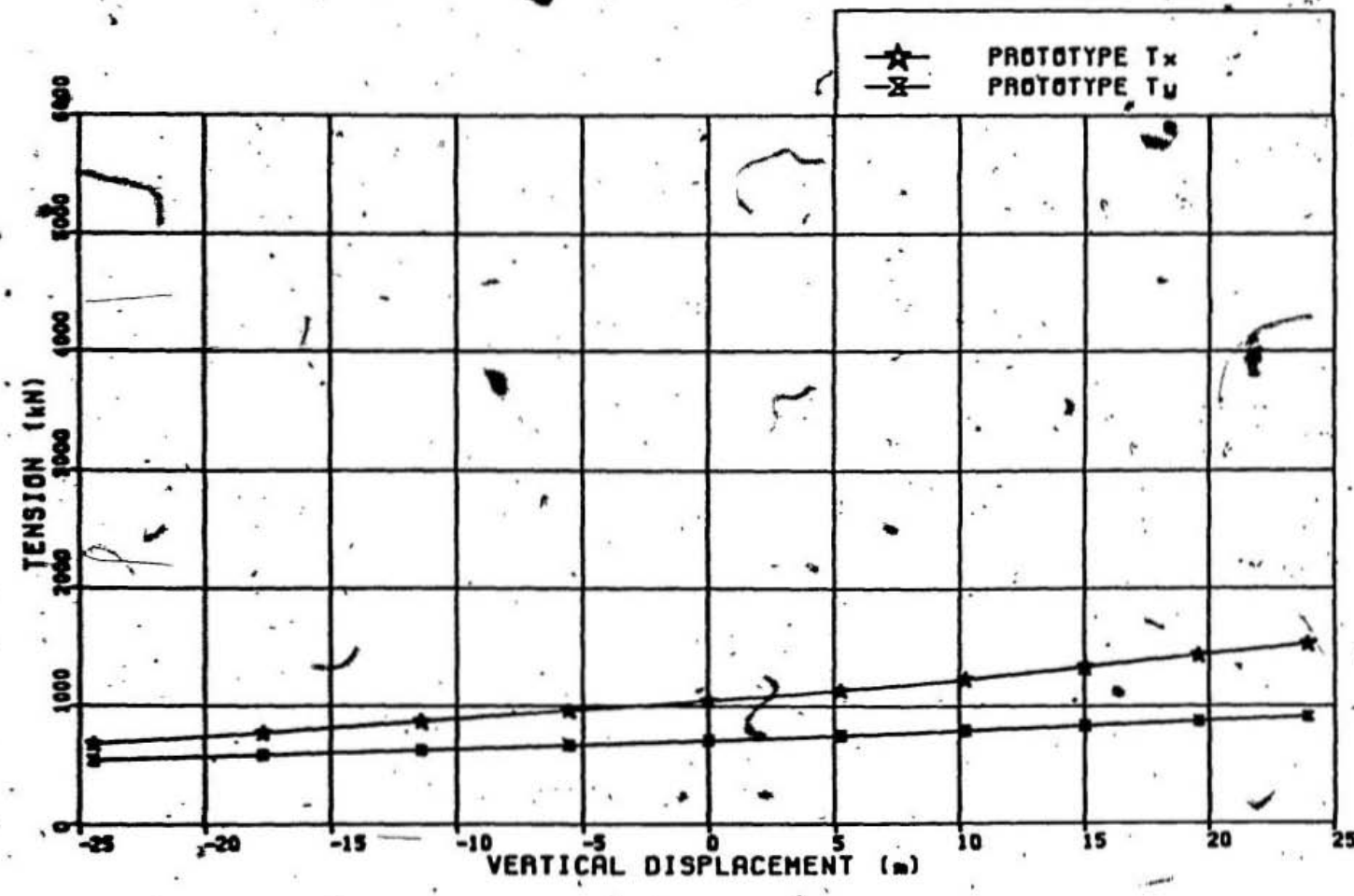

FIG. 4.4 Prototype Mooring; Line Tension as a Function of Vertical Excursion

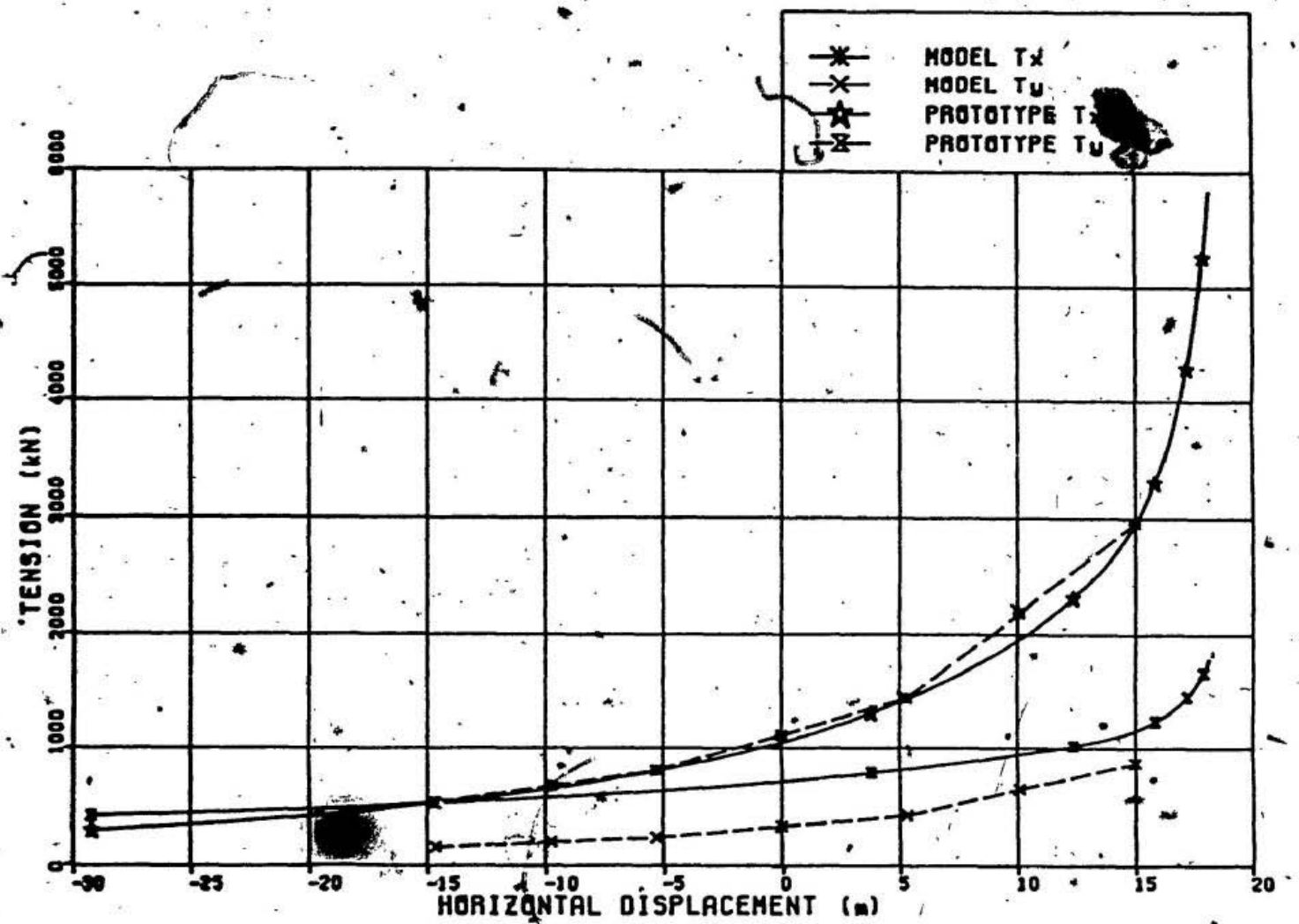

FIG. 4.5 Model Mooring; Line Tension as a Function of Horizontal Excursion

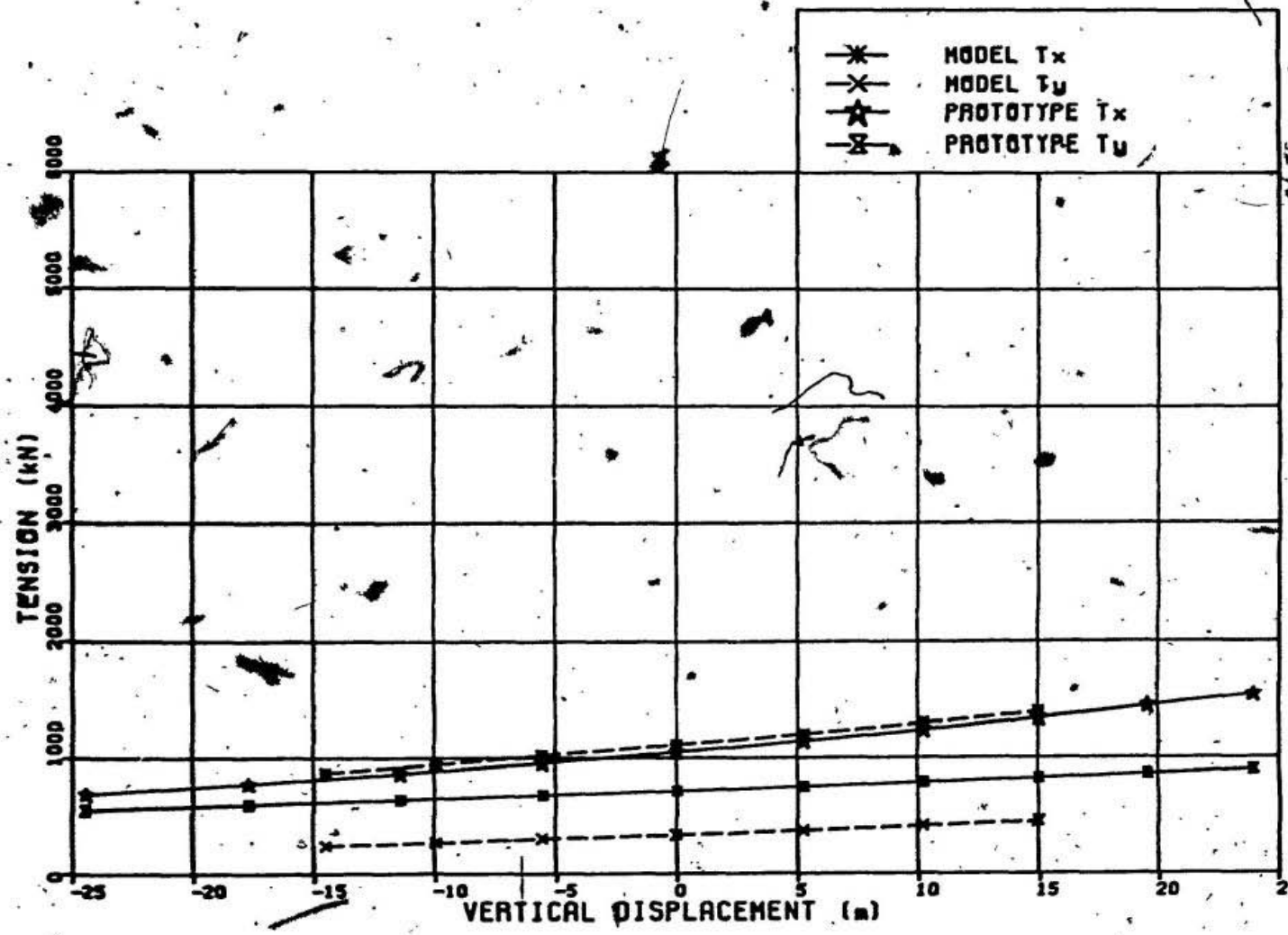

FIG. 4.6 Model Mooring; Line Tension as a Function of Vertical Excursion

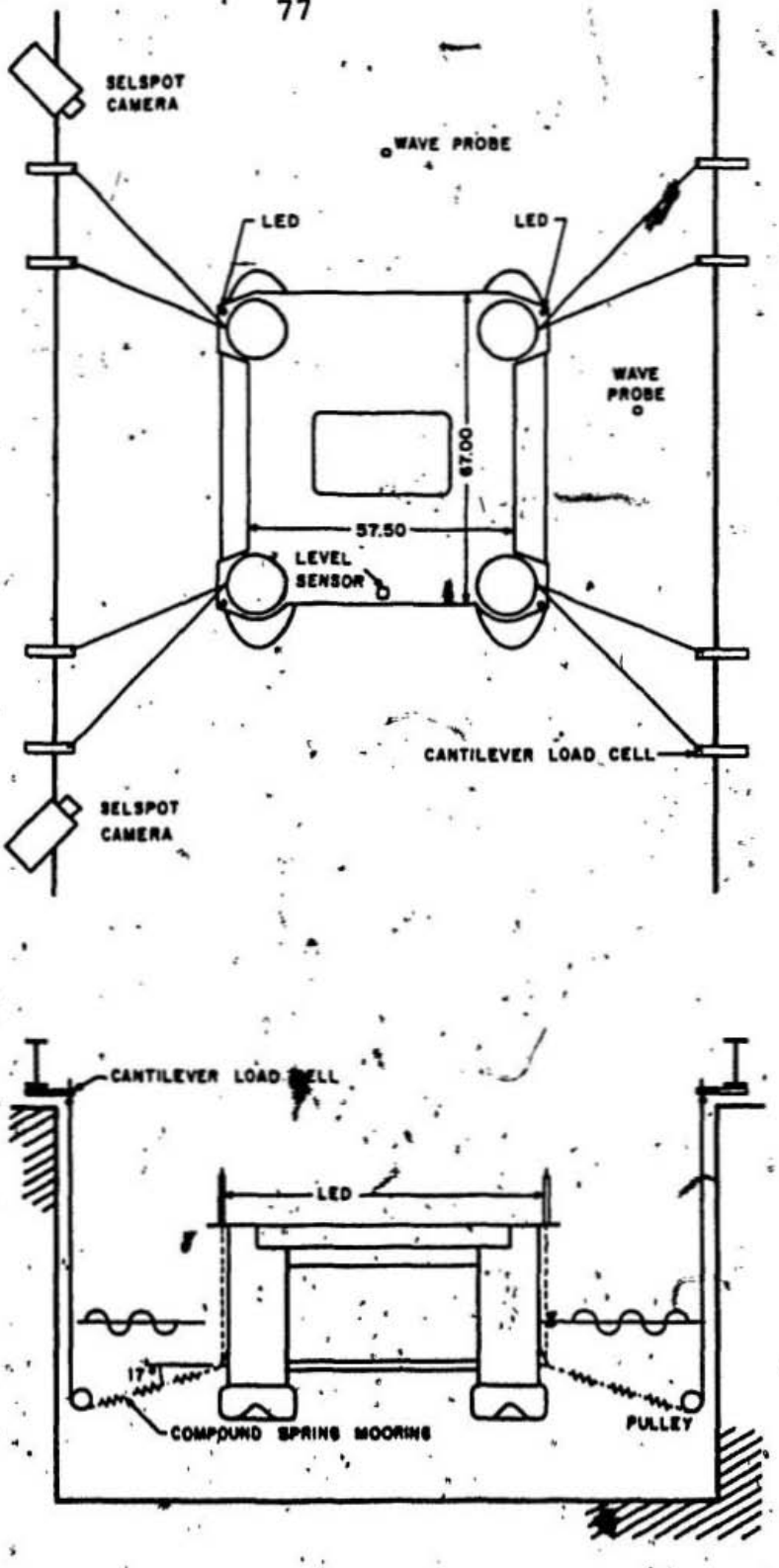

Fig. 5.1 Experimental Arrangement

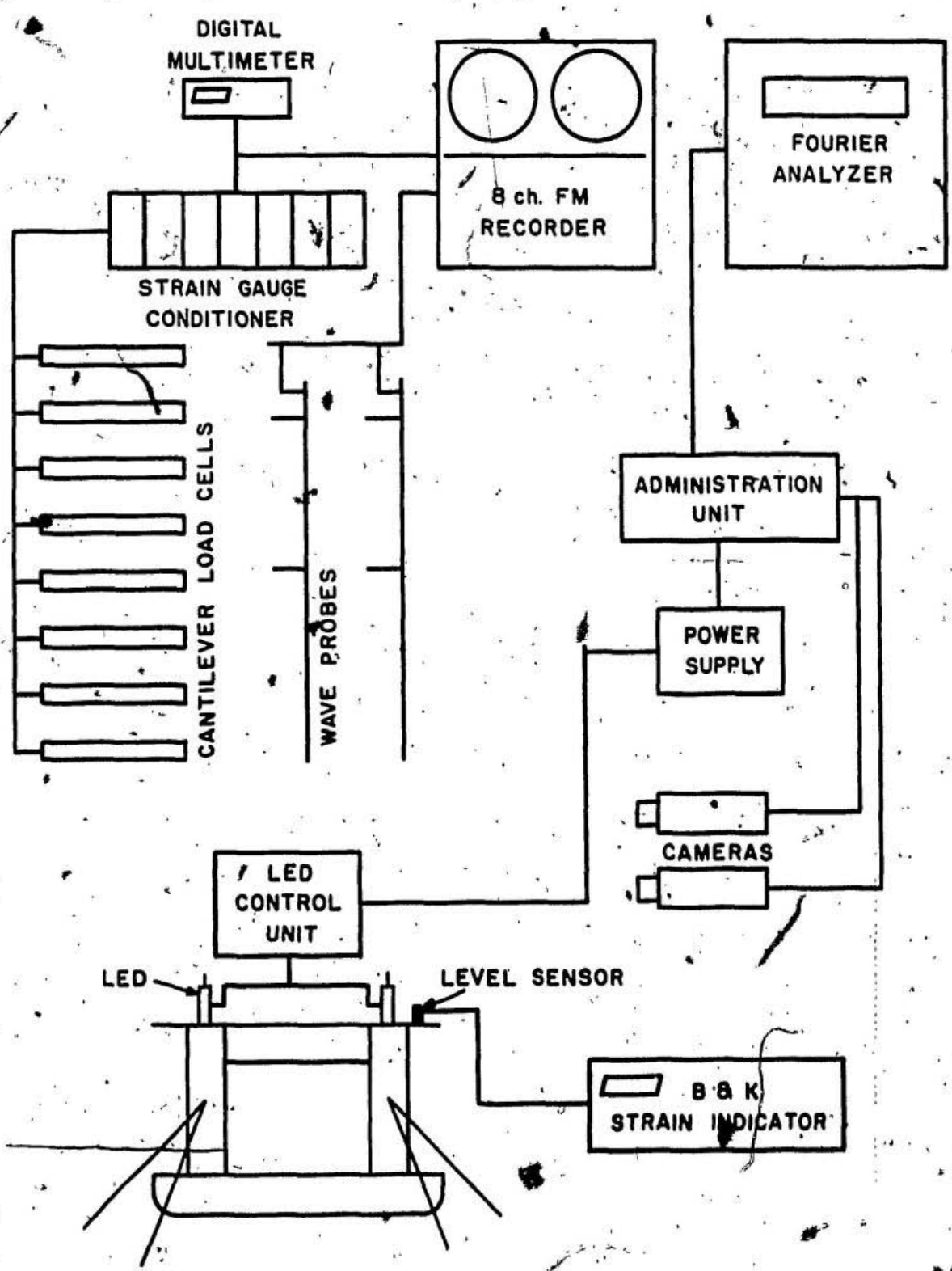

FIG. 5.2 INSTRUMENTATION AND DATA RECORDING SYSTEM

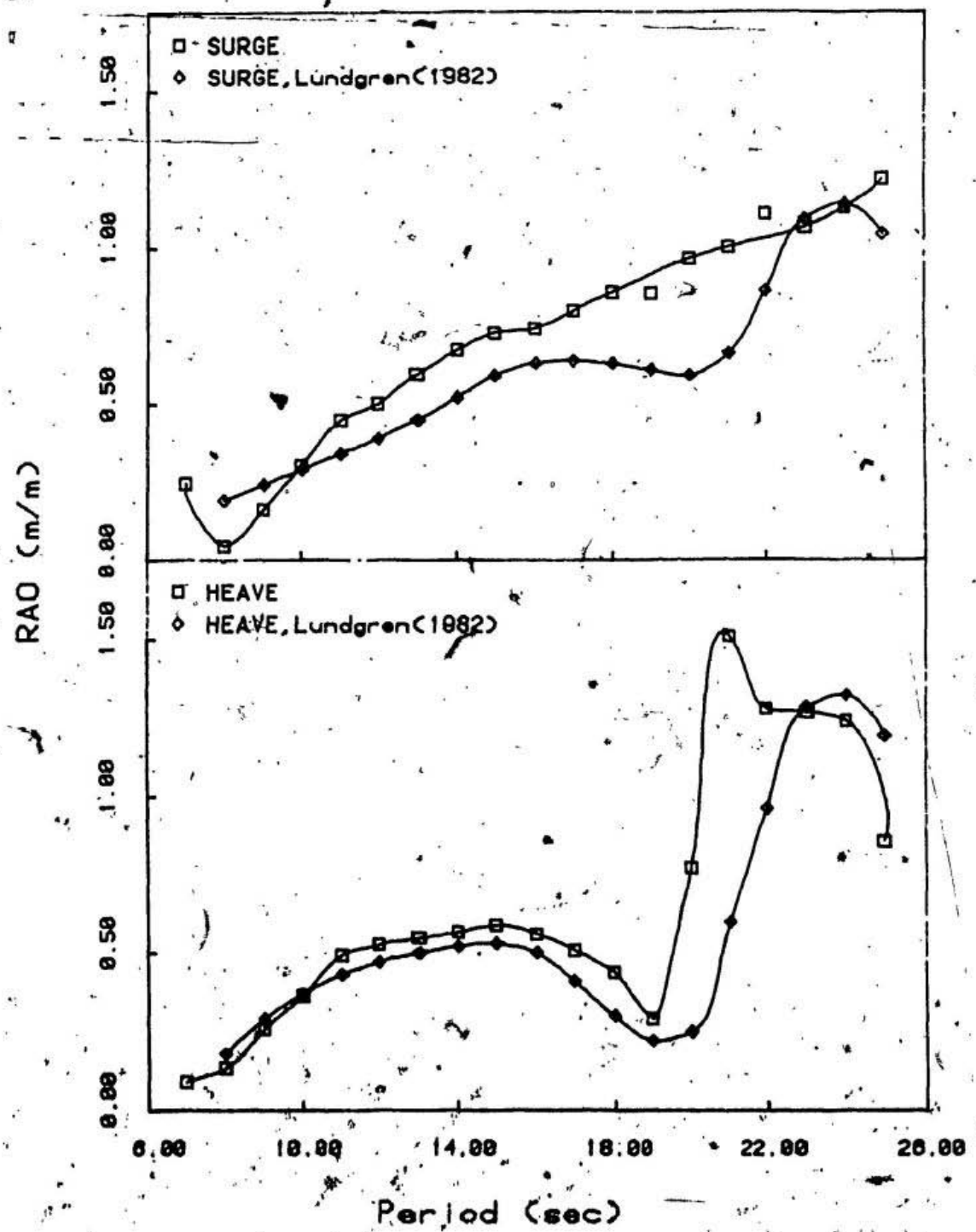

FIG. 6.1 HEAD SEA, EVEN KEEL, OPERATING DRAFT, SURGE AND HEAVE

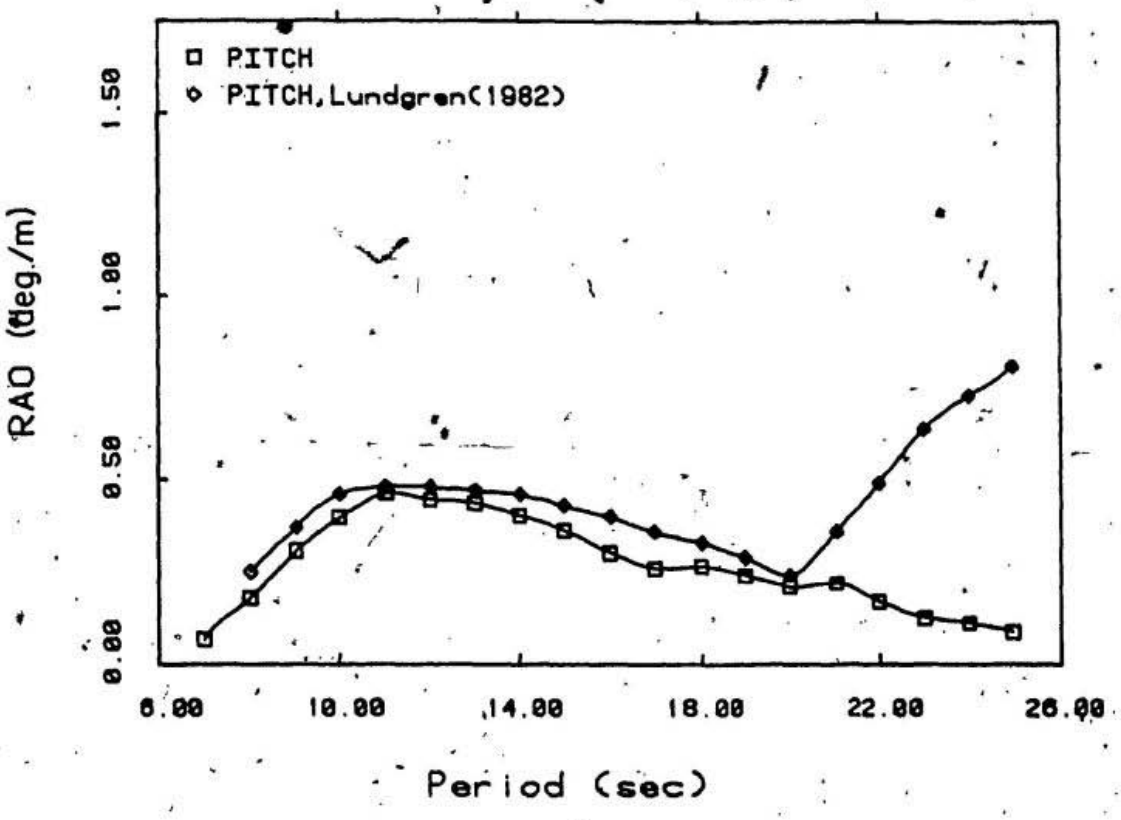

FIG. 6.2 HEAD SEA, EVEN KEEL, OPERATING DRAFT; PITCH

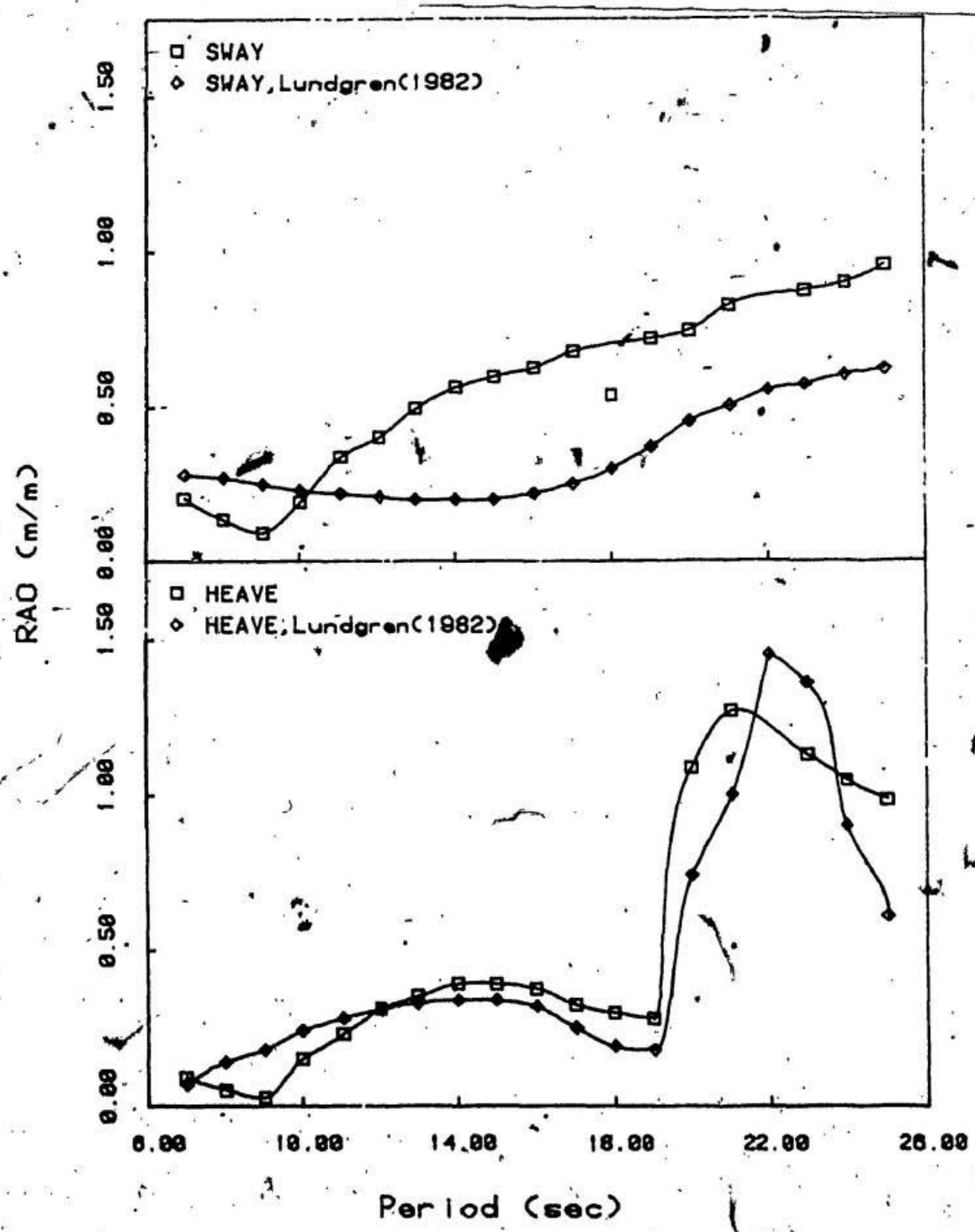

FIG. 6.3 BEAM SEA, EVEN KEEL, OPERATING DRAFT; SWAY AND HEAVE

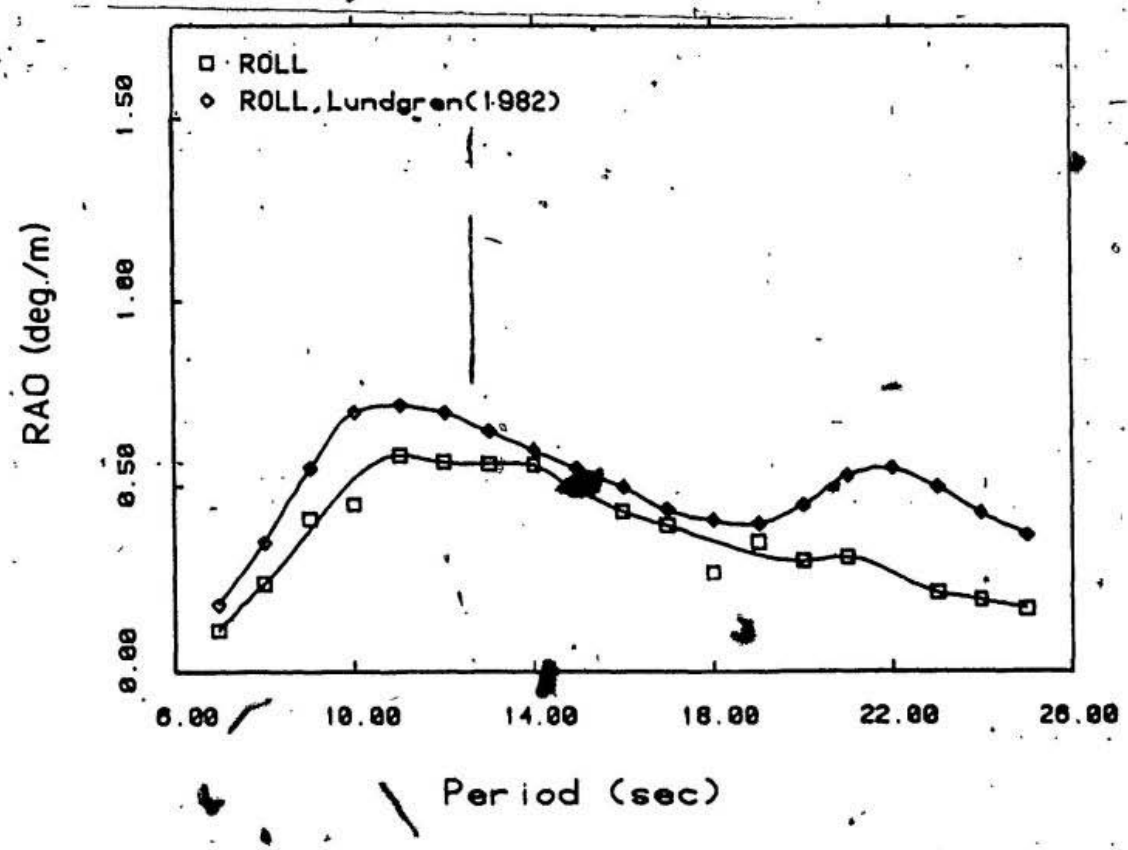

FIG. 6.4 BEAM SEA, EVEN KEEL, OPERATING DRAFT; ROLL

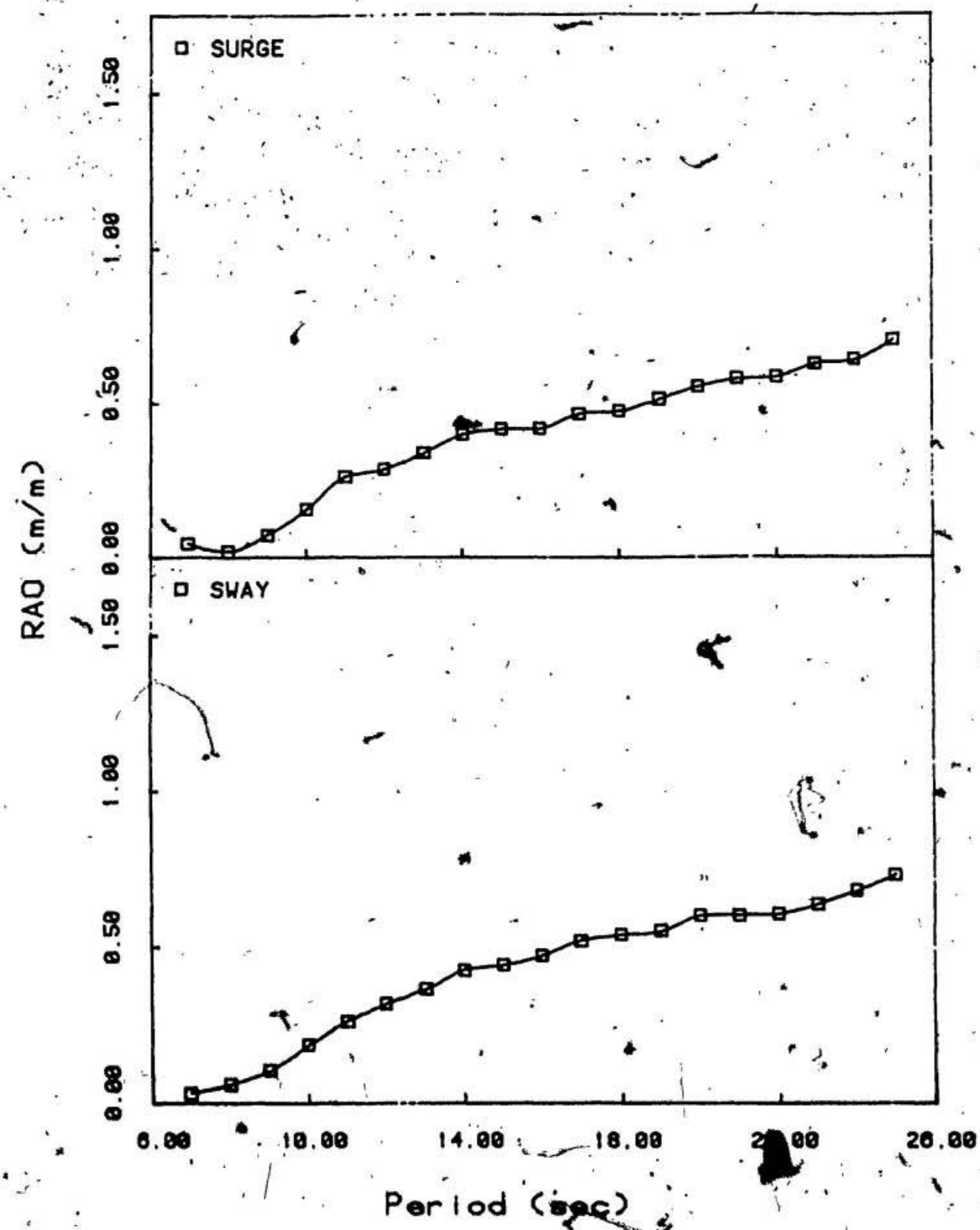

FIG. 6.5 QUARTERING SEA, EVEN KEEL, OPERATING DRAFT; SURGE AND SWAY

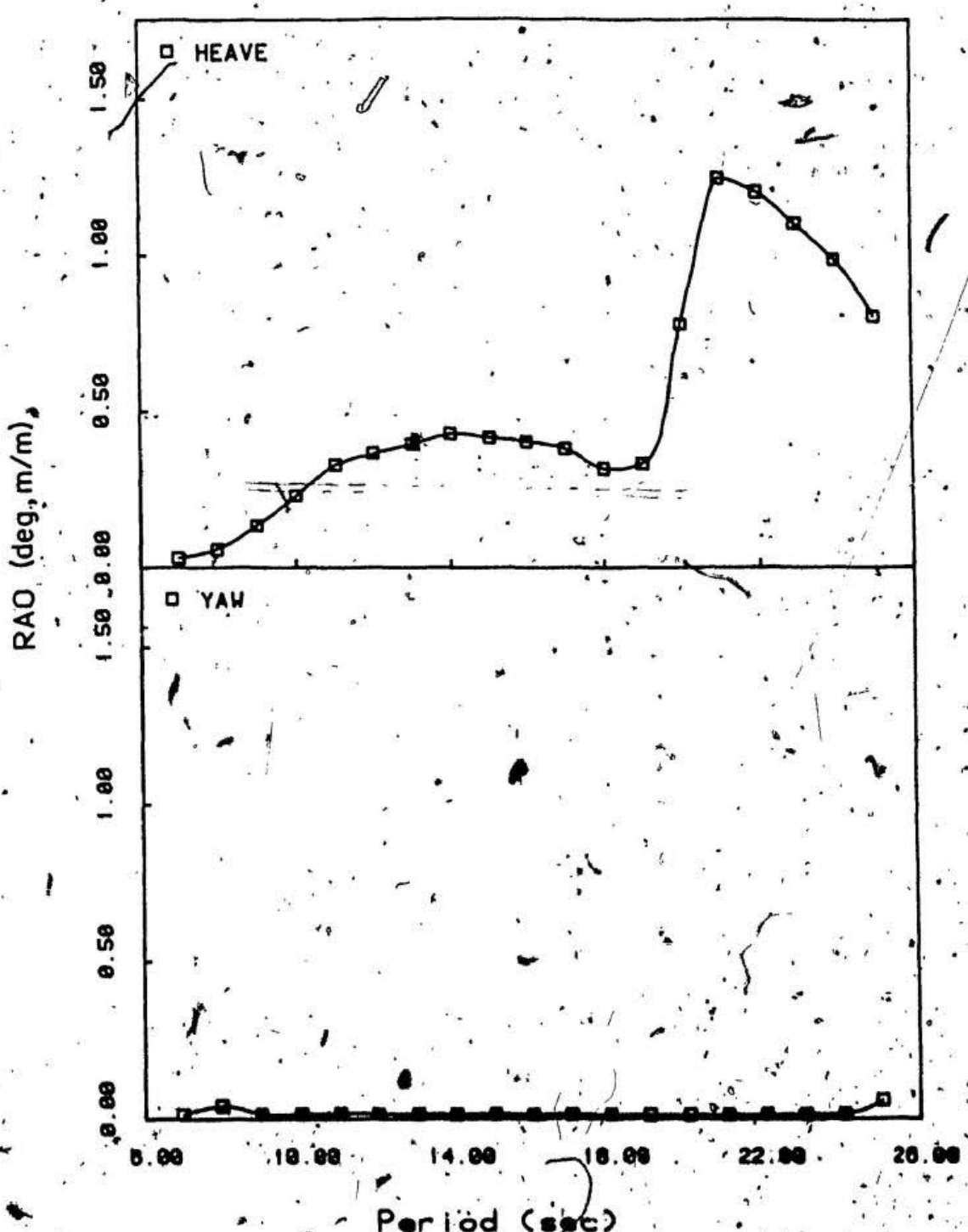

FIG. 6.6 QUARTERING SEA, EVEN KEEL, OPERATING DRAFT; HEAVE AND YAW

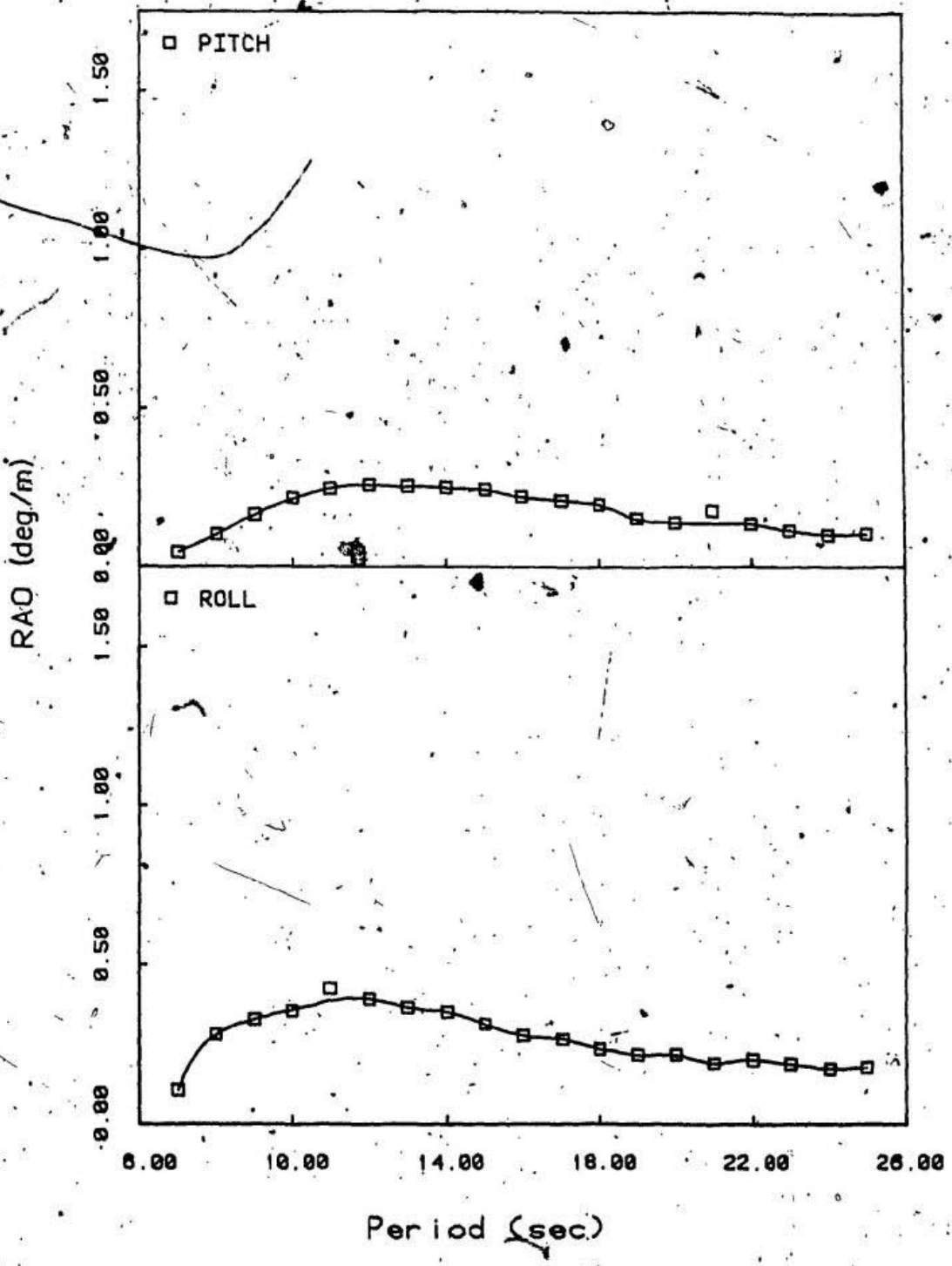

FIG. 6.7 QUARTERING SEA, EVEN KEEL, OPERATING DRAFT; PITCH AND ROLL

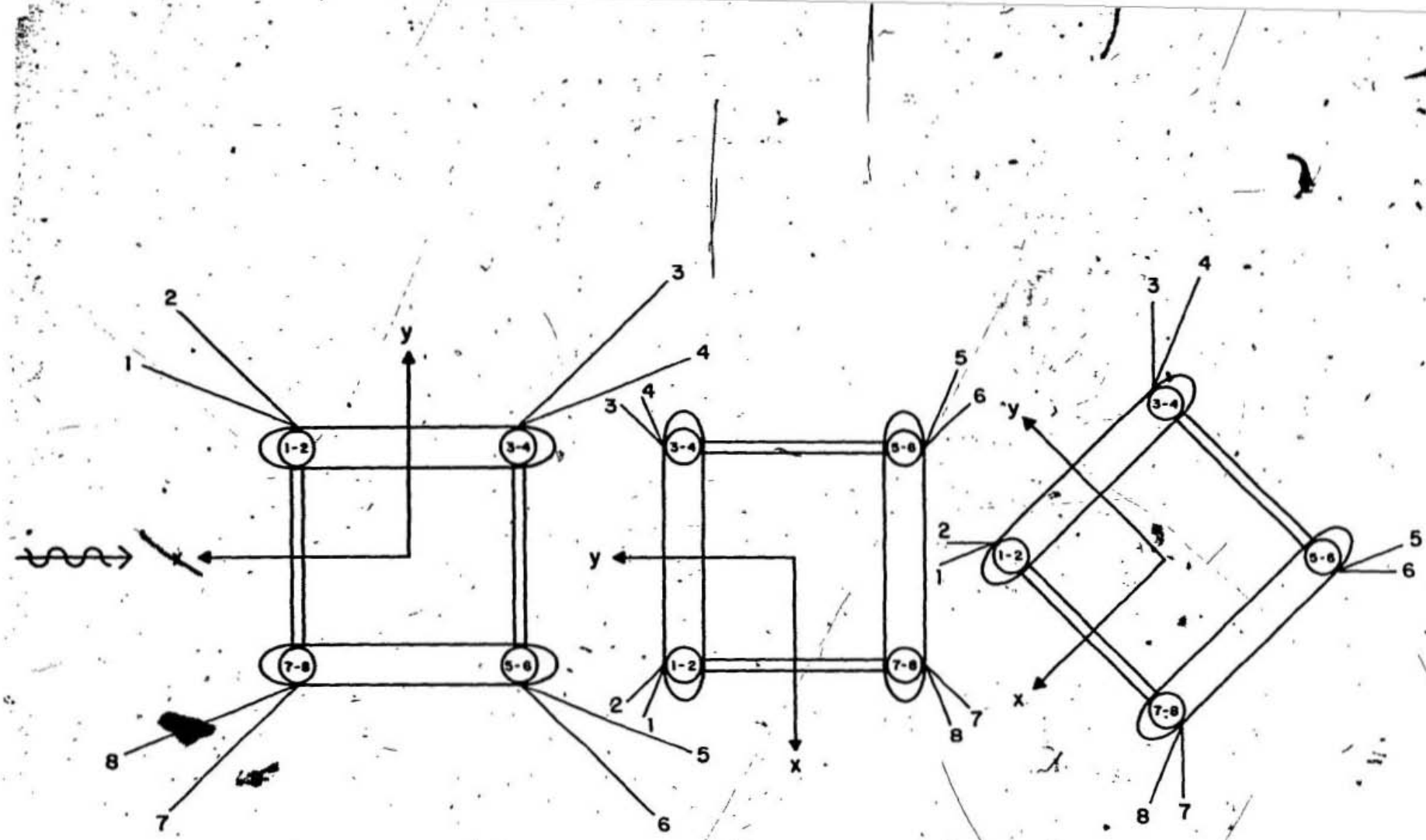

FIG. 6.8 MODEL ORIENTATIONS DURING TESTING

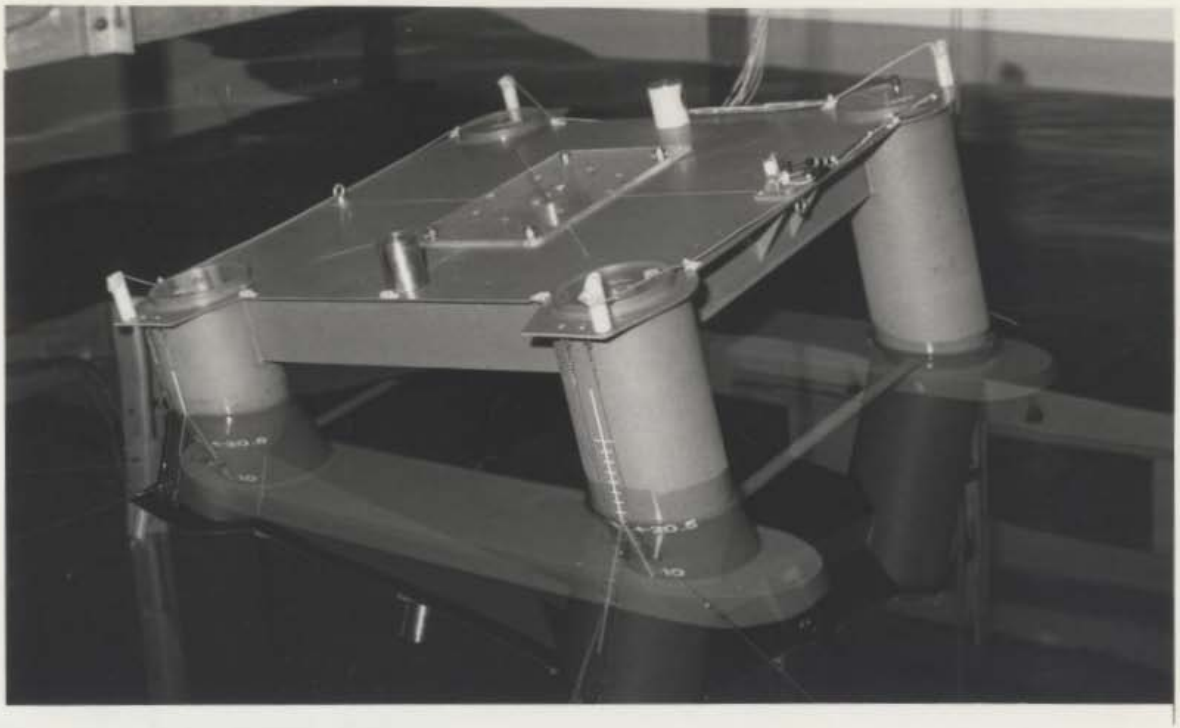

Fig. 6.9 Head Sea, Damage Condition +11.6 deg.

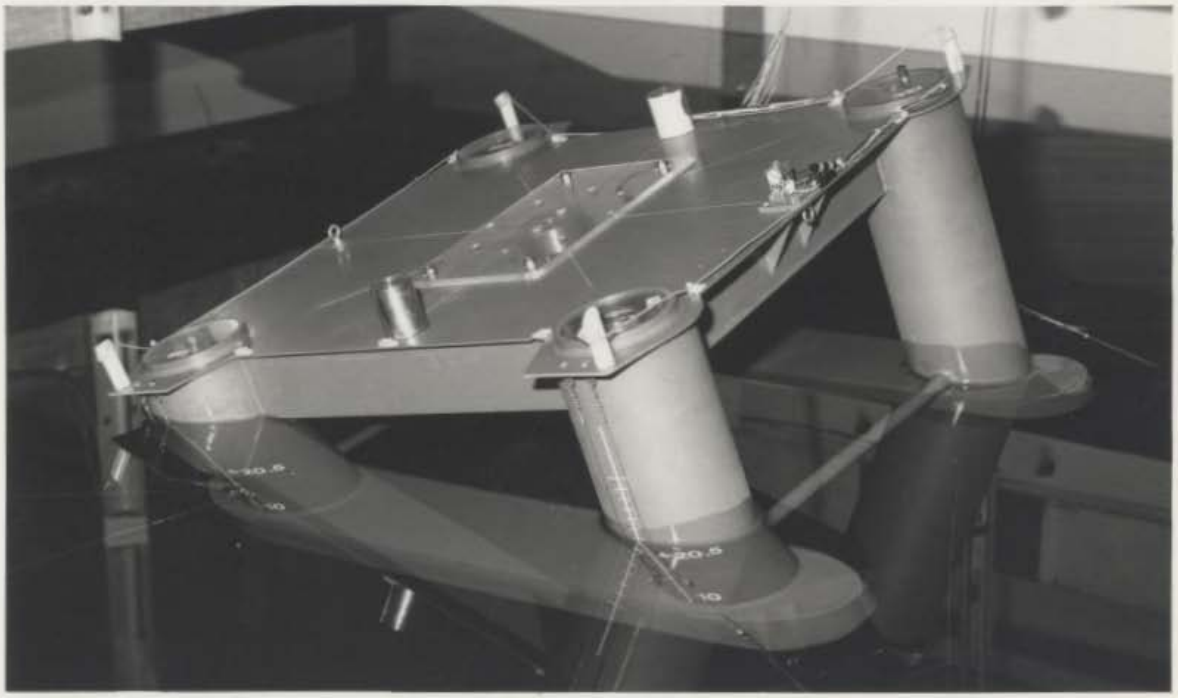

Fig. 6.10 Head Sea, Damage Condition +19.5 deg.

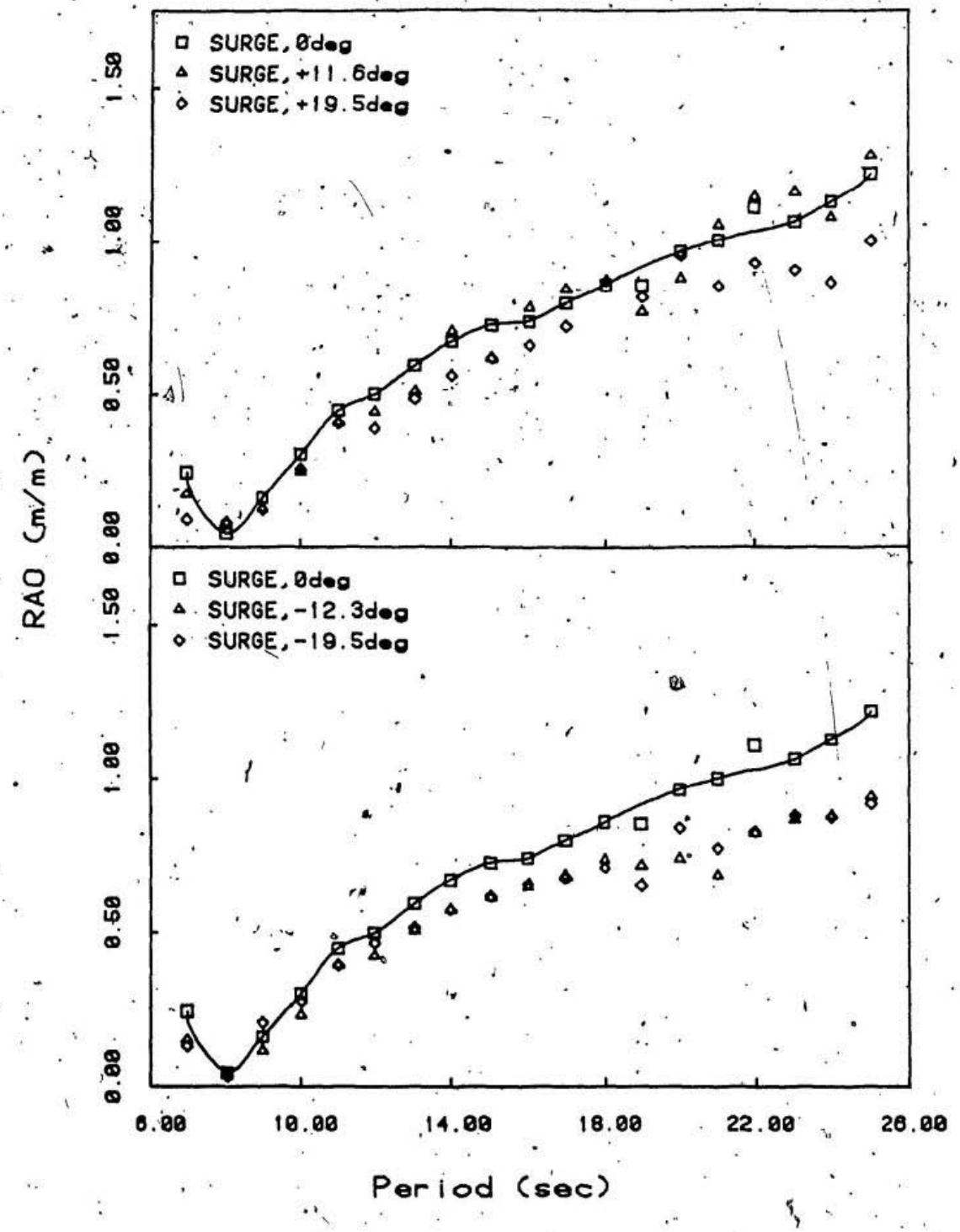

FIG. 6.11 HEAD SEAS; EVEN KEEL AND DAMAGE CONDITIONS; SURGE

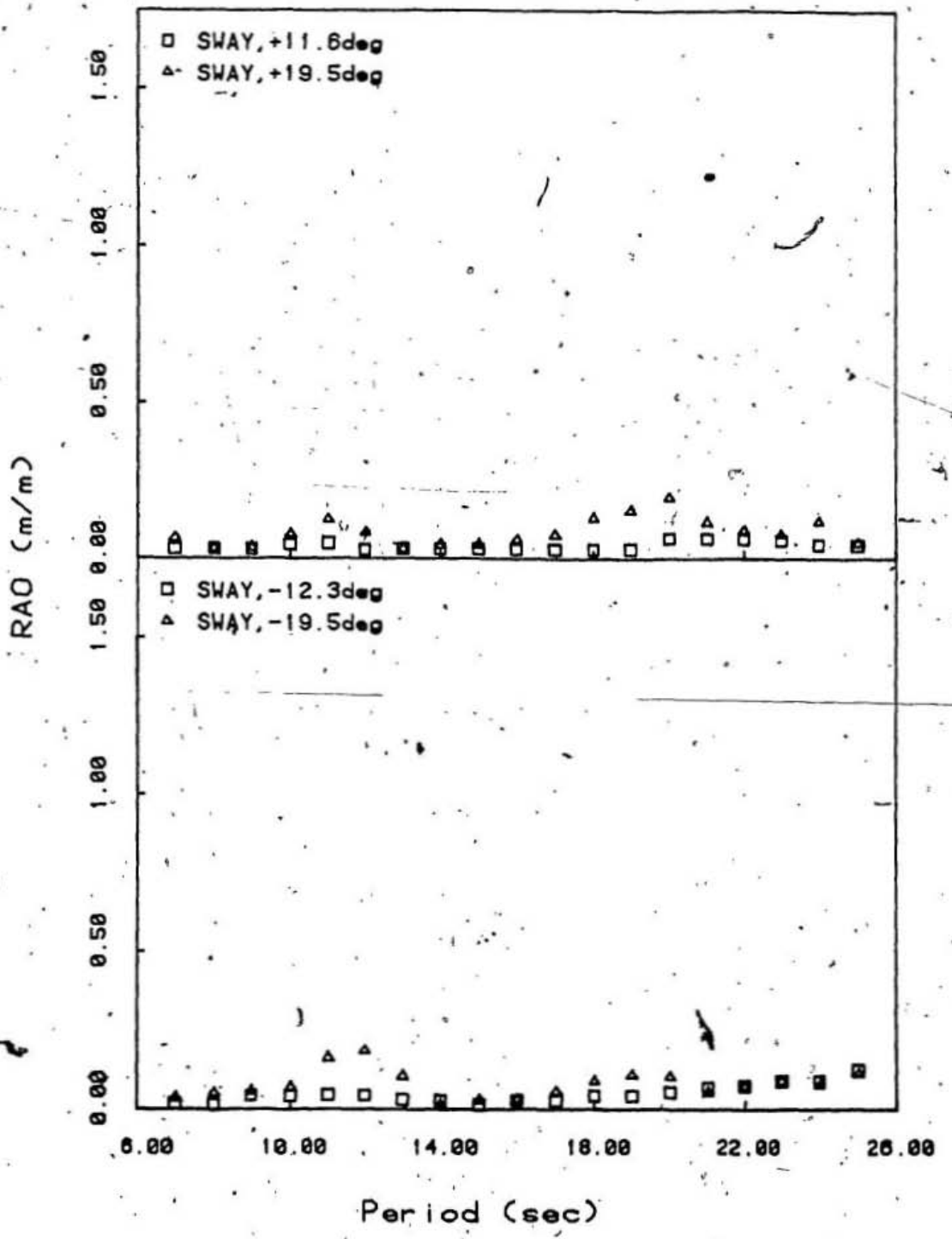

FIG. 6.12 HEAD SEAS; DAMAGE CONDITIONS, SWAY

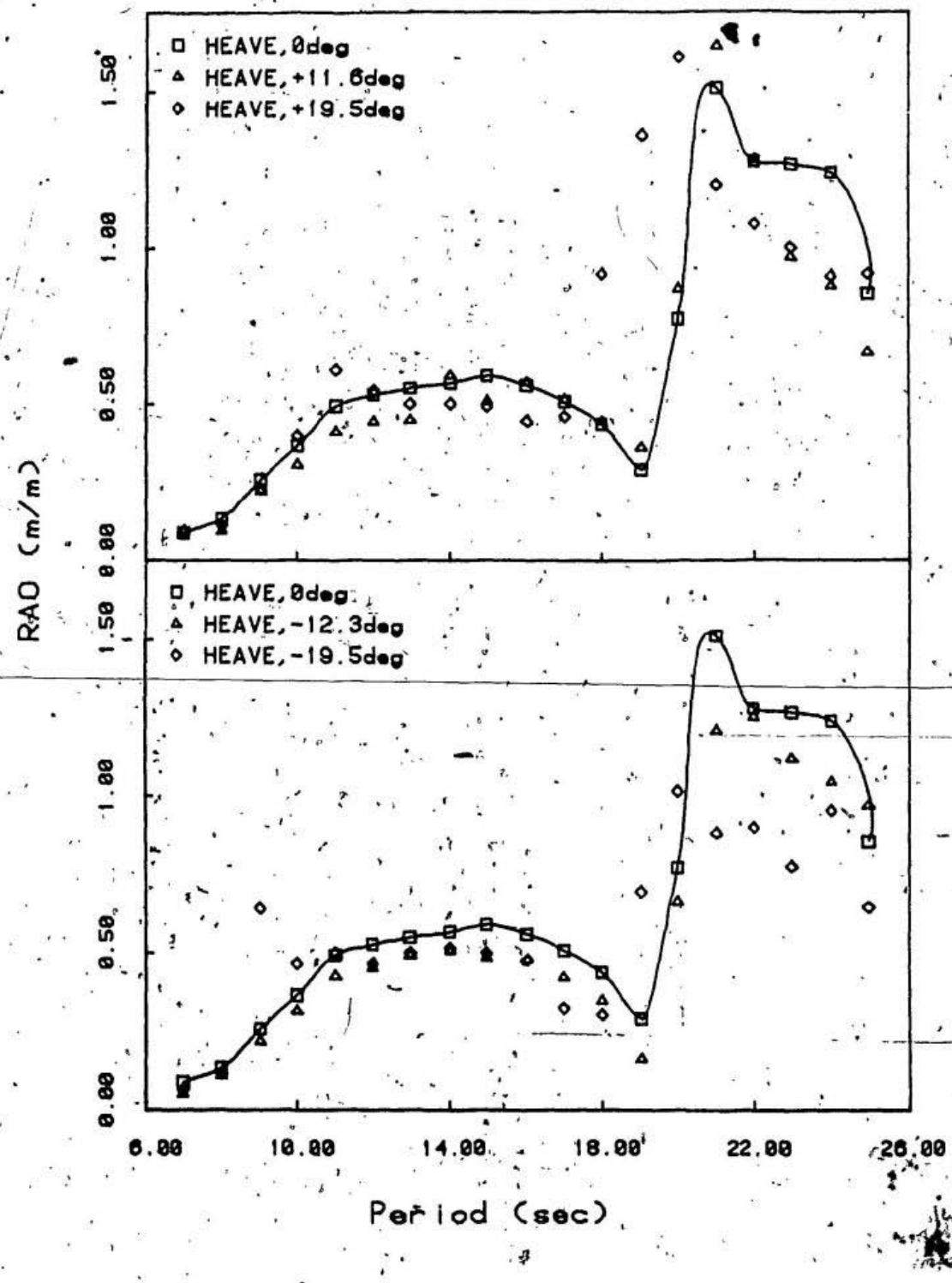

FIG. 6.13 HEAD SEAS; EVEN KEEL AND DAMAGE CONDITIONS; HEAVE

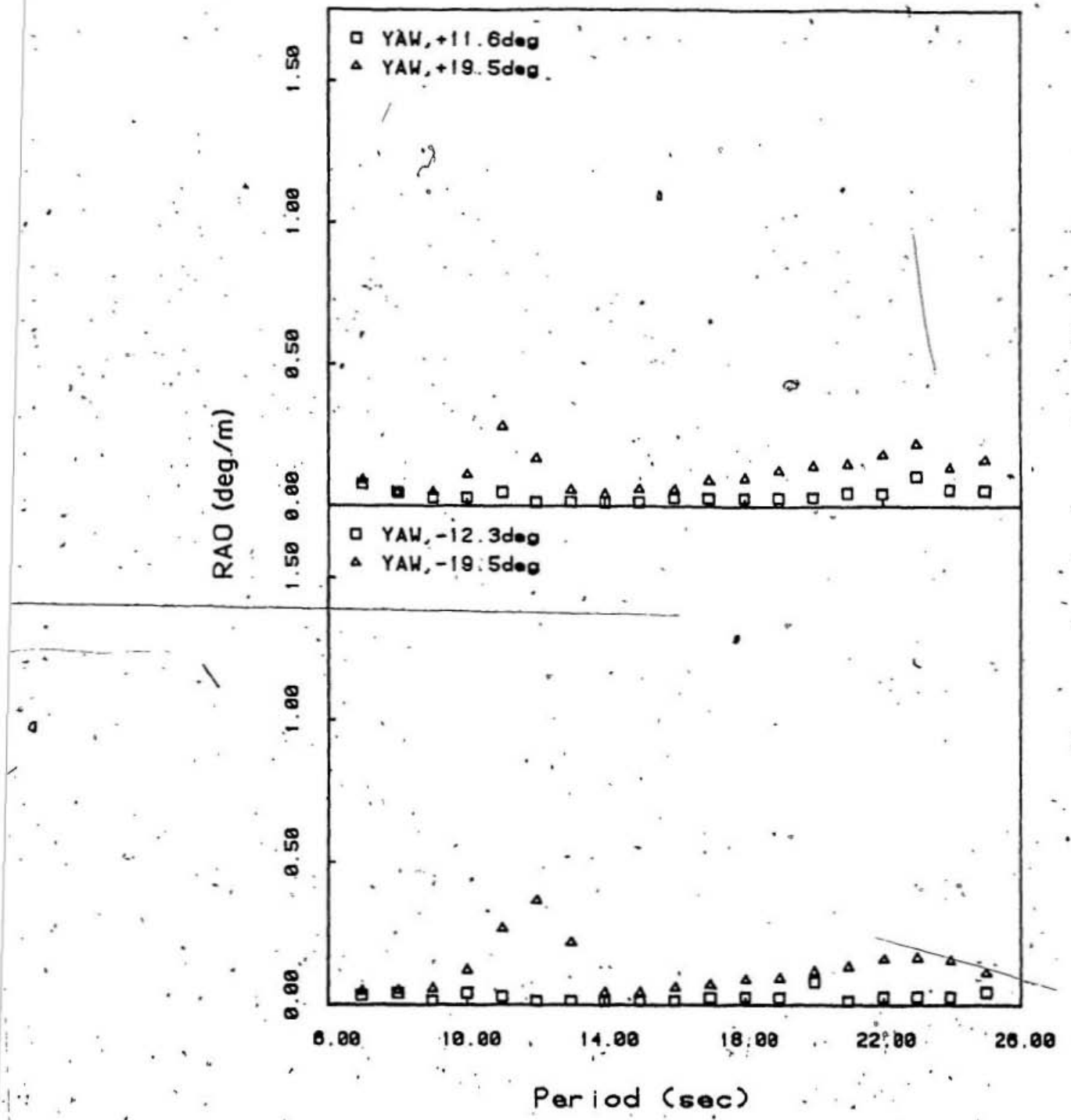

FIG. 6.14 HEAD SEAS, DAMAGE CONDITIONS; YAW

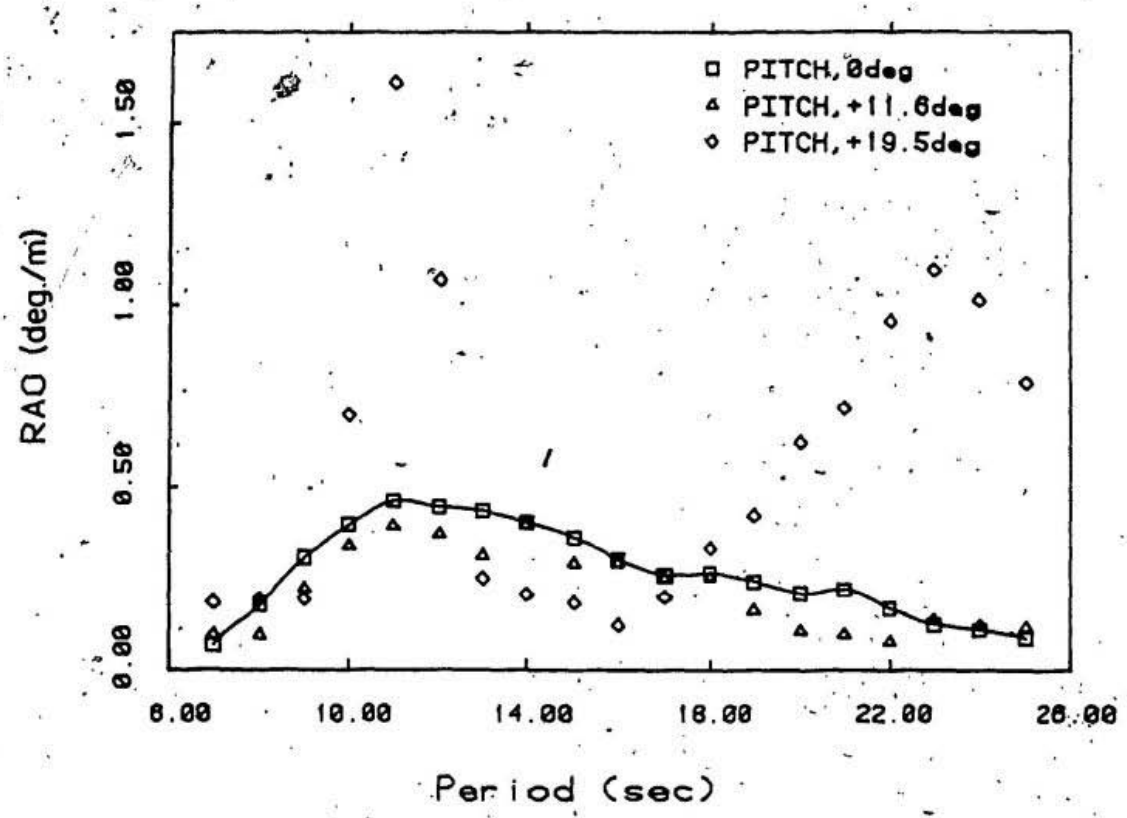

FIG. 6.15 HEAD SEAS: EVEN KEEL AND DAMAGE CONDITIONS; PITCH

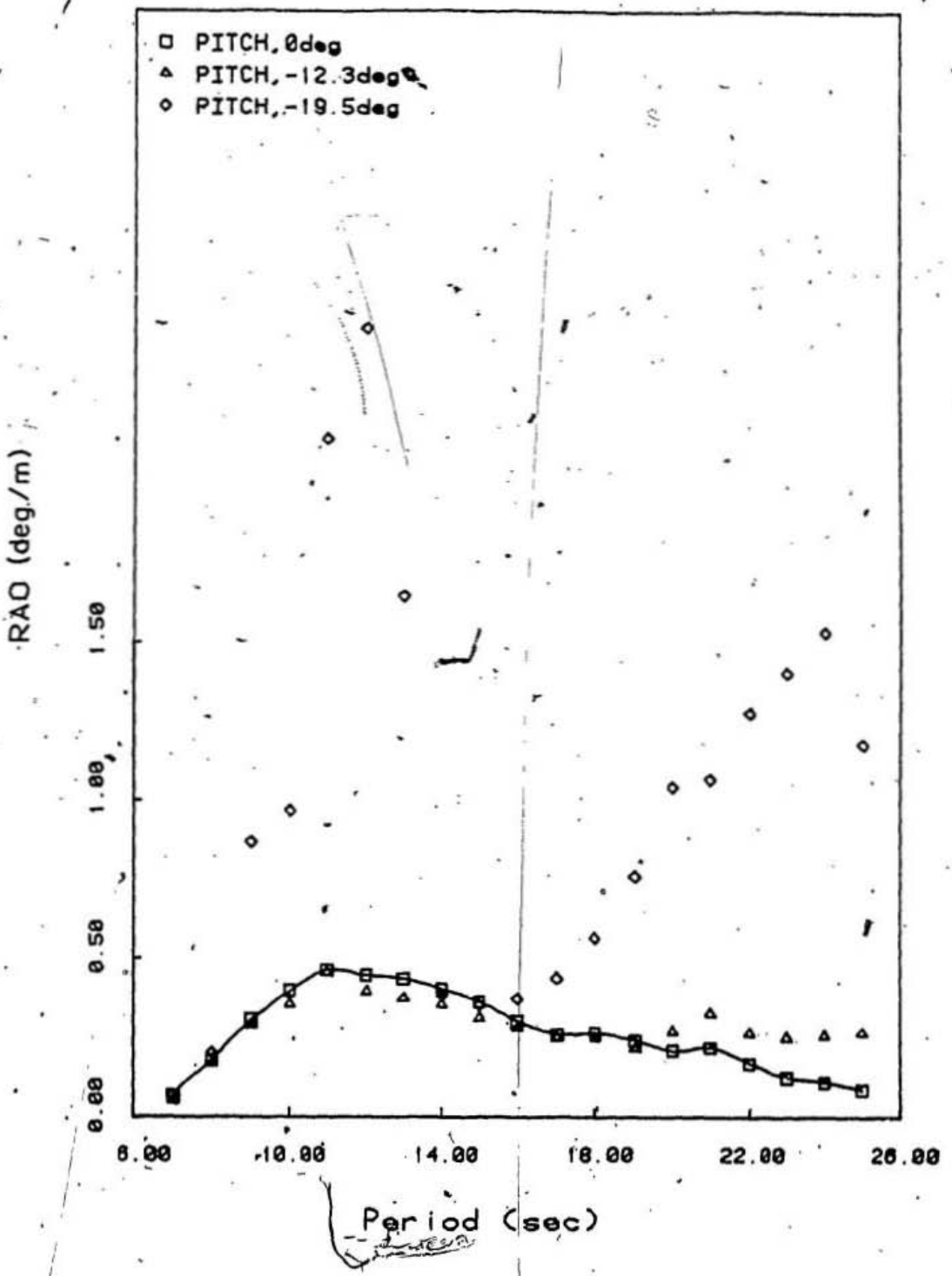

FIG. 6.16 HEAD SEAS; EVEN KEEL AND DAMAGE CONDITIONS; PITCH

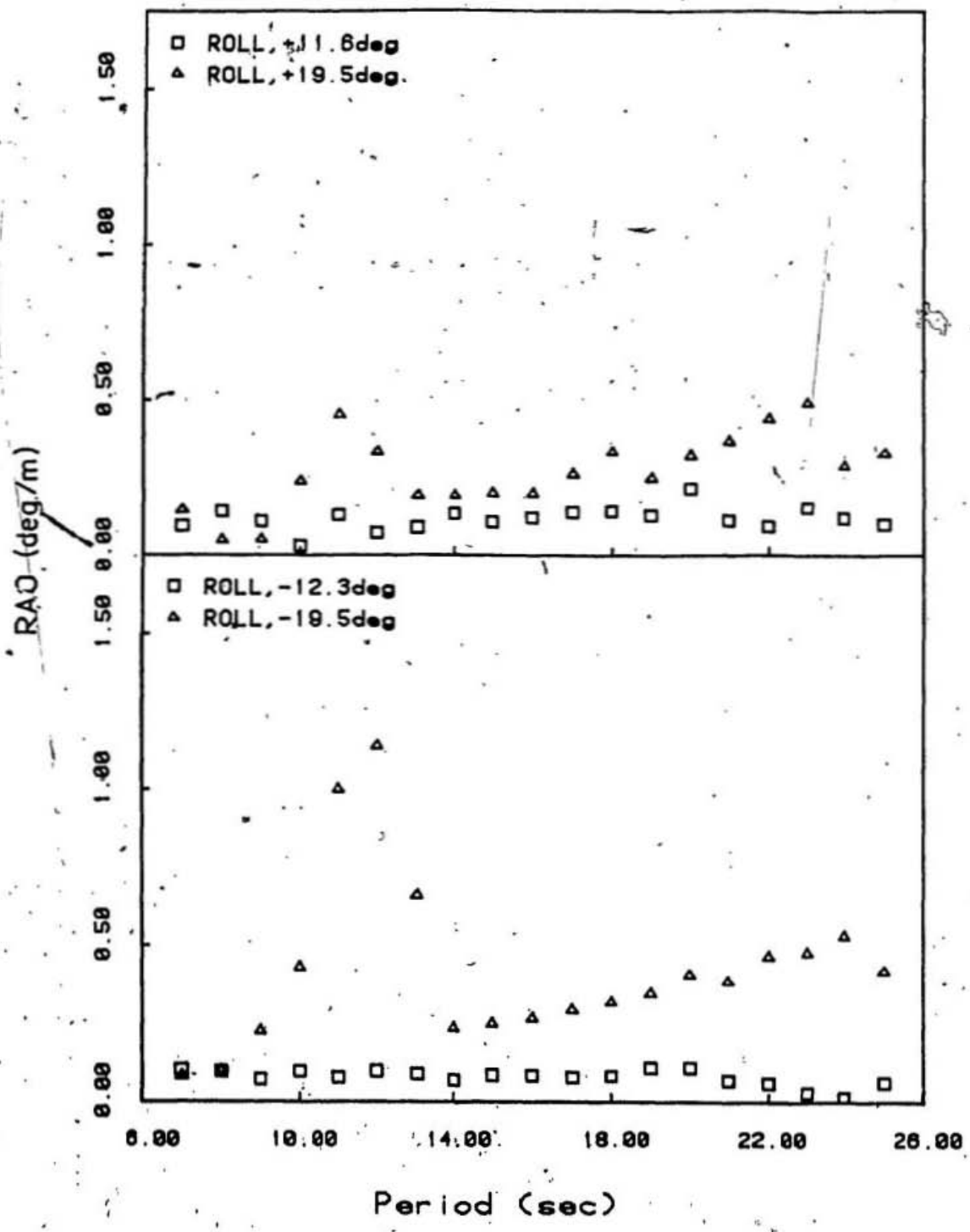

FIG. 6.17 HEAD SEAS; DAMAGE CONDITIONS; ROLL

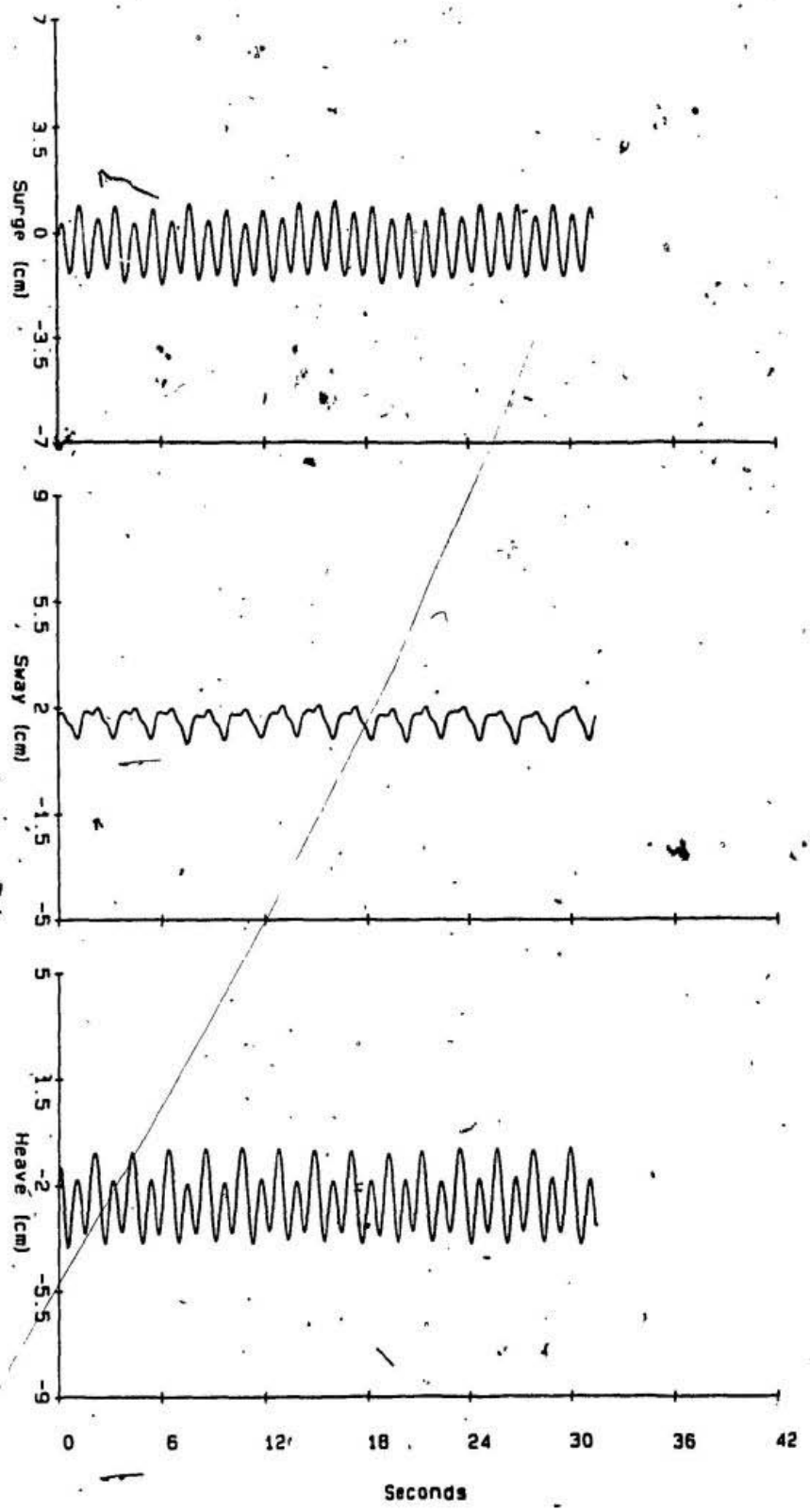

Fig. 6.18A Motion Time History; Head Sea, Damage Condition -19.5°, 11 sec. wave

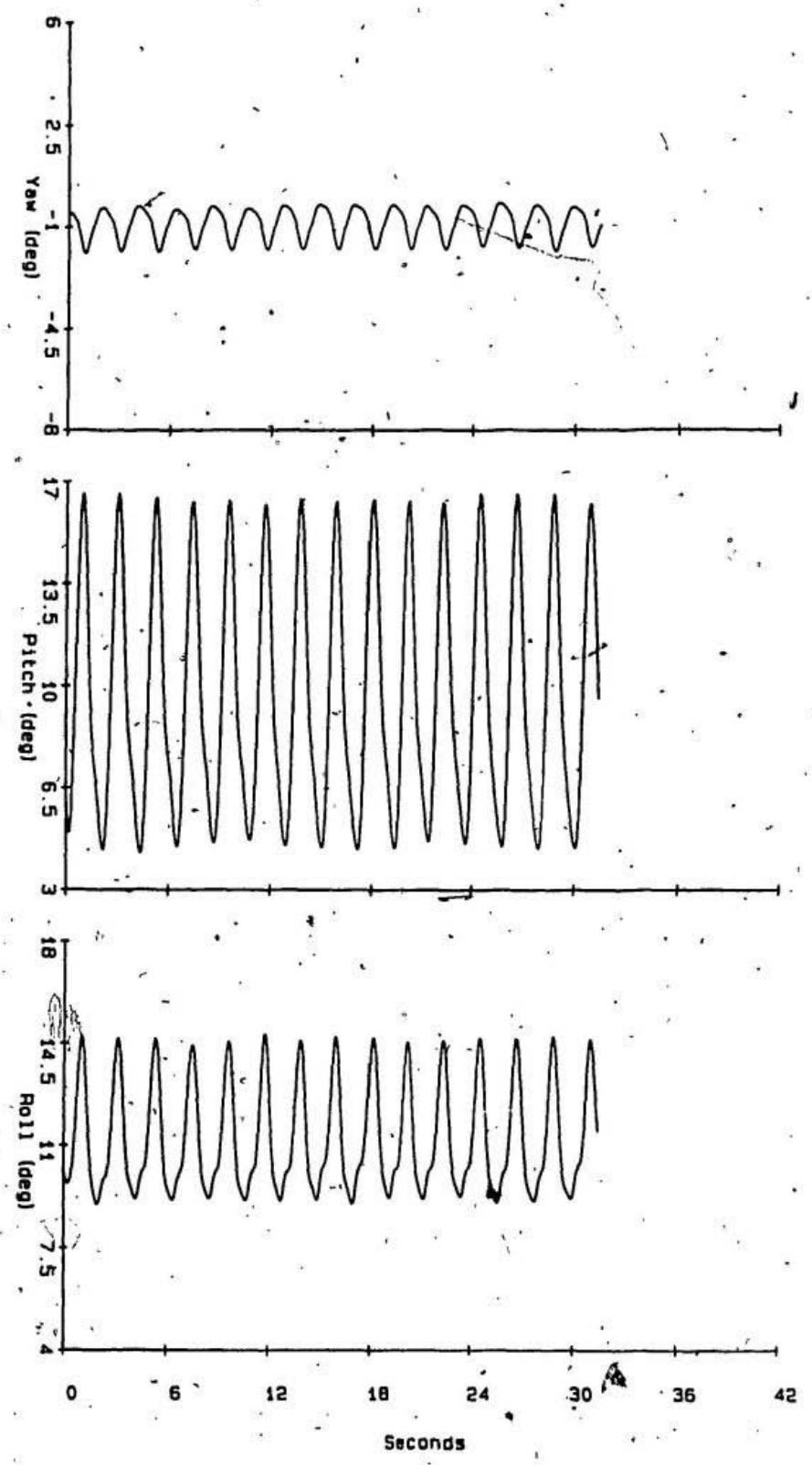

Fig. 6.18B Motion Time History; Head Sea, Damage Condition -19.5°, 11 sec. wave

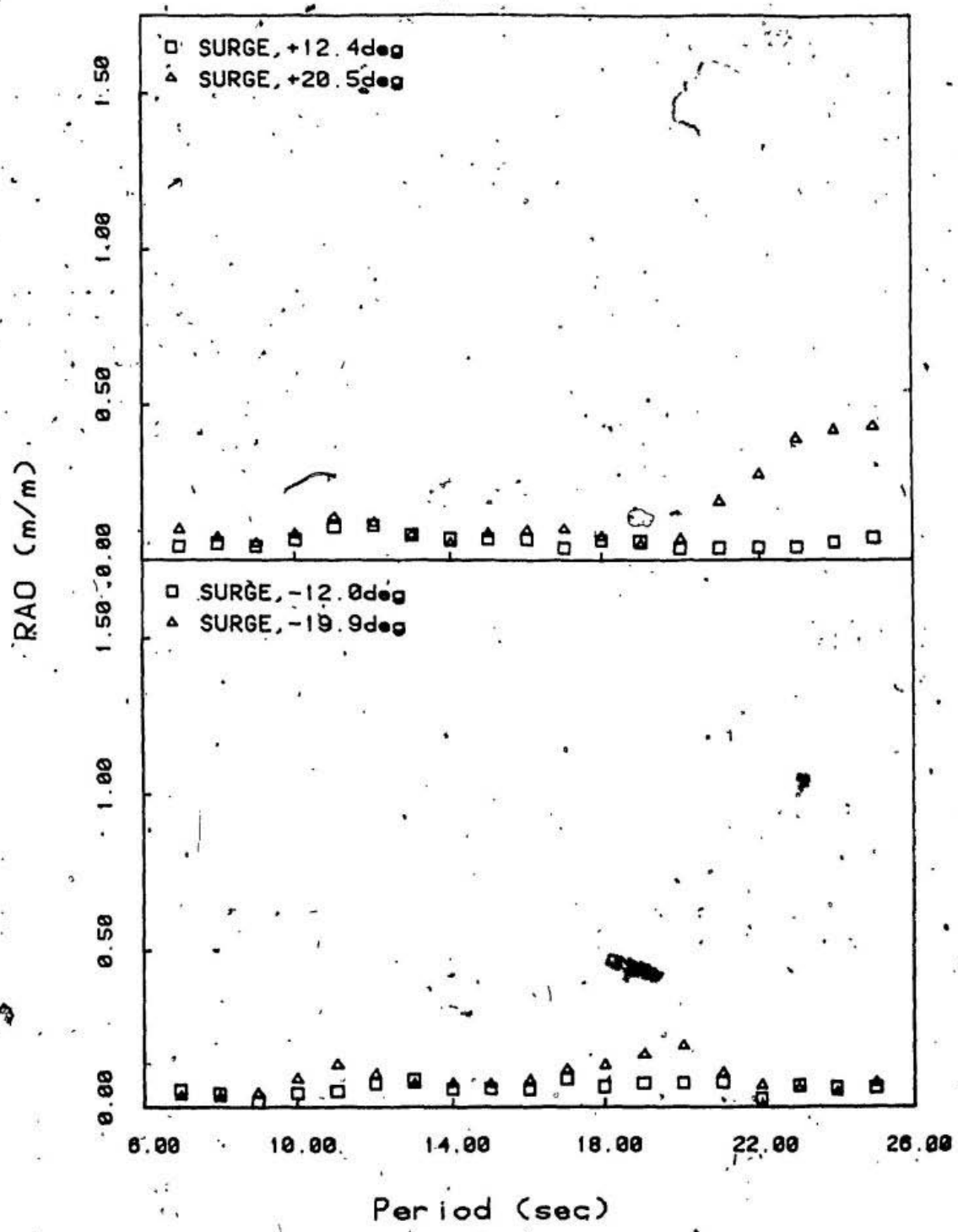

FIG. 6.19 BEAM SEAS; DAMAGE CONDITIONS; SURGE

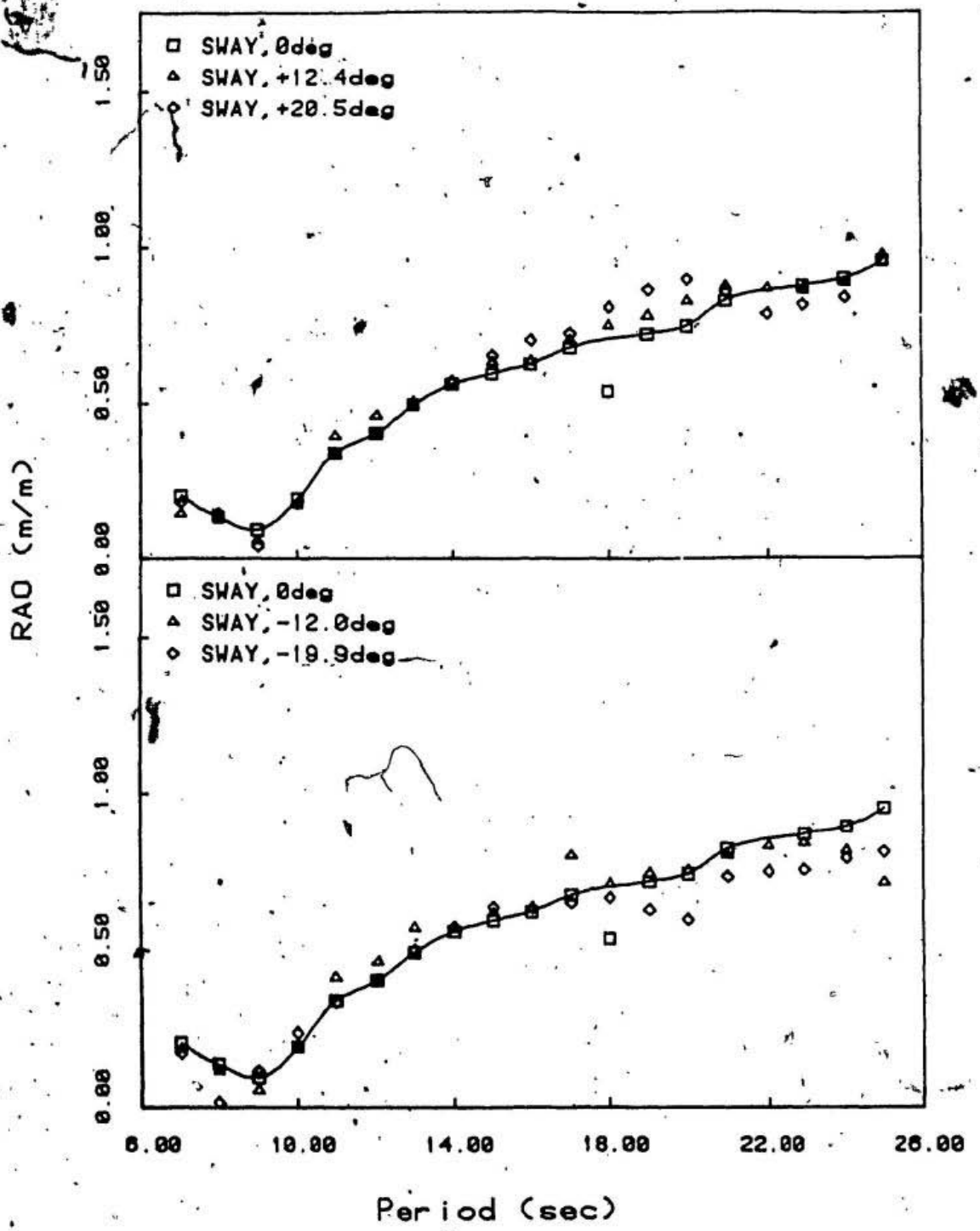

FIG. 6.20 BEAM SEAS; EVEN KEEL AND DAMAGE CONDITIONS; SWAY

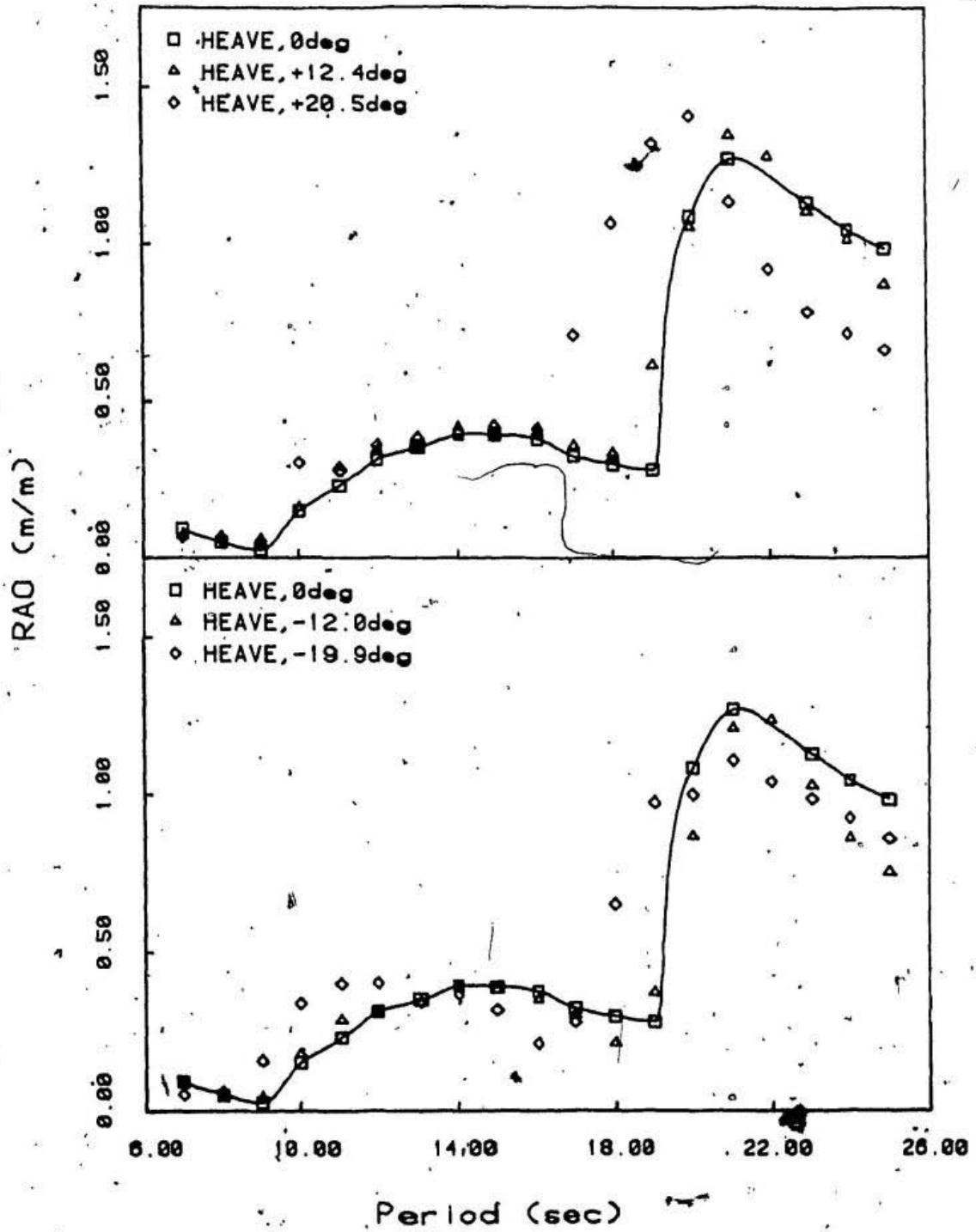

FIG. 6.21 BEAM SEAS; EVEN KEEL AND DAMAGE CONDITIONS; HEAVE

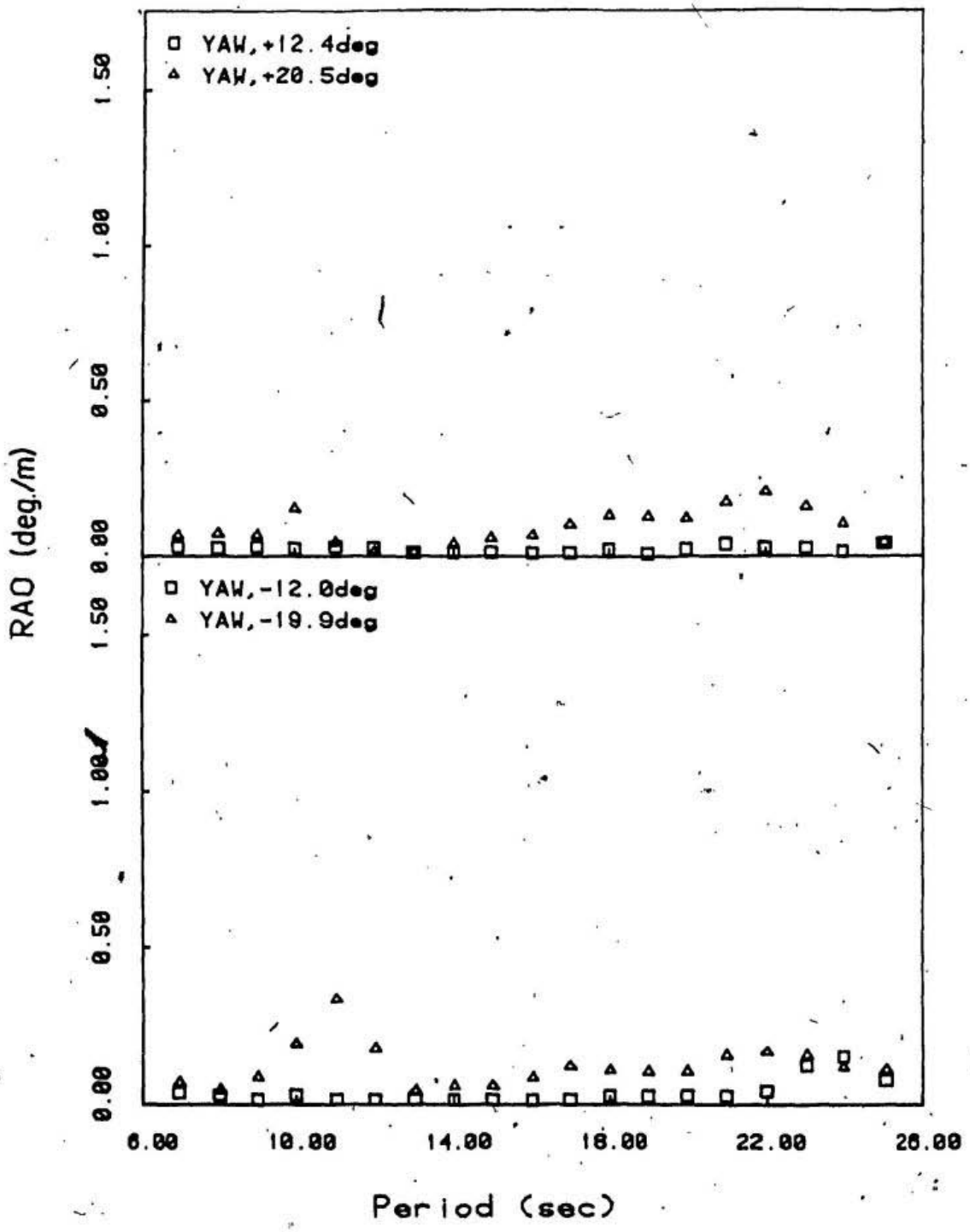

FIG. 6.22 BEAM SEAS; DAMAGE CONDITIONS; YAW

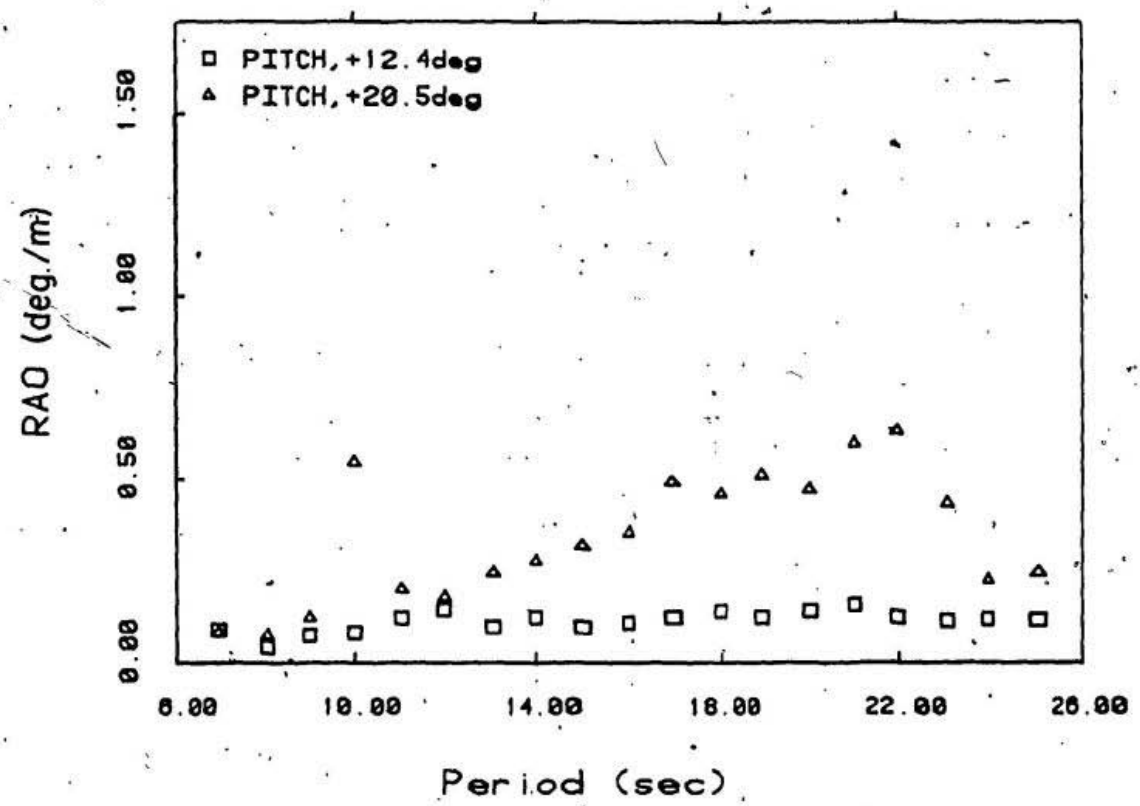

FIG. 6.23 BEAM SEAS; DAMAGE CONDITIONS; PITCH

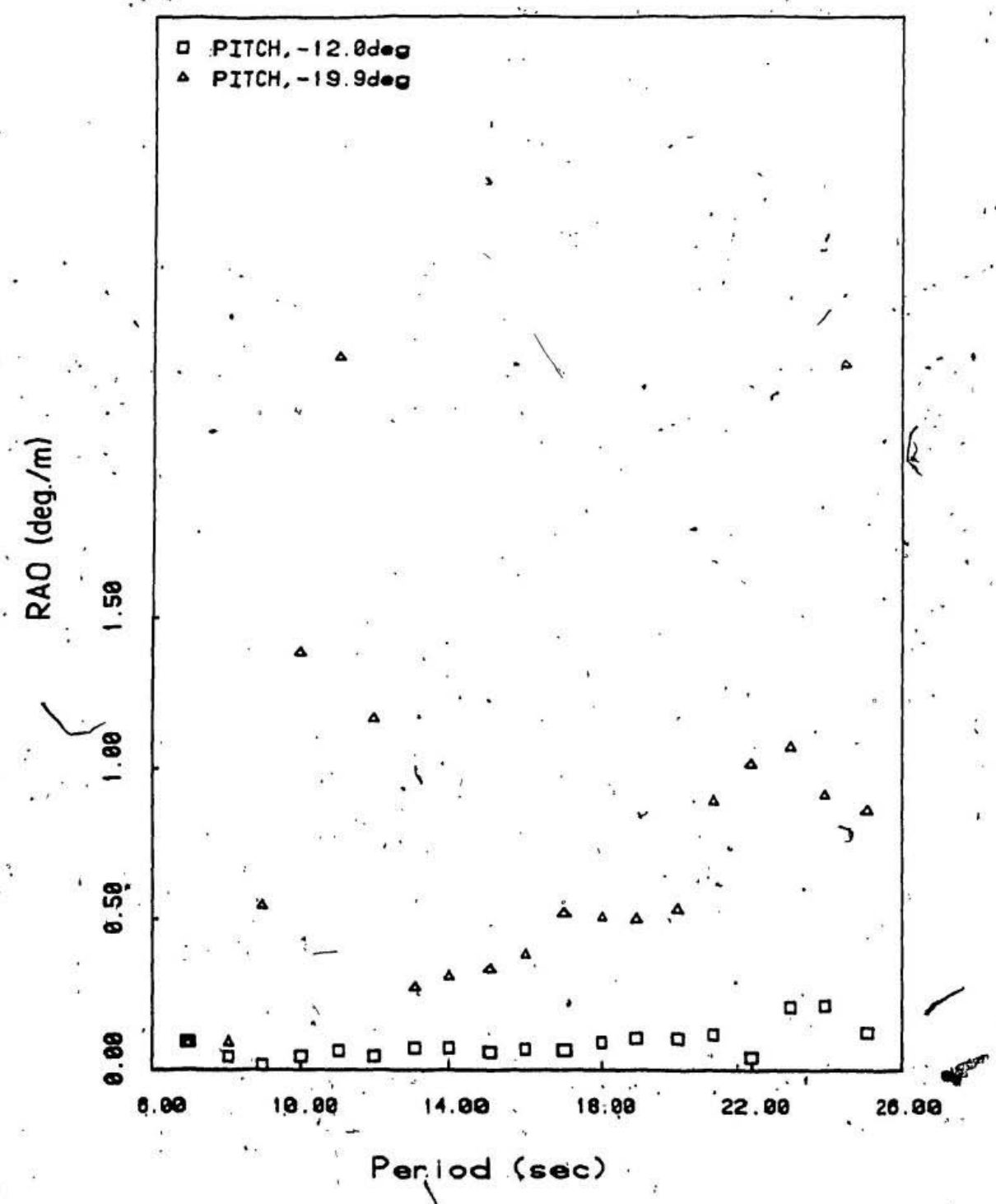

FIG. 6.24 BEAM SEAS; DAMAGE CONDITIONS; PITCH

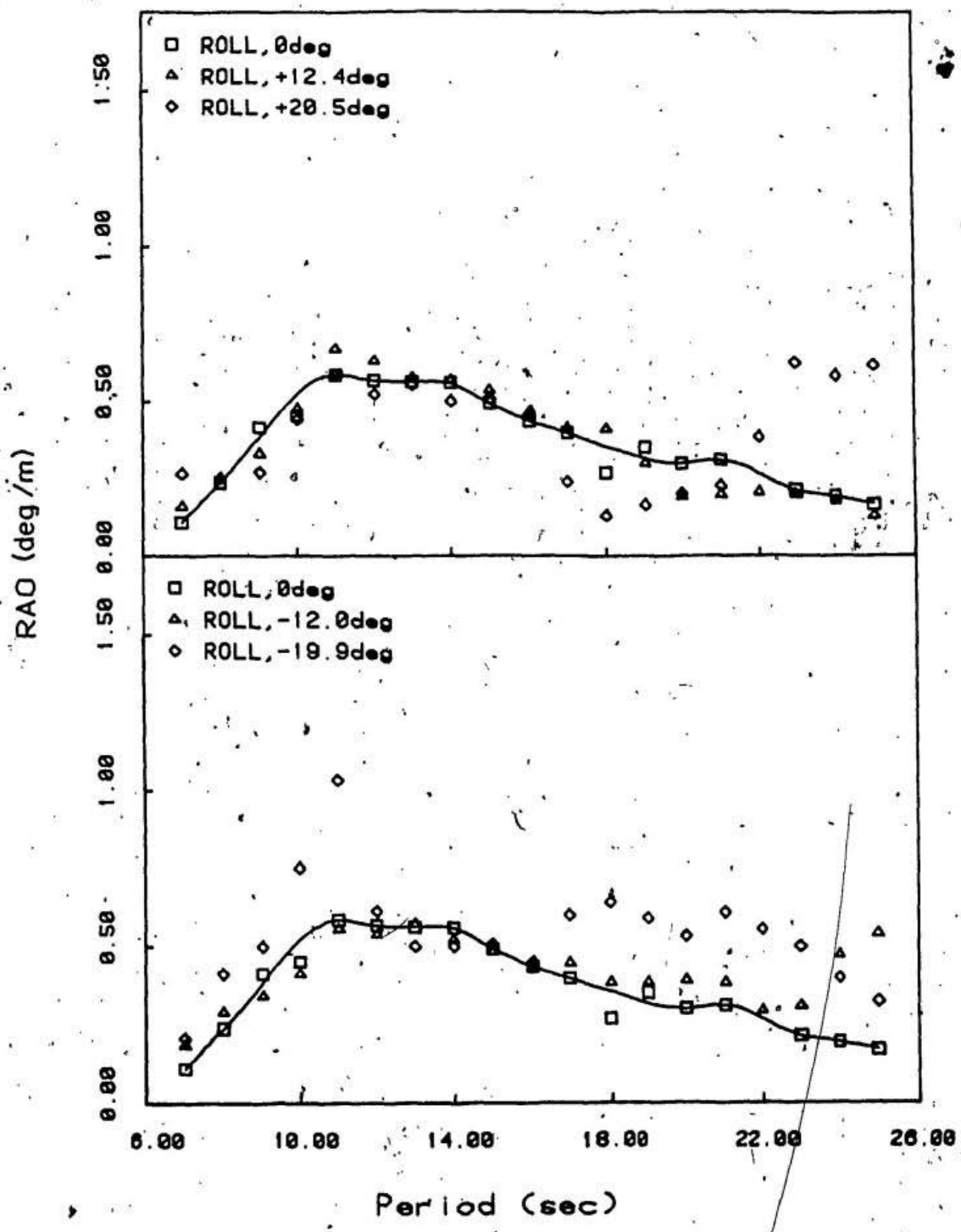

FIG. 6.25 BEAM SEAS; EVEN KEEL AND DAMAGE CONDITIONS; ROLL

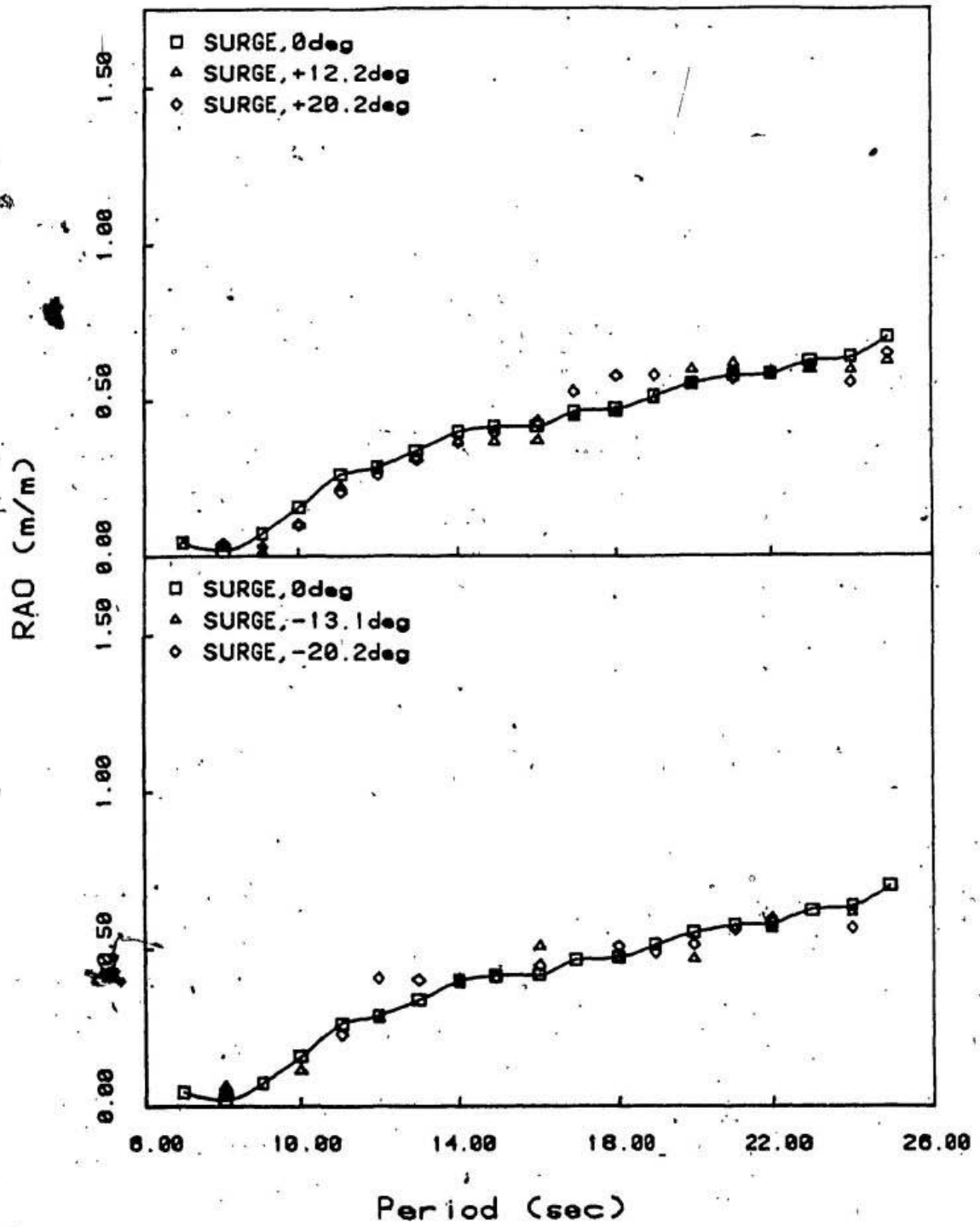

FIG. 6.26 QUARTERING SEAS; EVEN KEEL AND DAMAGE CONDITIONS; SURGE

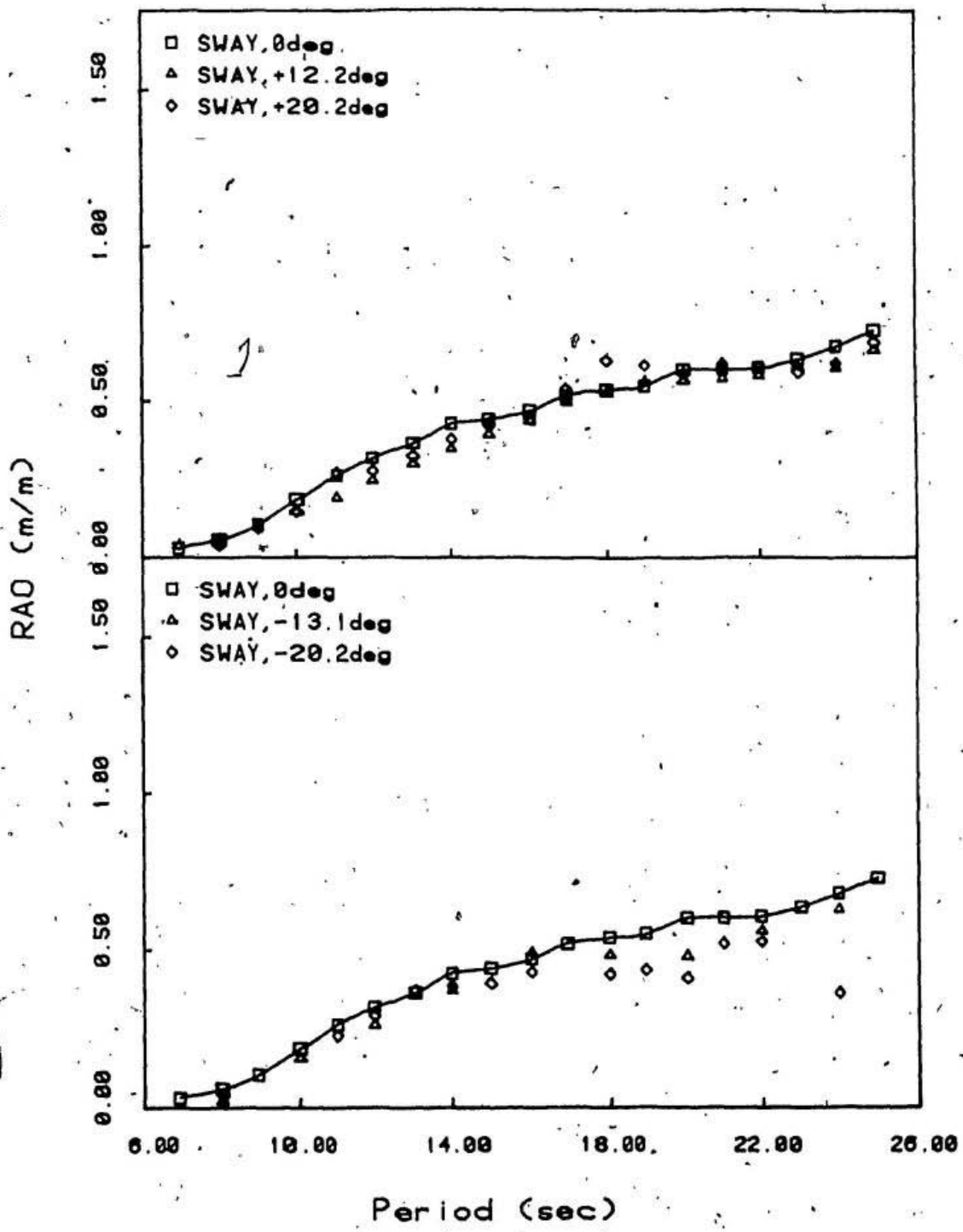

FIG. 6.27 QUARTERING SEAS; EVEN KEEL AND DAMAGE CONDITIONS; SWAY

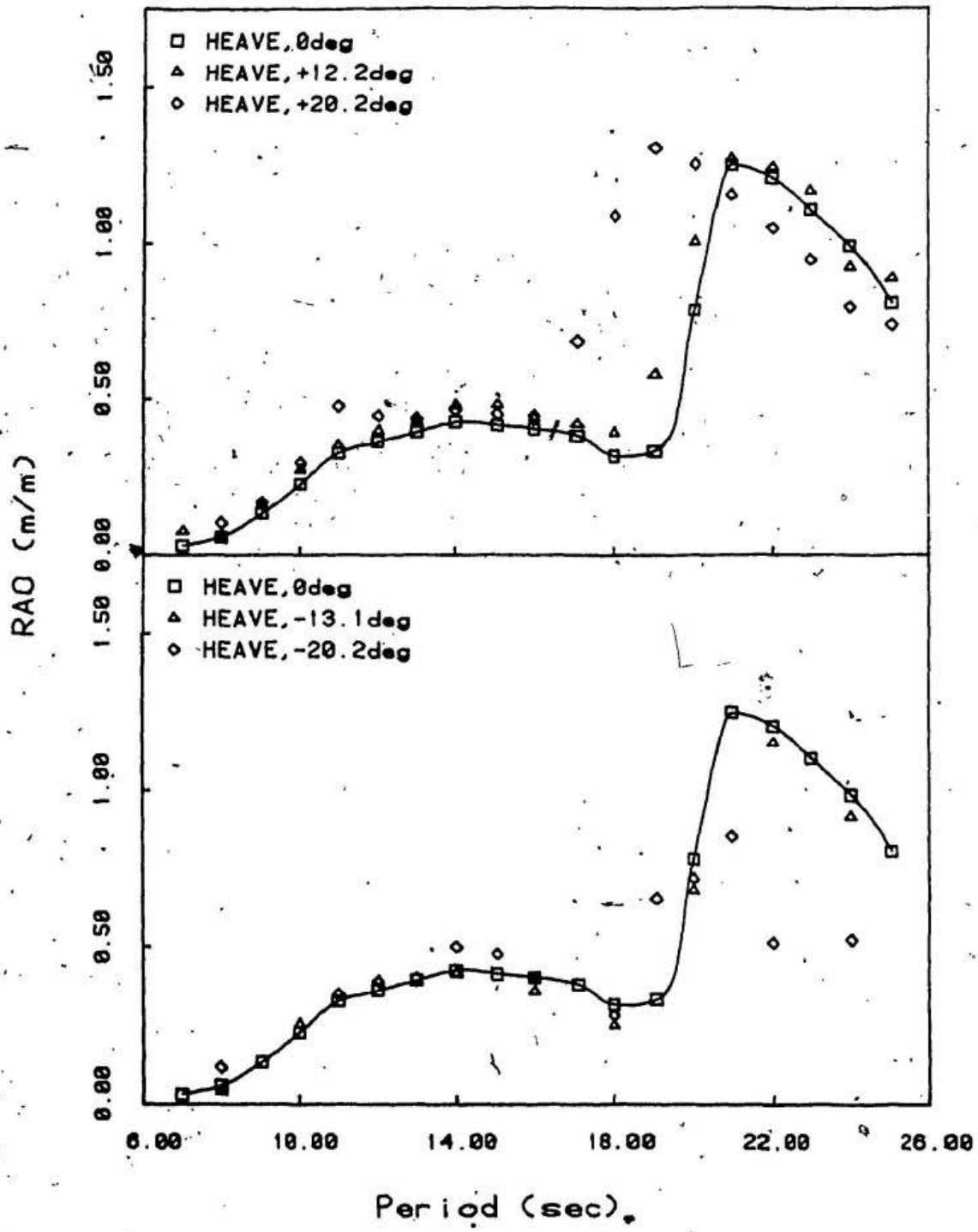

FIG. 6.28 QUARTERING SEAS; EVEN KEEL AND DAMAGE CONDITIONS; HEAVE

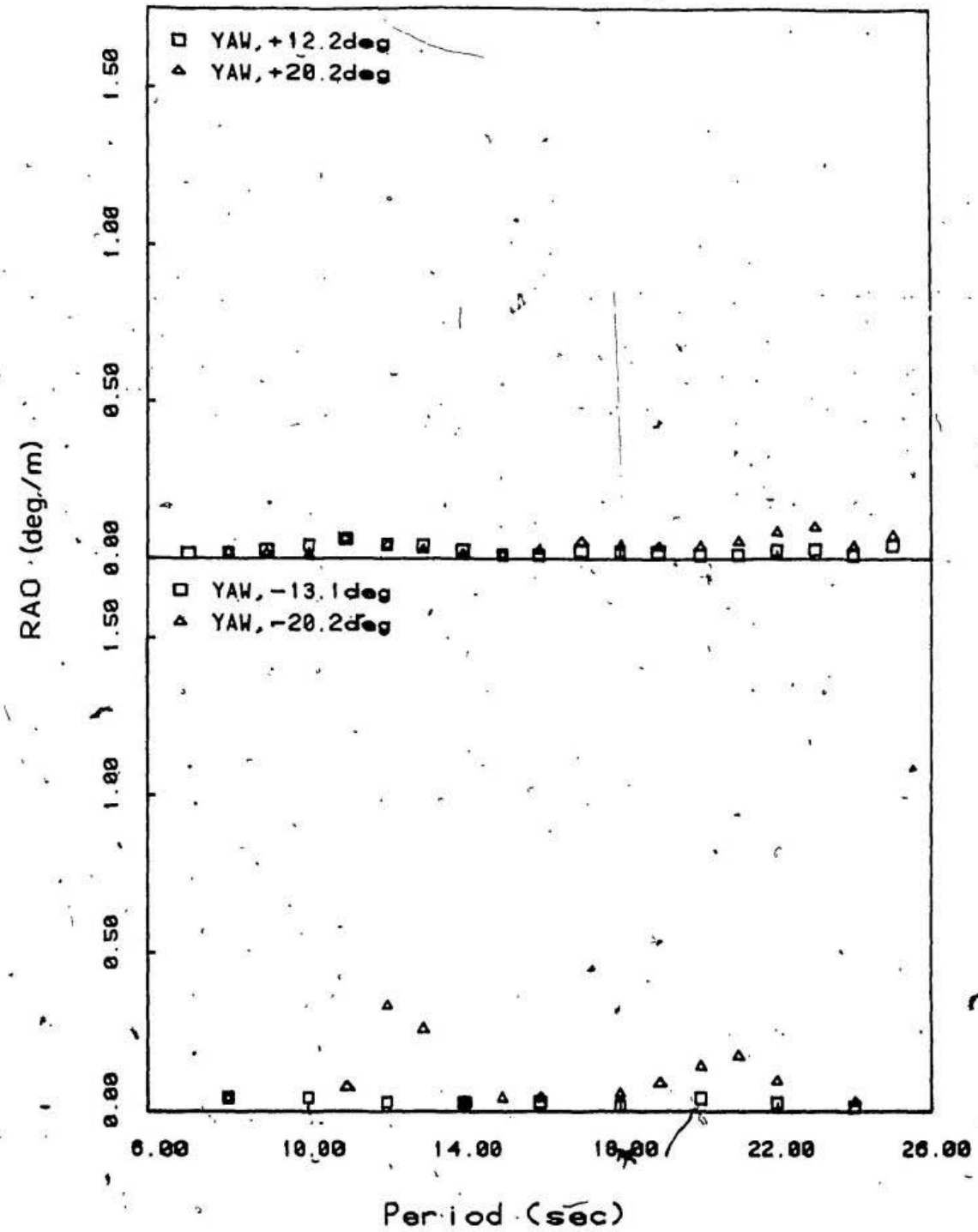

FIG. 6.29 QUARTERING SEAS; DAMAGE CONDITIONS; YAW

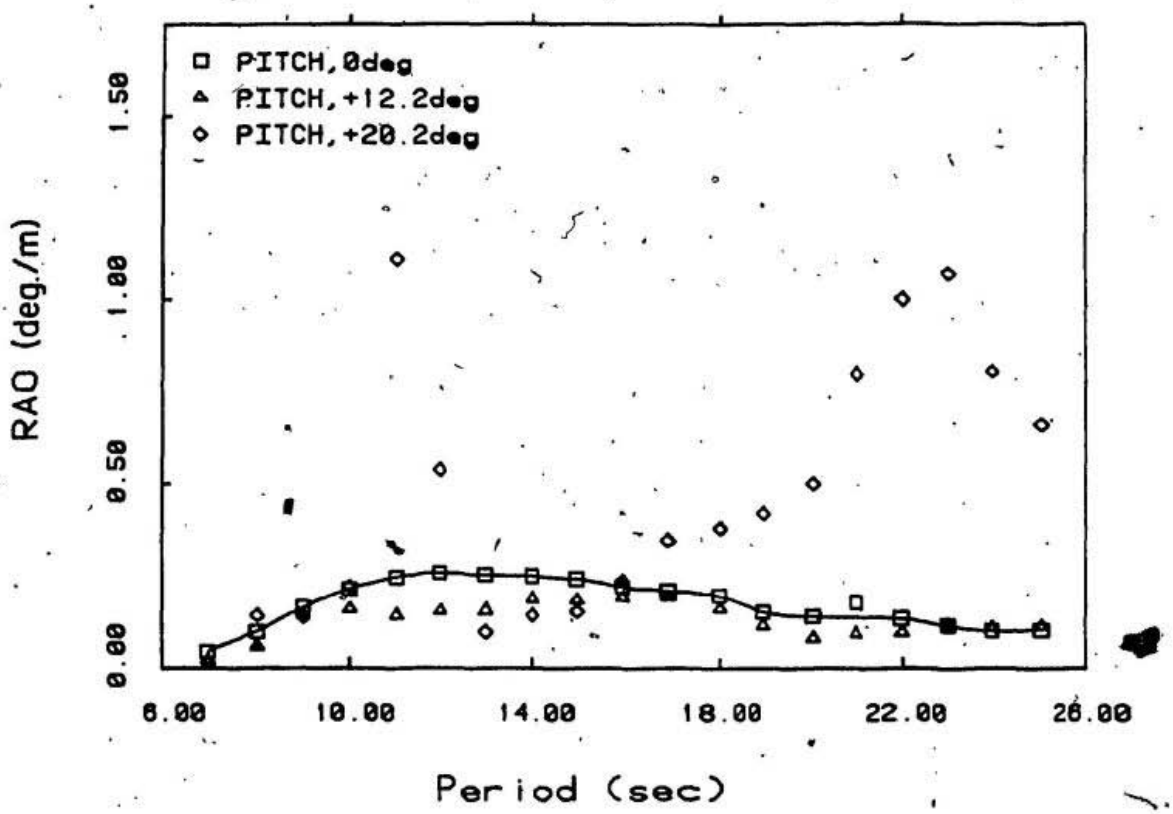

FIG. 6.30 QUARTERING SEAS; EVEN KEEL AND DAMAGE CONDITIONS; PITCH

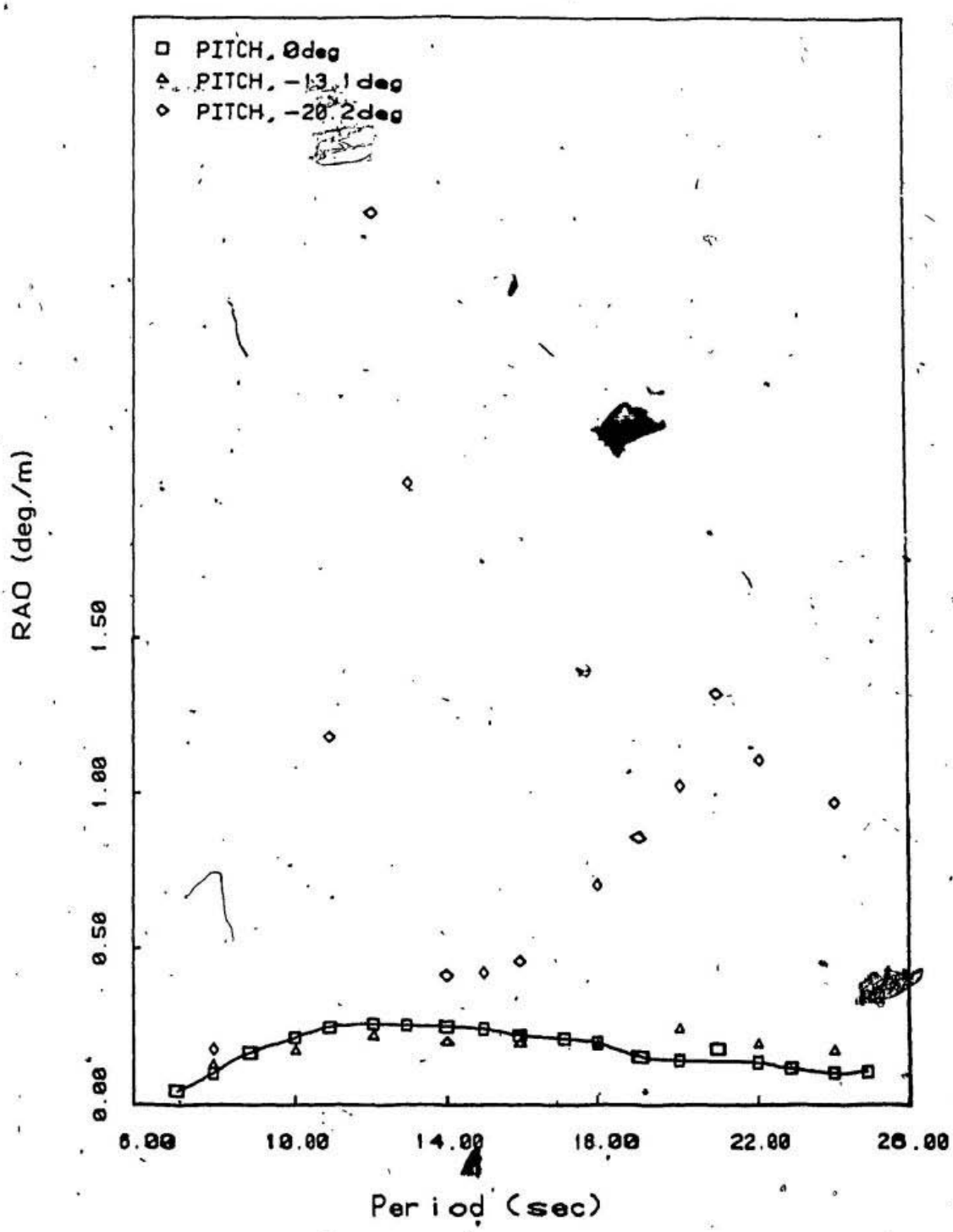

FIG. 6.31 QUARTERING SEAS; EVEN KEEL AND DAMAGE CONDITIONS; PITCH

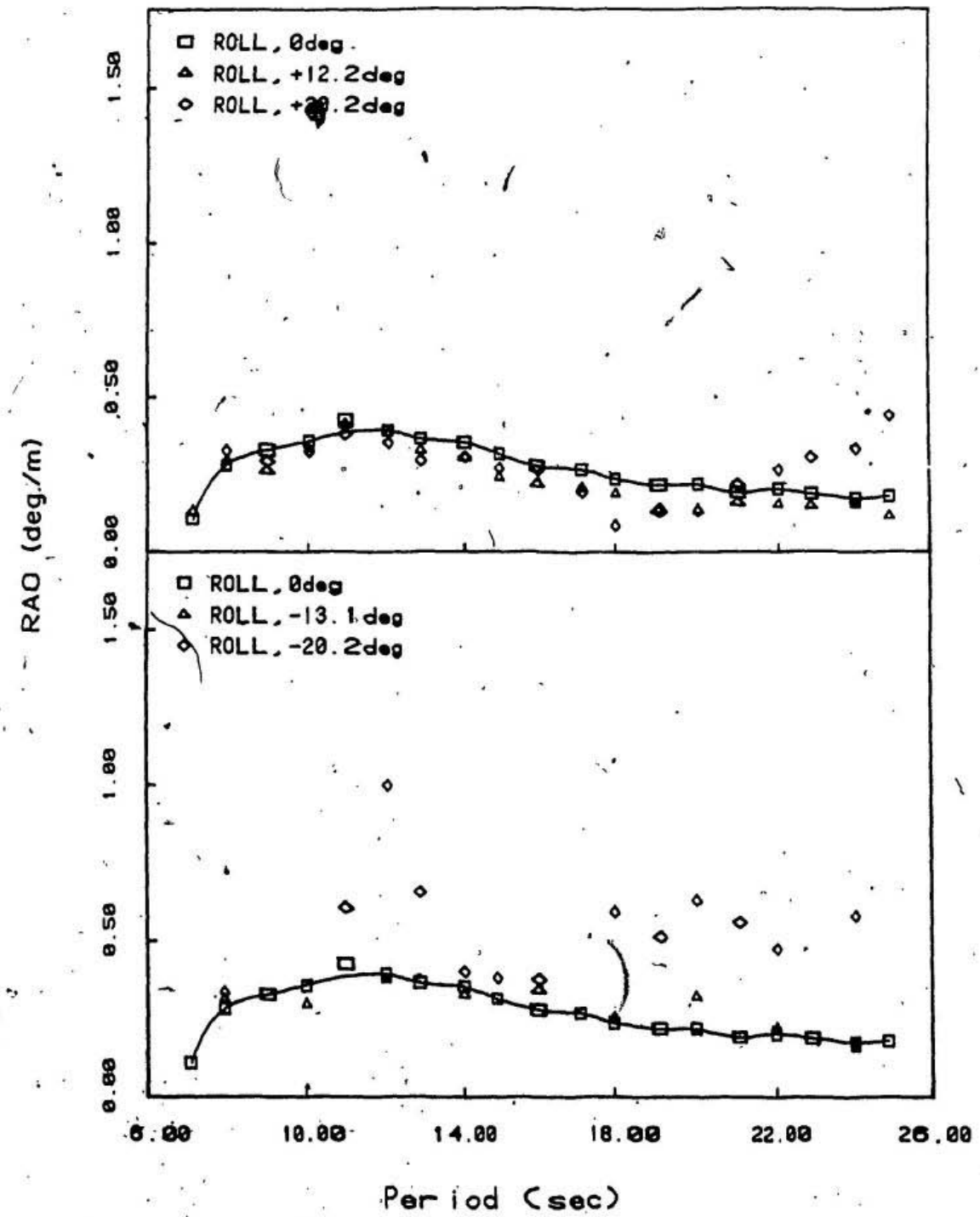

FIG. 6.32 QUARTERING SEAS; EVEN KEEL AND DAMAGE CONDITIONS; ROLL

APPENDIX A

Catenary Mooring Analysis - Computer Program

Catenary Mooring Analysis - Horizontal Excursion

```
      REAL*8  TX(225),T(225),TY(225),SI(225),SI0(225),S(225),
     1  UPRIM(225),U(225),SI1(225),SI01(225),HD(226),W,V,L,PI,
     1  SI2(225)
      DATA W,V,L,PI/1.1518,189.67,900.00,3.1415927/
      OPEN(UNIT=15,FILE='CAT1.DAT',TYPE='NEW')
      OPEN(UNIT=25,FILE='P1.DAT',TYPE='NEW')
      TT=500.00
      DO 75 I=1,225,1
      T(I)=TT
      TX(I)=T(I)-W*V
      ALP=1.0+1.0/(TX(I)/(W*V))
      TY(I)=TX(I)*SQRT((ALP**2)-1.0)
      PP=1.0/ALP
      SI(I)=ACOS(PP)
      SI0(I)=0.0
      S(I)=TY(I)/W
      IF(S(I).LT.900.00)THEN
      U(I)=(TX(I)/W)*(LOG(ALP+SQRT((ALP**2)-1.0))-SQRT
     1  ((ALP**2)-1.0))+L
      UPRIM(I)=L-S(I)
      ELSE
      PP=0.5*(W*V/T(I))*(L/V-V/L)+V/L
      SI(I)=ASIN(PP)
      TX(I)=T(I)*COS(SI(I))
      TY(I)=T(I)*SIN(SI(I))
      PPP=COS(SI(I))/(1.0-W*V/T(I))
      SI0(I)=ACOS(PPP)
      S(I)=L
      UPRIM(I)=0.0
      U(I)=(TX(I)/W)*LOG((1.0/COS(SI(I))+TAN(SI(I)))/
     1  (1.0/COS(SI0(I))+TAN(SI0(I))))
      END IF
      TT=TT+25.0
   75 CONTINUE
      DO 88 K=1,225,1
      SI1(K)=(180.00*SI(K))/PI
      SI01(K)=(180.00*SI0(K))/PI
   88 SI2(K)=SI1(K)*100.0
      DO 95 L=1,225,1
   95 HD(L)=U(L)-U(32)
      WRITE(25,30)(HD(M),T(M),SI2(M),M=4,221,1)
   30 FORMAT(3F14.4/)
      WRITE(15,24)
   24 FORMAT(1X,'MOORING LINE CATENARY ANALYSIS,
     1  LINE TENSION(T)/HORIZONTAL DISPLACEMENT(U)',//)
      WRITE(15,23)
   23 FORMAT(9X,'T',13X,'TX',12X,'TY',12X,'SI',11X,'SI0',12X,'S',
     1  13X,'UPRIM',10X,'U',11X,'HD',//)
```

```
      WRITE(15,22)(T(J),TX(J),TY(J),SI1(J),SI01(J),S(J),UPRIM(J),
     1  U(J),HD(J),J=1,225,1)
   22 FORMAT(9F14.4/)
      CLOSE UNIT=15
      STOP
      END
```

Catenary Mooring Analysis - Vertical Excursion

```
      REAL*8 T(225),TX(225),TY(225),V(225),SI(225),SI1(225),SIO(225)
     1 SIO1(225),S(225),UP(225),U(225),VD(225),SI2(225),W,UC,L,A,PI,
     1 TT,VP
      DATA W,UC,L,PI/1.1618,860.5383,900.00,3.1415927/
      OPEN(UNIT=15,FILE='CAT2.DAT',TYPE='NEW')
      OPEN(UNIT=25,FILE='P2.DAT',TYPE='NEW')
      TT=500.00
      VP=100.00
      DO 75 I=1,225,1
      T(I)=TT
      IF(I.GT.III.AND.III.GT.1)GOTO 20
15    A=1.0+1.0/((T(I)/(W*VP))-1.0)
      U(I)=((T(I)-(W*VP))/W)*(LOG(A+SQRT(A**2-1.0))-(SQRT(A**2-1.0)))+L
      IF(ABS(U(I)-UC).LE.0.001)GOTO 57
      VP=VP+0.001
      GOTO 15
57    V(I)=VP
      TX(I)=T(I)-W*V(I)
      TY(I)=TX(I)*SQRT(A**2-1.0)
      SI(I)=ACOS(1.0/A)
      SIO(I)=0.0
      S(I)=TY(I)/W
      IF(S(I).LT.900.00)THEN
      UP(I)=L-S(I)
      ELSE
      VP=V(I-1)
20    PPPP=(W*VP)/(2.0*T(I))*(L/VP-VP/L)+VP/L
      SI(I)=ASIN(PPPP)
      TX(I)=T(I)*COS(SI(I))
      TY(I)=T(I)*SIN(SI(I))
      QQQQ=COS(SI(I))/(1.0-W*VP/T(I))
      SIO(I)=ACOS(QQQQ)
      S(I)=L
      UP(I)=0.0
      U(I)=(TX(I)/W)*LOG((1.0/COS(SI(I))+TAN(SI(I)))/
     1 (1.0/COS(SIO(I))+TAN(SIO(I))))
      V(I)=VP
      IF(ABS(U(I)-UC).LE.0.001)GOTO 67
      VP=V(I)+0.001
      GOTO 20
67    III=I
      END IF
      TT=TT+25.0
75    CONTINUE
99    KK=I-1
      DO 88 K=1,KK,1
      SI1(K)=(180.00*SI(K))/PI
      SIO1(K)=(180.00*SIO(K))/PI
```

```
88      SI2(K)=SI1(K)*100.0
        DO 95 L=1,225,1
95      VD(L)=V(L)-189.67
        WRITE(26,30)(VD(M),T(M),SI2(M),M=16,48,1)
30      FORMAT(3F14.4/)
        WRITE(16,24)
24      FORMAT(1X,'MOORING CATENARY ANALYSIS,LINE TENSION(T)/
     1  VERTICAL DISPLACEMENT(V)',//)
        WRITE(16,23)
23      FORMAT(9X,'T',13X,'TX',12X,'TY',12X,'SI',11X,'SI0',
     1  12X,'S',13X,'UP',13X,'U',13X,'V',//)
        WRITE(16,22)(T(J),TX(J),TY(J),SI1(J),SI01(J),S(J),UP(J),U(J),
     1  V(J),J=1,KK,1)
22      FORMAT(9F14.4/)
        CLOSE UNIT=16
        STOP
        END
```